

---

**Proteolysis of the Receptor for Advanced  
Glycation End Products by Matrix Metalloproteinases**

Dissertation  
Zur Erlangung des Grades  
Doktor der Naturwissenschaften

Am Fachbereich Biologie  
Der Johannes Gutenberg-Universität Mainz

**Ling Zhang**  
geb. am 22-10-1972 in Wuhan, China

Mainz 2006

## Table of Contents

Table of Contents.....	ii
<b>1. Introduction.....</b>	<b>1</b>
<b>1.1 The A<math>\beta</math> peptide.....</b>	<b>1</b>
<b>1.1.1 A<math>\beta</math> peptide production and its pathologic role in Alzheimer’s disease (AD).....</b>	<b>1</b>
<b>1.1.2 A<math>\beta</math> peptide clearance from the brain.....</b>	<b>2</b>
<b>1.2 RAGE (receptor for advanced glycation end products).....</b>	<b>4</b>
<b>1.2.1 Structure.....</b>	<b>4</b>
<b>1.2.2 Expression patterns.....</b>	<b>5</b>
<b>1.2.3 Extracellular ligands and their pathophysiologic functions.....</b>	<b>5</b>
<b>1.2.4 Intracellular signaling.....</b>	<b>7</b>
<b>1.2.5 RAGE-A<math>\beta</math> interaction.....</b>	<b>8</b>
<b>1.2.6 Isoforms of RAGE.....</b>	<b>9</b>
<i>1.2.6.1 Full-length RAGE.....</i>	<i>9</i>
<i>1.2.6.2 C-terminal truncated RAGE.....</i>	<i>10</i>
<i>1.2.6.3 Soluble RAGE (sRAGE).....</i>	<i>10</i>
<i>1.2.6.4 N-truncated RAGE.....</i>	<i>12</i>
<b>1.3 Protein Ectodomain Shedding.....</b>	<b>12</b>
<b>1.3.1 Ectodomain shedding.....</b>	<b>12</b>
<i>1.3.2.1 A disintegrin and metalloproteinases (ADAMs).....</i>	<i>14</i>
<i>1.3.2.2. Matrix metalloproteinases (MMPs).....</i>	<i>14</i>
<b>2. Aim of the study.....</b>	<b>19</b>
<b>3. Materials and Methods.....</b>	<b>21</b>
<b>3.1 Materials.....</b>	<b>21</b>
<b>3.1.1 Chemicals and Media.....</b>	<b>21</b>
<b>3.1.2 Enzyme and Kit systems.....</b>	<b>22</b>
<b>3.1.3 Laboratory instruments and accessories.....</b>	<b>23</b>
<b>3.1.4 Solutions, buffers and media.....</b>	<b>24</b>
<b>3.1.5 Antibodies.....</b>	<b>26</b>
<b>3.1.6 Bacterial strains and cell lines.....</b>	<b>28</b>
<b>3.1.7 Plasmids.....</b>	<b>29</b>
<b>3.1.8 Oligonucleotides.....</b>	<b>32</b>
<b>3.1.9 Inhibitors and Activators.....</b>	<b>33</b>
<b>3.2 Methods.....</b>	<b>34</b>
<b>3.2.1 Molecular biology.....</b>	<b>34</b>
<i>3.2.1.1 Maintenance of bacterial strains.....</i>	<i>34</i>
<i>3.2.1.2 Preparation of competent bacteria.....</i>	<i>34</i>
<i>3.2.1.3 Transformation of E. coli.....</i>	<i>34</i>
<i>3.2.1.4 Plasmid Minipreparation.....</i>	<i>34</i>
<i>3.2.1.5 Plasmid Maxipreparation.....</i>	<i>35</i>
<i>3.2.1.6 Enzymatic modification of DNA.....</i>	<i>36</i>
<i>3.2.1.7 DNA electrophoresis.....</i>	<i>37</i>
<i>3.2.1.8 DNA purification.....</i>	<i>38</i>
<i>3.2.1.9 DNA Sequencing.....</i>	<i>38</i>
<i>3.2.1.10 Polymerase Chain Reaction (PCR).....</i>	<i>38</i>
<b>3.2.2 Protein biochemical methods.....</b>	<b>40</b>
<i>3.2.2.1 Determination of protein concentration (Bradford assay).....</i>	<i>40</i>
<i>3.2.2.2 TCA precipitation of proteins.....</i>	<i>40</i>
<i>3.2.2.3 Chloroform-Methanol precipitation of proteins.....</i>	<i>41</i>
<i>3.2.2.4 SDS-polyacrylamide gel electrophoresis.....</i>	<i>41</i>

3.2.2.5 Western Blot .....	42
3.2.2.6 Coomassie staining of polyacrylamide gels .....	43
3.2.2.7 Biotinylation of cell surface proteins .....	43
3.2.2.8 Gelatin zymography assay .....	44
3.2.3 Cell biology methods .....	44
3.2.3.1 Cell culture .....	44
3.2.3.2 Trypsinizing adhesive cells .....	44
3.2.3.3 Subculture adhesive cells .....	45
3.2.3.4 Freezing cells .....	45
3.2.3.5 Thawing cells .....	45
3.2.3.6 Transfect cells with lipofectamine 2000 .....	45
3.2.3.7 Transfect cell with DEAE-Dextran reagent .....	46
3.2.3.8 Selection of stable transfectants .....	46
3.2.4 Methods for analysis of ectodomain shedding .....	46
3.2.4.1 General procedures .....	46
3.2.4.2 Handling of secretion medium .....	48
3.2.4.3 Handling of cells .....	48
3.3 Data analysis .....	48
4. Result .....	49
4.1 Overexpression of myc-RAGE or wild-type RAGE in Flp-In 293 cells as well as COS-7 cells .....	49
4.2 Human soluble RAGE is released from the cell membrane .....	50
4.2.1 Cleavage products of full-length RAGE .....	50
4.2.2 Glycosylation of secreted RAGE (sRAGE) .....	51
4.2.3 Full-length human RAGE is cell surface associated and the cleavage of RAGE occurs at the plasma membrane .....	51
4.3 Proteolysis of RAGE is both constitutive and regulated .....	52
4.3.1 Constitutive and PMA stimulated shedding of RAGE .....	53
4.3.2 APMA stimulated shedding of RAGE .....	53
4.3.3 Calcium ionophore stimulated shedding of RAGE .....	54
4.3.4 PD98059 does not affect shedding of RAGE whereas Chelerythrine enhances shedding of RAGE .....	56
4.4 The cleavage of RAGE is unaffected by several different proteases inhibitors .....	57
4.5 Shedding of RAGE is inhibited by metalloproteinase inhibitors .....	60
4.6 ADAM10 and ADAM17 are not essential for constitutive or stimulated shedding of RAGE .....	63
4.7 Overexpression of MT1-MMP does not affect constitutive and stimulated shedding of RAGE .....	68
4.8 Shedding of RAGE by MMP9 .....	69
4.8.1 MMP9 zymography assay .....	69
4.8.2 Enhancement of shedding of RAGE via overexpression of MMP9 .....	71
4.8.3 Knockdown of MMP9 expression by RNAi reduces constitutive and PMA-stimulated shedding of RAGE .....	73
4.8.3.1 Efficient suppression of MMP9 expression in MMP9-COS-7 cells as well as in myc-RAGE-Flp-In 293 cells by a RNAi strategy .....	74
4.8.3.2 MMP9 silencing severely reduces shedding of RAGE .....	75
4.9 The cytoplasmic domain of RAGE is not essential for constitutive and PMA stimulated shedding of RAGE .....	78
4.9.1 Deletion of cytoplasmic domain does not abrogate ectodomain shedding of RAGE .....	78
4.9.2 RAGE deleted of its cytoplasmic domain is membrane-anchored and proteolysed at the cell surface .....	79
4.10 Analysis of the RAGE cleavage site .....	81
5. Discussion .....	83
5.1 Human soluble RAGE is glycosylated and is generated by proteolysis .....	83

<b>5.2 Several stimuli can stimulate the release of soluble RAGE</b> .....	85
<b>5.3 RAGE shedding seems to be PKC and MAPK independent</b> .....	86
<b>5.4 The cleavage of RAGE is mediated by a metalloproteinase</b> .....	87
<b>5.5 The cleavage of RAGE is not sequence specific</b> .....	90
<b>5.6 The cytoplasmic domain of RAGE is not essential for shedding and membrane localization of RAGE</b> .....	91
<b>5.7 Significance of RAGE shedding</b> .....	92
<b>6. Summary</b> .....	94
<b>Reference</b> .....	95
<b>Abbreviations</b> .....	108
<b>Index of Tables and Figures</b> .....	109
<b>Acknowledgments</b> .....	<b>Error! Bookmark not defined.</b>
<b>Curriculum Vitae</b> .....	<b>Error! Bookmark not defined.</b>

## 1. Introduction

### 1.1 The A $\beta$ peptide

#### 1.1.1 A $\beta$ peptide production and its pathologic role in Alzheimer's disease (AD)

AD is a neurodegenerative disease and is the most prevalent cause of dementia. AD affected individuals develop a gradual and progressive decline in cognitive and functional abilities as well as behavioral and psychiatric symptoms leading to a vegetative state and ultimately death (Tanzi 1999). The presence of senile plaques and intracellular neurofibrillary tangles are main neuropathological hallmarks of AD (Selkoe 2001a). The primary constituents of the senile plaques are heterogenous, 39-43 amino acid peptides, the amyloid  $\beta$  peptides (A $\beta$  peptides). A $\beta$  peptides are generated by the sequential proteolytic processing of its precursor, the amyloid precursor protein (APP), by  $\beta$  and  $\gamma$ -secretases (Gandy 2005). APP processing follows two competing pathways: the amyloidogenic pathway and the non-amyloidogenic pathway. In the brain, the non-amyloidogenic pathway is mediated by  $\alpha$ -secretase which generates sAPP $\alpha$  (soluble APP $\alpha$ ) and the C-terminal fragment- $\alpha$  (CTF- $\alpha$ , also known as C83). After subsequent cleavage of C83 by  $\gamma$ -secretase a truncated non-toxic peptide (named P3) is generated. Therefore, the non-amyloidogenic pathway precludes A $\beta$  peptide formation. In contrast, the amyloidogenic pathway is initiated by cleavage at Asp1 of the A $\beta$  sequence mediated by  $\beta$ -secretase and generates sAPP $\beta$  (soluble APP $\beta$ ) and a unique C-terminal membrane-retained fragment, termed CTF- $\beta$  (or C99). Subsequent cleavage of CTF- $\beta$  by  $\gamma$ -secretase results in the production of A $\beta$  peptides and an intracellular product named APP Intracellular Domain (AICD). AICD is very short lived and has been identified only recently (Cao and Sudhof 2001). The generation of A $\beta$  peptides from APP is illustrated in Figure 1.

According to the amyloid cascade hypothesis (Hardy and Higgins 1992), which states that the development of AD is due to abnormal accumulation of A $\beta$  in the brains of AD patients causing neurodegeneration and finally the clinical symptoms of dementia, A $\beta$  is considered to play a central role in the pathogenesis of AD. First of all, A $\beta$  is directly toxic to cultured neurons because of its ability to generate reactive oxygen species in solution and produce an accumulation of H<sub>2</sub>O<sub>2</sub> and lipid peroxides in the cells (Behl *et al.* 1994). Secondly, A $\beta$  is also a potent inducer of the transcription factor, NF- $\kappa$ B, in primary neurons and astrocytes (Kaltschmidt *et al.* 1997). Thirdly, being chemotactic, A $\beta$  causes migration of microglia, thereby contributing to an increased accumulation of microglial cells surrounding the amyloid plaques (Klegeris *et al.* 1994). Finally, A $\beta$  was found to potentiate cytokine secretion (IL-6 and IL-8) in IL-1 $\beta$ -activated human astrocytoma cells (Gitter *et al.* 1995). The predominant forms of A $\beta$  are the A $\beta$ 40 and A $\beta$ 42

fragments. Soluble A $\beta$ 40 is the major form of circulating A $\beta$  and cerebrovascular amyloid, whereas amyloidogenic A $\beta$ 42, the major constituent of senile plaques, accounts for minor amounts in the circulation (Giri *et al.* 2002). The origin of the A $\beta$  deposited in cerebral vasculature and brain is uncertain. According to the “neuronal theory”, A $\beta$  is produced locally in brain. In contrast, the “vascular theory” proposes that A $\beta$  originates from the entire body, and that circulating soluble A $\beta$  can contribute to neurotoxicity if it crosses the blood–brain-barrier (BBB) (Zlokovic 1997).

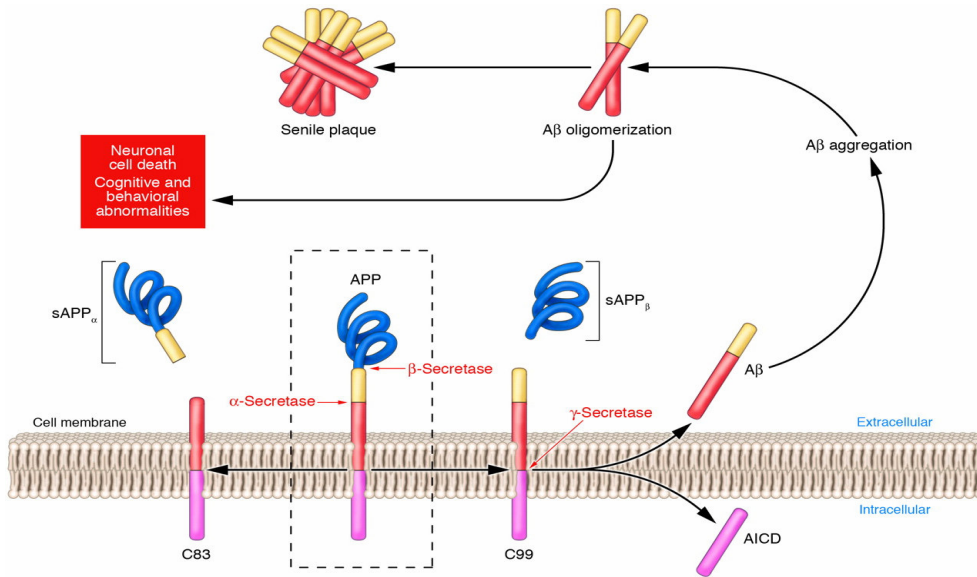


**Figure 1. Processing of APP and consequential accumulation of A $\beta$ .**

Processing of APP occurs *in vivo* by two competitive pathways. The non-amyloidogenic pathway is mediated by  $\alpha$ -secretase, resulting in release of sAPP $\alpha$ ; while the amyloidogenic pathway involves sequential cleavage by  $\beta$ -secretase and  $\gamma$ -secretase, releasing intracellular fragment AICD and A $\beta$  ranging in length from 39 to 43 amino acids. A $\beta$  is prone to aggregation and accumulated as oligomers, which are most toxic and contribute to AD pathogenesis. (From Gandy 2005)

### 1.1.2 A $\beta$ peptide clearance from the brain

The life-long accumulation of A $\beta$  in the brain is determined by the rate of A $\beta$  generation versus A $\beta$  clearance. Strategies to treat AD have focused on both decreasing the production of A $\beta$  and enhancing its clearance from the brain. Clearance can be accomplished via two major pathways: proteolytic degradation and receptor-mediated export from the brain.

Degradation of A $\beta$  in the central nervous system (CNS) could play an important role in clearance (Iwata *et al.* 2001). The proteases capable of degrading A $\beta$ , e.g. neprilysin, insulin-degrading enzyme (insulysin), plasmin, tissue plasminogen activator,

endothelin-converting enzyme and matrix metalloproteinase-9, have been recently reviewed (Selkoe 2001b).

A $\beta$  lowering strategies based on receptor mediated-A $\beta$  transport has just recently begun to receive more attention (Figure 2). Increasing lines of evidence suggest that the low-density lipoprotein receptor-related protein (LRP) and the receptor for advanced glycation end products (RAGE) are involved in receptor-mediated flux of A $\beta$  across the BBB (Zlokovic 2004). While LRP appears to mediate the efflux of A $\beta$  from the brain to the periphery, RAGE is implicated in A $\beta$  influx back into the CNS. In addition, evidence also exists to suggest that 10-15% of A $\beta$  can enter into the cerebral spinal fluid (CSF) from the brain interstitial fluid and onward into the blood stream (Shibata *et al.* 2000).

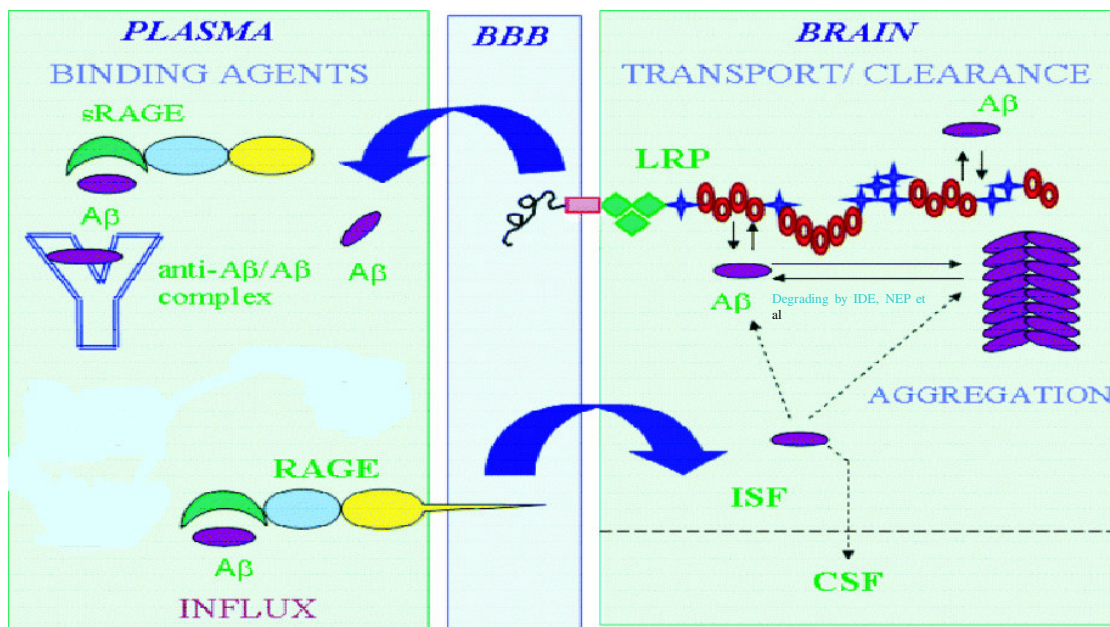


**Figure 2. Transport-clearance model for A $\beta$  regulations in the brain.**

(1) Transport-mediated clearance of A $\beta$  across the BBB and via the interstitial fluid (ISF)/cerebrospinal fluid (CSF) route: LRP mediates rapid A $\beta$  transport across the BBB out of the CNS. Soluble A $\beta$  can also be removed slowly via the ISF bulk flow into the CSF and from there into the bloodstream. (2) Transport of plasma-derived A $\beta$  across the BBB: RAGE mediates influx of free, unbound circulating A $\beta$  across the BBB into the CNS. (3) A $\beta$  plasma binding agents such as anti-A $\beta$  IgG, gelsolin and/or GM1, or sRAGE can sequester A $\beta$  in plasma, thus reducing its influx across the BBB. (Modified from Zlokovic, 2004)

RAGE was identified as human BBB receptors for A $\beta$ 40 in 1998 (Mackic *et al.* 1998). Moreover, recently it was found that RAGE contributes to the transport of A $\beta$  into the CNS and furthermore, recombinant soluble RAGE (sRAGE) reduced accumulation of A $\beta$  in brain parenchyma of transgenic APP mice (Deane *et al.* 2003). Transportation of circulating A $\beta$  into the brain results in expression of proinflammatory cytokines in neurovascular cells and elaboration of endothelin-1, causing decreased cerebral blood flow. Besides RAGE, gp330/megalin may also transport circulating A $\beta$  in a complex with apoJ (Zlokovic *et al.* 1996). However, gp330/megalin is normally saturated by high levels of plasma apoJ which precludes significant influx of A $\beta$  into the CNS under physiological conditions. This leaves RAGE as a probable major influx receptor for A $\beta$  at the BBB.

## **1.2 RAGE (receptor for advanced glycation end products)**

### **1.2.1 Structure**

RAGE was first identified as a cell surface receptor for the products of nonenzymatic glycation and oxidation of proteins, the advanced glycation end products (AGEs). The RAGE gene was cloned and characterized from mouse lung in 1992 (Neeper *et al.* 1992). Later the RAGE gene was located on chromosome 6p21.3 in a gene-rich region containing a number of inflammatory genes and components of the major histocompatibility complex (MHC) (Sugaya *et al.* 1994).

Human RAGE gene encodes a type I transmembrane protein of 404 amino acids (Srikrishna *et al.* 2002), composed of an extracellular domain with 344 amino acids, a transmembrane domain with 19 residues and a cytosolic domain with 43 amino acids (Figure 3). The large extracellular domain of RAGE contains a N-terminal signal sequence of 22 amino acids and three immunoglobulin (Ig)-like regions, which define RAGE protein as a member of the immunoglobulin superfamily. These Ig-like regions include one “V”-type domain (IgV sequence from residue 41 to residue 126) followed by two “C”-type domains (IgC sequence from residue 127 to residue 234 and IgC’ from residue 235 to residue 344). The “V”-type domain confers ligand binding and contains two putative N-glycosylation sites. Deglycosylation was shown to affect RAGE binding of certain ligands (Srikrishna *et al.* 2002). The shorter cytoplasmic domain shows greatest identity to the B-cell activation marker CD20 and is critical for signaling downstream of receptor-ligand interaction. Furthermore, RAGE shares significant homology with MUC18, a glycoprotein which also belongs to the immunoglobulin superfamily and with neural cell adhesion molecule (NCAM). (Neeper *et al.* 1992; Schmidt *et al.* 1992; Schmidt *et al.* 1994).



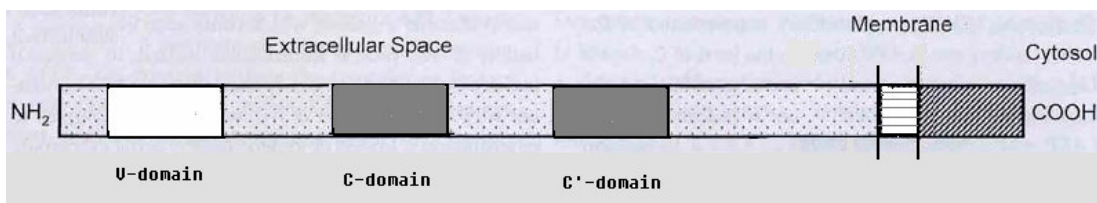


**Figure 3. Structure of Receptor for advanced glycation end products.**

The large extracellular domain of RAGE contains an N-terminal signal sequence and three Ig-like regions including one “V”-type domain followed by two “C”-type domains. The “V”-type domain confers ligand binding and contains two putative N-glycosylation sites. The short cytoplasmic domain is critical for downstream signaling.

### 1.2.2 Expression patterns

RAGE transcription is controlled by several transcription factors, including SP-1, AP-2, NF- $\kappa$ B, and NF-IL6 (Li and Schmidt 1997). During development, RAGE is highly expressed in the nervous system such as in the developing embryonic rat brain (Hori *et al.* 1995; Sakaguchi *et al.* 2003). In striking contrast, in mature animals there is relatively little expression of RAGE in most tissues except lung and skin. At the cellular level, RAGE is expressed in a variety of cell types, including endothelial, vascular smooth muscle, mononuclear phagocytes, microglial cells, astrocytes and neuronal cells (Brett *et al.* 1993). RAGE expression is highly up-regulated frequently under pathological conditions such as diabetic vascular disease, chronic inflammation, Alzheimer’s disease and tumors (Bucciarelli *et al.* 2002). In conclusion, RAGE is expressed in both constitutive and inducible manner, depending on the cell type and pathophysiologic conditions.

### 1.2.3 Extracellular ligands and their pathophysiologic functions

RAGE was first identified as a cell surface receptor for AGEs. In addition to AGEs, it has become evident that a variety of ligands with diverse structural features also interact with RAGE. These ligands include: Amphoterin (also known as high mobility group I DNA-binding protein, HMG-1), amyloid- $\beta$  peptide, amyloid A and S100/calgranulins. RAGE also interacts with surface molecules on bacteria, prions, and leukocytes (Bierhaus *et al.* 2005). The engagement of RAGE by its ligands contributes to various pathologic processes ranging from proinflammatory responses, accelerated diabetic atherosclerosis, Alzheimer’s disease to tumor cell invasion (Schmidt *et al.* 2001) (Table 1).

On the other hand, RAGE also has physiological functions. As judged from the expression patterns of RAGE described in 1.2.2, it is reasonable to assume that RAGE could play roles in development. Indeed, a few reports have suggested that RAGE might contribute to the development of the CNS. For instance, amphoterin can bind RAGE and contribute to axonal sprouting which accompanies neuronal development (Hori *et al.* 1995). Recently, RAGE was shown to promote neurite outgrowth in vivo in a unilateral sciatic nerve crush model and the trophic effects could be blocked by sRAGE or antibodies against either RAGE or amphoterin, thus confirming the neurotrophic functions of RAGE (Rong *et al.* 2004). These results are in accord with the fact that RAGE is expressed at a high level in the nervous system during development (Hori *et al.* 1995). However, RAGE null mice develop normally, live a natural life span, and are fertile (Bierhaus *et al.* 2004), indicating that RAGE may contribute to the development of nervous system, but redundant molecules can compensate for the loss of RAGE.

Another recent study revealed the possibility of an involvement of RAGE in the regulation of differentiation (Bartling *et al.* 2005). In this context, down-regulation of RAGE may be considered as a critical step in tissue reorganization and the formation of lung tumors. Considering that lung is one of the few tissues in which RAGE is constitutively expressed at high levels, we can suppose that in normal lung tissues RAGE can keep cells in the differentiated state and inhibits tumor genesis. Upon down-regulation of RAGE, cells may become undifferentiated and tumor growth may ensue. Undoubtedly, further experiments are needed to confirm whether RAGE indeed regulates cell differentiation.

**Table 1. Ligands for RAGE and their associated pathophysiologic roles**

Ligands for RAGE	Ligand property	Pathophysiologic impact
Advanced glycation end products (Neeper <i>et al.</i> 1992) (e.g., CML-adducts)	Non-enzymatically glycated adducts	Diabetes, renal failure, amyloidoses, inflammation, oxidant stress, aging, neurodegenerative disorders
Amyloid- $\beta$ peptide & $\beta$ -sheet fibrils (Yan <i>et al.</i> 1996)	Main constituent of the senile plaques and cerebrovascular deposits in Alzheimer's disease	Alzheimer's disease amyloidosis
S100/calgranulins (Hofmann <i>et al.</i> 1999)	proinflammatory cytokine-like mediators	Development, inflammation, tumors, neurodegenerative disorders
Amphoterin (Hori <i>et al.</i> 1995)	DNA binding protein	Development, neurite outgrowth inflammation, tumors

### 1.2.4 Intracellular signaling

As a transmembrane receptor, the engagement of RAGE by its ligands has been reported to trigger intracellular signaling pathways (Figure 4). In most cases, RAGE induces the activation of the immune/inflammatory-associated transcription factor, nuclear factor  $\kappa$ B (NF- $\kappa$ B). Notably, the human RAGE promoter contains two NF- $\kappa$ B responsive elements (Li and Schmidt 1997) that act to form a positive feedback loop such that RAGE is up-regulated where its ligands are present. In addition to NF- $\kappa$ B, RAGE can induce a range of signal transduction pathways including activation of small GTPases like Cdc42 and Rac (Huttunen *et al.* 1999), mitogen-activated protein kinase (MAPK) and c-Jun N-terminal kinase (Taguchi *et al.* 2000) and extracellular signal-regulated kinases 1 and 2 (Simm *et al.* 1997), as well as activation of the cAMP response element-binding factor (Huttunen *et al.* 2002). The diversity of signaling cascades identified in RAGE-mediated cellular signaling implies that different RAGE ligands might induce different pathways and thus make the RAGE network more complicated. Although a number of reports suggested that the cytoplasmic domain of RAGE is essential for intracellular signaling, a challenging task will be to elucidate the exact bridging molecules that engage the cytoplasmic domain of RAGE upon activation of the receptor.

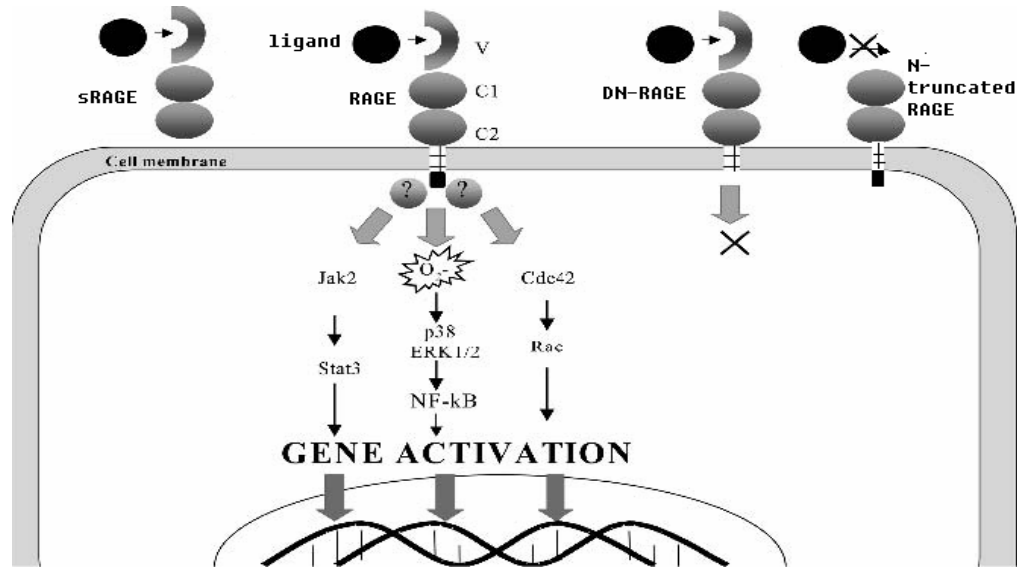


**Figure 4. RAGE signaling pathways.**

RAGE is activated upon binding to ligands via the extracellular V-type domain. This leads to recruitment of unidentified cytoplasmic proteins to the intracellular domain of RAGE and activation of numerous downstream signaling proteins such as stat3, ERK and Rho, which consequently activate gene transcription. RAGE isoforms including sRAGE, dominant negative RAGE (DN-RAGE) and N-truncated RAGE that lack either V-type domain or the intracellular domain are unable to mediate RAGE signaling and have potential to block harmful effects mediated by RAGE signaling. Modified from (Hudson and Schmidt 2004).

### 1.2.5 RAGE-A $\beta$ interaction

It has been demonstrated that expression of RAGE is increased in AD patients and furthermore, expression of RAGE was colocalized with that of A $\beta$  in human AD brain tissues, in neurons, microglia and vascular elements (Yan *et al.* 1996; Yan *et al.* 1998), thus indicating the possibility of a RAGE/A $\beta$  interaction in pathogenesis of AD. It has been suggested that RAGE may be the nerve cell receptor for A $\beta$  (Yan *et al.* 1997; Li *et al.* 1998; Du *et al.* 1997). Indeed, RAGE binds soluble A $\beta$  in a dose-dependent manner in the nanomolar range (Yan *et al.* 1996). Studies using an in vitro model of the human BBB showed that RAGE mediated the binding of soluble A $\beta$ 1–40 at the apical side of brain capillary endothelium and RAGE was also involved in soluble A $\beta$ 1–40 transcytosis (Mackic *et al.* 1998). In addition, it has been demonstrated in an animal model that RAGE mediates transport of pathophysiologically relevant concentration of plasma A $\beta$  across the BBB, while deletion of the RAGE gene protects the A $\beta$  CNS pool from influences of its peripheral pool by eliminating transport of free circulating A $\beta$  into the brain (Deane *et al.* 2003).

Indeed, transport of circulating A $\beta$  into the brain results in expression of proinflammatory cytokines in neurovascular cells and elaboration of endothelin-1, causing decreased cerebral blood flow. Because of the presence of two NF- $\kappa$ B responsive elements in the human RAGE promoter, RAGE-A $\beta$  interaction might induce a possible feedback loop. Thereby, A $\beta$ -induced oxidant stress activates NF- $\kappa$ B which subsequently binds to the RAGE promoter and upregulates RAGE expression. The interaction of RAGE with A $\beta$  is followed by a series of intracellular activities that may trigger inflammatory pathways, which could contribute to the progression of AD (Du *et al.* 1997). Furthermore, a mouse model was developed to assess the impact of RAGE in an A $\beta$ -rich environment by employing transgenic mice with targeted neuronal overexpression of RAGE or DN-RAGE. Double transgenic mice of RAGE and mutant APP displayed early abnormalities in spatial learning/memory, accompanied by altered activation of markers of synaptic plasticity and exaggerated neuropathologic findings, before such changes were found in mutant APP mice. In contrast, double transgenic mice bearing mutant DN-RAGE and APP displayed preservation of spatial learning/memory and diminished neuropathologic changes. These data strongly indicate that RAGE is a cofactor for A $\beta$ -induced neuronal pathology in AD models and suggest its potential as a therapeutic target to ameliorate dysfunction associated with AD (Arancio *et al.* 2004).

## 1.2.6 Isoforms of RAGE

It is important to be aware of that there are 3 major different forms of RAGE (Figure 5). These isoforms can be defined as the full-length RAGE, soluble RAGE (sRAGE) and C-terminal truncated RAGE (C-truncated RAGE).

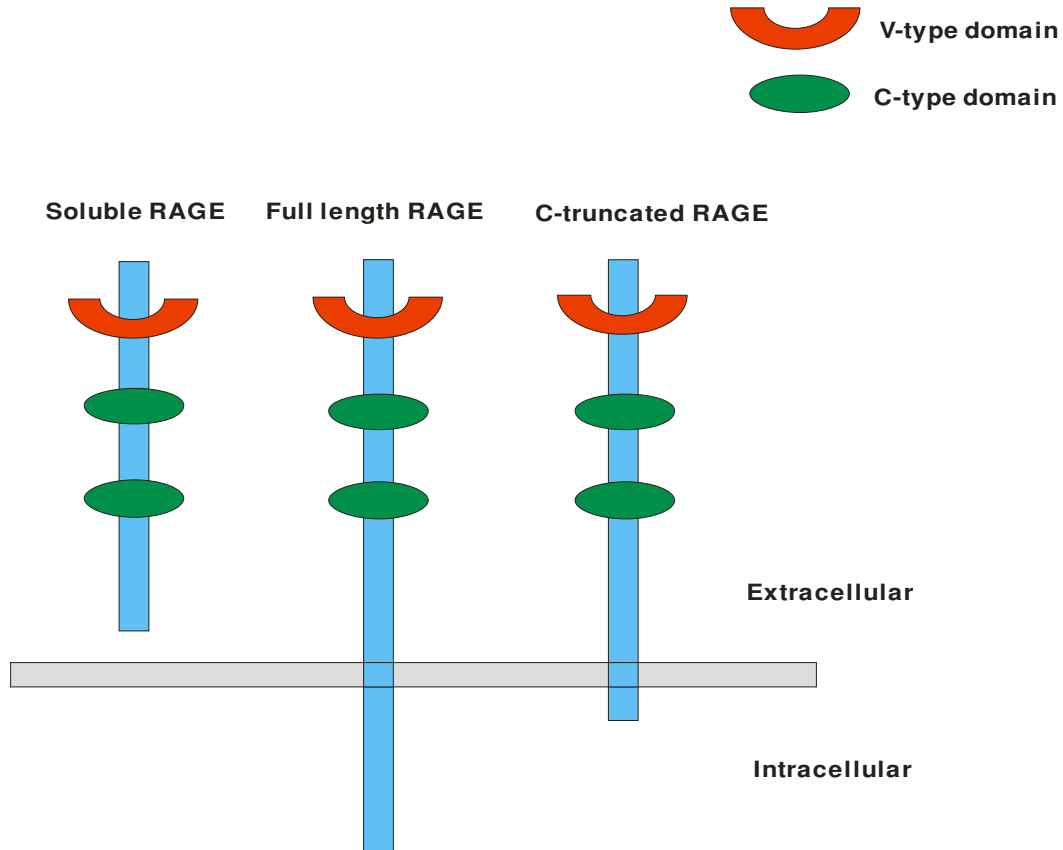


**Figure 5. Multiple isoforms of RAGE.**

There are 3 major isoforms of RAGE including full-length RAGE, soluble RAGE and C-terminal truncated RAGE (C-truncated RAGE). The existence of these 3 isoforms suggests that the ability of any RAGE ligands to induce RAGE signaling depends on the coordinated effects of different RAGE isoforms. (Adapted from Ding and Keller, 2005)

### 1.2.6.1 Full-length RAGE

Among the 3 major isoforms of RAGE full-length RAGE is by far the most studied. The structure and function of full-length RAGE has been described in detail in part 1.2.1-1.2.5.

### ***1.2.6.2 C-terminal truncated RAGE***

C-terminal truncated RAGE contains the extracellular and transmembrane domain of RAGE, but lacks the C-terminal intracellular domain important for signal transduction. Therefore, by competing for the binding of RAGE ligands recombinant C-terminally truncated RAGE prevents the activation of full-length RAGE. For this reason C-terminally truncated RAGE is also named dominant negative RAGE (DN-RAGE) (Yan *et al.* 1996). Recently, it was shown that the expression level of DN-RAGE in the human brain is similar to that of full-length RAGE (Ding and Keller 2005b). Unfortunately, it is still unknown whether or/and how the ratio of full-length RAGE versus DN-RAGE is changed under different physiological or pathological conditions. Since a number of RAGE ligands such as AGE and A $\beta$  have devastating effects on cells, binding of these ligands to DN-RAGE would lead to diminished binding to full-length RAGE and consequently, less deleterious effects mediated by full-length RAGE.

But it is important to keep in mind that although engagement of harmful ligands by DN-RAGE may be beneficial during the initial periods of ligand binding, the long term effects may be less advantageous. This is based on the supposition that the engagement of the ligands at the cell surface by DN-RAGE may lead to the initiation of further ligand recruitment, oxidation, and aggregation, which unfavorably enhances the activation of full-length RAGE (Ding and Keller 2005a). Of course further experimentation is decisive to test whether the above supposition is true or not. It is undisputed that a detailed understanding of the regulation of DN-RAGE generation is crucial to evaluate DN-RAGE as a target to modulate signaling mediated by full-length RAGE.

### ***1.2.6.3 Soluble RAGE (sRAGE)***

The soluble form of RAGE contains only the extracellular domain of RAGE, while lacking the transmembrane and the cytoplasmic domains. Thereby, sRAGE is released from the cell surface into the extracellular space as a soluble form.

#### **1.2.6.3.1 Functional significance of sRAGE**

Lack of the transmembrane domain renders sRAGE serving as a decoy for the ligands and blocking signaling by preventing ligands from gaining access to full-length RAGE. Furthermore, recombinant sRAGE is able to block or reduce RAGE mediated pathological situation. Use of recombinant sRAGE has been shown to prevent diabetic atherosclerosis (Park *et al.* 1998), reduce diabetic late complications (Goova *et al.* 2001), inhibit tumor metastases and invasion (Taguchi *et al.* 2000) and block transport of A $\beta$  across BBB (Deane *et al.* 2003). However, it is important to note that sRAGE provides a decoy strategy, i.e., sRAGE sequesters ligands and prevents their interaction with RAGE and, potentially, other receptors as well. So it is imperative to investigate

whether sRAGE has any inhibitory effects on normal functions of other receptors before therapy based on sRAGE can be implemented.

#### 1.2.6.3.2 Generation of sRAGE

Soluble forms of membrane-associated receptors can be generated via two distinct pathways. The first involves the alternative splicing of mRNA transcripts that usually encode membrane-associated receptors. Alternative splicing is an important way to generate soluble forms of cell surface receptor, examples include the TGF- $\beta$  receptor family (T $\beta$ R-I, activin receptor-like kinase 7) (Choi 1999), the TNFR superfamily (TNFRSF6/Fas/CD95, TNFRSF9/4-1BB/CD137) (Michel *et al.* 1998), and the IL-17R (Haudenschild *et al.* 2002).

By far several different alternatively spliced RAGE mRNA encoding secretory proteins have been reported (Yonekura *et al.* 2003; Schlueter *et al.* 2003; Park *et al.* 2004; Malherbe *et al.* 1999; Ding and Keller 2005b) and they are summarized in Table 2.

**Table 2. Splicing forms of RAGE**

RAGE Splicing forms	Tissue or cell types	Existing forms	References
Full-length RAGE	Human EC, pericyte	cell surface associated RAGE	Yonekura <i>et al.</i> 2003
	Human lung, lymph node, breast cancer, myometrium, fibroblasts, Hela cell		Schlueter <i>et al.</i> 2003
hRAGEsec	Human fetal lung	soluble	Malherbe <i>et al.</i> 1999
sRAGE1,sRAGE2,sRAGE3	Human lung, lymph node, breast cancer, myometrium, fibroblasts, Hela cell	soluble	Schlueter <i>et al.</i> 2003
C-truncated RAGE	Human EC, pericyte	soluble	Yonekura <i>et al.</i> 2003
N-truncated RAGE	Human EC, pericyte	cell surface associate RAGE	Yonekura <i>et al.</i> 2003
NtRAGE $\Delta$ ,sRAGE $\Delta$ ,sRAGE	Human brain	soluble	Ding and Keller 2005b
NtRAGE, RAGE $\Delta$	Human brain	cell surface associate RAGE	Ding and Keller 2005b

Although nearly all of the data implicated that sRAGE is derived from alternative splicing of RAGE mRNA, most recent evidence indicated that sRAGE in mice may be generated as the result of protein cleavage instead of splicing (Hanford *et al.* 2004). Actually, proteolysis based ectodomain shedding might be the second pathway that contributes to the production of sRAGE.

#### **1.2.6.4 N-truncated RAGE**

The least discussed RAGE isoform is N-truncated form, which is derived from splicing variants of RAGE mRNA that encode proteins that lack the N-terminal V-type Ig-like domain and is retained in the plasma membrane (Yonekura *et al.* 2003; Ding and Keller 2005a). As a result of the deletion of the V-type Ig domain, N-truncated RAGE is significantly impaired in its ability to bind RAGE ligands. However, the functional significance of N-truncated RAGE remains elusive.

### **1.3 Protein Ectodomain Shedding**

#### **1.3.1 Ectodomain shedding**

The extracellular domains of various cell surface proteins are released through proteolytic cleavage. This type of proteolysis occurs at or near the plasma membrane and has been known as ectodomain shedding (Arribas and Borroto 2002). The shedding of cell surface proteins can occur either in non-stimulated cells (known as constitutive shedding) or activated by several independent mechanisms (known as stimulated shedding) (Arribas and Borroto 2002). Stimulants which can induce shedding include phorbol esters (Lammich *et al.* 1999), calcium ionophores (Sanderson *et al.* 2005) and serum factors (Hirata *et al.* 2001). Ectodomain shedding event has been observed for a surprisingly large number of cell surface proteins with distinct functions. Targets of this process include cytokines and cytokine receptors (CD44,IL15R $\alpha$ ) (Nakamura *et al.* 2004; Kajita *et al.* 2001; Budagian *et al.* 2004), growth factors (proTNF- $\alpha$ ,proTGF- $\alpha$ ) (Black *et al.* 1997; Peschon *et al.* 1998), adhesion molecules (L1)(Mechtersheimer *et al.* 2001), enzymes (ACE) (Parkin *et al.* 2003), and proteins associated with neuropathological disorders (APP, cellular prion protein) (Allinson *et al.* 2004; Cisse *et al.* 2005) (summarized in Table 3).

It appears increasingly apparent that proteolytic shedding of cell surface proteins is an important cellular post-translational regulatory process. Soluble shed proteins commonly consist of the extracellular portions or ectodomains of their membrane-bound precursors and thereby retain the ability to bind ligands. They may further serve to affect the nature of cell signaling events by acting as antagonists, carrier molecules or chaperones to protect the ligands from binding to membrane-bound proteins (Mortier *et al.* 2004), and in some cases act as biological agonists (Vollmer *et al.* 1996). Cleavage of various membrane proteins contributes to mitogenesis, cell migration, differentiation, and various diseased states such as inflammation, tumorigenesis, spongiform encephalopathies, and Alzheimer's disease (Hooper *et al.* 1997). Thus, ectodomain shedding can potentially regulate most cellular functions mediated by transmembrane proteins and, therefore, has attracted more and more attention.



**Table 3. Examples of proteins undergoing ectodomain shedding and the corresponding sheddases**

	proteins		sheddases	reference
Transmembrane growth factors and cytokines	proTNF $\alpha$ (tumor necrosis factor- $\alpha$ )		TACE , ADAM19	Black et al. 1997; Moss et al. 1997
	proTGF $\alpha$ (transforming growth factor- $\alpha$ )		TACE	Peschon et al. 1998
	pro-HB-EGF(Heparin-binding EGF-like growth factor)		ADAM9 , ADAM10, ADAM12, TACE	Higashiyama and Nanba 2005
	IGFBP-3 (insulin growth factor binding protein-3)		ADAM12-S	Loechel <i>et al.</i> 2000
Membrane receptors	p75NTR (p75 neurotrophin receptor)		TACE	Weskamp <i>et al.</i> 2004
	Notch		ADAM10 , TACE	Vooijs <i>et al.</i> 2004
	IL-6R $\alpha$		TACE	Vollmer et al. 1996
	CD30		TACE	Hansen <i>et al.</i> 2004
Adhesion molecules	L-Selectin		TACE	Smalley and Ley 2005
	L1		ADAM10	Mechtersheimer et al. 2001
	VCAM		TACE	Garton <i>et al.</i> 2003
	CX3CL1 (fractalkine)		ADAM10,TACE	Hundhausen <i>et al.</i> 2003; Garton <i>et al.</i> 2001
	CD44		MT1-MMP	Kajita <i>et al.</i> 2001
proteins associated with neuropathological disorders	APP		ADAM10 , TACE,	Allinson <i>et al.</i> 2004
	Prion protein		ADAM9	Cisse <i>et al.</i> 2005
	ACE, ACE2		No identified	

### **1.3.2 Proteases involved in Ectodomain shedding**

Proteases which are responsible for mediating ectodomain shedding are denoted as “sheddases” or “secretases” and appear to be members of the metzincin superfamily of zinc-dependent proteases including ADAMs and MMPs.

#### ***1.3.2.1 A disintegrin and metalloproteinases (ADAMs)***

ADAMs are type-I transmembrane proteins that contain a disintegrin-like and a metalloproteinase-like domain. Up to date, 33 ADAMs have been identified. ADAMs have been implicated in most of the known shedding events (Seals and Courtneidge 2003; Black and White 1998; Schlondorff and Blobel 1999; Primakoff and Myles 2000; Kheradmand and Werb 2002). ADAM17, also known as TACE (tumor necrosis factor- $\alpha$  converting enzyme) was the first protease shown to be responsible for shedding events. A number of diverse cell surface proteins including APP, TNF- $\alpha$ , TNFRs I and II, TGF- $\alpha$ , L-selectin, IL-6R, CD30, growth factor receptor, and others undergo proteolysis mediated by TACE. Other members of the ADAM family of proteinases, particularly ADAM9, ADAM10, and ADAM12, have been implicated as sheddases for a wide range of proteins such as APP, Pro-HB-EGF, CX3CL1 and Notch (Table 3). In addition to mediating ectodomain shedding, ADAMs play an important role in epithelial and neural development, fertilization, myoblast fusion, and cell-cell interactions.

#### ***1.3.2.2. Matrix metalloproteinases (MMPs)***

MMPs, also known as matrixins, are a large family of zinc-dependent metalloproteinases that degrade extracellular matrix and basement membrane components (Dzwonek *et al.* 2004). Till now, more than 20 endopeptidases have been classified as MMPs. Based on substrate specificity and the presence of distinct structural domains, MMPs are categorized into 6 subfamilies (Hartung and Kieseier 2000): collagenases, gelatinases, stromelysins, matrilysins, membrane type MMPs (MT-MMPs) and other MMPs (Table 4). The MMPs are homogeneous enzymes and share common structural elements. All members of this family contain a pro-domain and a catalytic domain. The pro-domain is cleaved upon activation while the catalytic domain contains the catalytic machinery including the zinc binding site and a conserved methionine. The metal ions maintain the three dimensional structure of MMPs and are necessary for stability and enzymatic activities. Additionally, fibronectin like repeats, transmembrane domains and C-terminus hemopexin-like domains are present in different groups of MMPs respectively. Table 4

summarizes the classifications of the MMPs and their substrate specificities. The architecture of MMPs is illustrated in Figure 6.

**Table 4. Category of MMPs and their substrates (adapted from Chakraborti *et al.* 2003)**

Enzyme	MMP	ECM substrate	Non ECM substrate
<b>Collagenases</b>			
Collagenase-1	MMP-1	Collagens (I, II, III, VII, VIII and X), gelatin, proteoglycans, aggrecan, versican, tenascin, entactin	$\alpha$ 1-PI, IL-1, pro-TNF, IGFBP-3, MMP-2, MMP-9
Collagenase-2	MMP-8	Collagens (I, II, III, V, VII, VIII and X), gelatin, aggrecan	$\alpha$ 1-PI, $\alpha$ 2-antiplasmin
Collagenase-3	MMP-13	Collagens (I, II, III, IV, IX, X, XIV), gelatin, aggrecan, perlecan, large tenascin-C, fibronectin, osteonectin	MMP-9, plasminogen activator inhibitor-2
Collagenase-4	MMP-18	ND	ND
<b>Gelatinases</b>			
Gelatinase A	MMP-2	Collagens (I, IV, V, VII, X, XI and XIV), gelatin, elastin, fibronectin, laminin-1, laminin-5, galectin-3, aggrecan, decorin, versican, proteoglycans, osteonectin	IL-1, $\alpha$ 1-PI, prolysin oxidase fusion protein, MMP-1, MMP-9, MMP-13
Gelatinase B	MMP-9	Collagens (IV, V, VII, X, and XIV), gelatin, elastin, galectin-3, aggrecan, fibronectin, versican, proteoglycans, entactin, osteonectin	$\alpha$ 1-PI, IL-1 $\beta$ , plasminogen
<b>Stromelysins</b>			
Stromelysin-1	MMP-3	Collagens (III, IV, V and IX), gelatin, aggrecan, versican, perlecan, decorin, proteoglycans, large tenascin-C, fibronectin, laminin, entactin, osteonectin	$\alpha$ 1-PI, antithrombin-III, ovosstatin, substance P, IL-1 $\beta$ , serum amyloid A, IGFBP-3, plasminogen, MMP-2/TIMP-2, MMP-7, -8, -9, -13
Stromelysin-2	MMP-10	Collagens (III, IV and V), gelatin, casein, aggrecan, elastin, proteoglycans	MMP-1, -8
Stromelysin-3	MMP-11	Casein, laminin, fibronectin, gelatin, collagen IV	$\alpha$ 1-PI, casein, IGFBP-1
<b>Membrane type MMPs</b>			
MT1-MMP	MMP-14	Collagens (I, II and III), casein, elastin, fibronectin, gelatin, laminin, vitronectin, large tenascin-C, entactin, proteoglycans	$\alpha$ 1-PI, MMP-2, -13
MT2-MMP	MMP-15	Large tenascin-C, fibronectin,	MMP-2

		laminin, entactin, aggrecan, perlecan	
MT3-MMP	MMP-16	Collagen-III, gelatin, casein, fibronectin	MMP-2
MT4-MMP	MMP-17	ND	ND
MT5-MMP	MMP-24	ND	ND
MT6-MMP	MMP-25	ND	ND
<b>Matrilysins and Others</b>			
Matrilysin-1 (Matrilysin)	MMP-7	Collagens IV and X, gelatin, aggrecan, decorin, fibronectin, laminin, entactin, large and small tenascin-C, osteonectin, $\beta$ 4 integrin, elastin, casein, transferrin	MMP-1, -2, -9 MMP-9/TIMP-1, $\alpha$ 1-Pi, plasminogen
Matrilysin-2	MMP-26	Collagen IV, gelatin, fibronectin	ProMMP-9, fibrinogen, $\alpha$ 1-Pi
Metalloelastase	MMP-12	Collagen IV, gelatin, elastin, casein, laminin, proteoglycan monomer, fibronectin, vitronectin, enactin	$\alpha$ 1-Pi, fibrinogen, fibrin, plasminogen, myelin basic protein
	MMP-19	Gelatin	ND
Enamelysin	MMP-20	Amelogenin	ND

Abbreviations:  $\alpha$ 1-Pi,  $\alpha$ 1-proteinase inhibitor; IGFBP, insulin-like growth factor binding protein; IL-1, interleukin-1; TNF, tumor necrosis factor; ND, not determined.

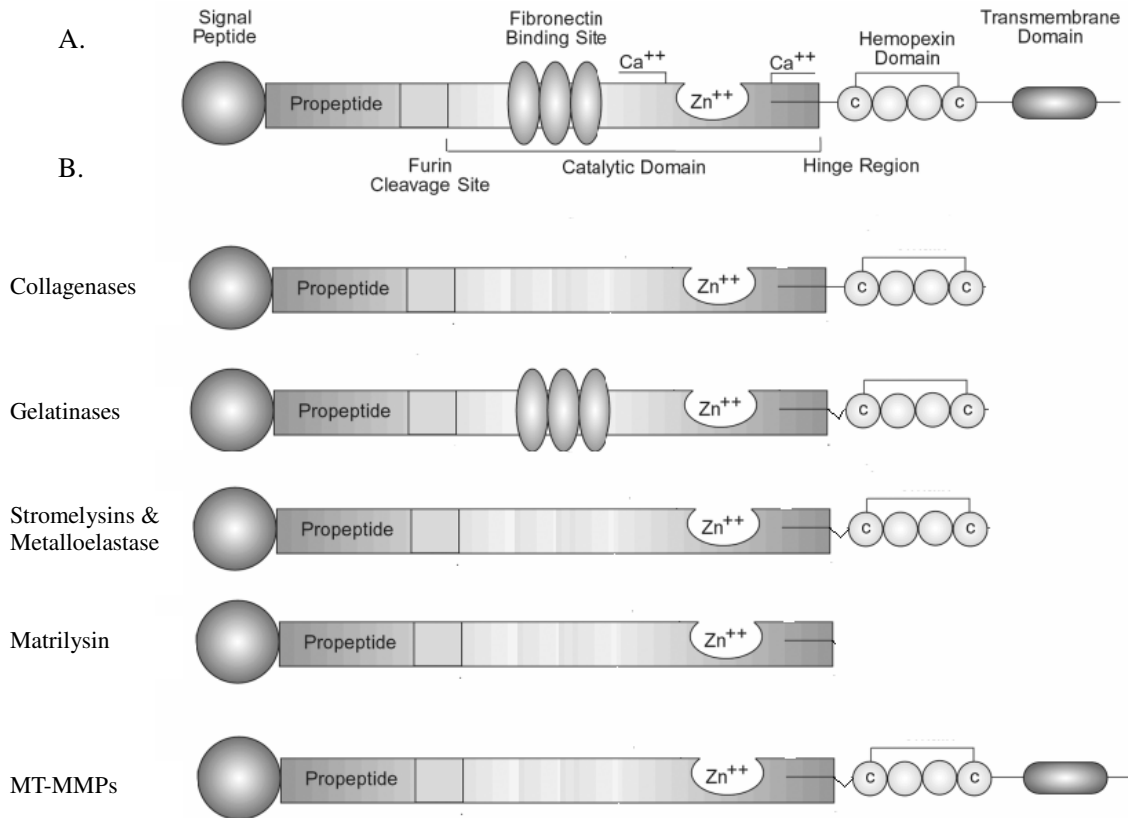


**Figure 6. Modular domain structures of MMPs.**

(A) Composite protein representing modular domains found in all kinds of MMPs. (B) Individual MMPs contain different combinations of the domains shown in (A). Of note is that all MMPs contain the signal peptide, a propeptide region, a furin cleavage site, as well as a catalytic domain with zinc and calcium ions. In addition, a fibronectin binding site is present in gelatinases and a transmembrane domain is present in MT-MMPs. A hemopexin domain is present in all MMPs except matrilysins.

MMPs have broad, but not necessarily overlapping substrate specificities. Because MMPs can degrade all protein components of ECM, their main function has been presumed to ECM remodeling (Nagase *et al.* 2006). Physiologically, MMPs are thought to be important in wound healing, angiogenesis and bone remodeling (Lakka *et al.* 2005; Yu and Han 2006). On the other hand, MMPs also have pathological roles in a variety of disease processes such as tumor invasion and metastasis, rheumatoid arthritis, periodontal disease and atherosclerosis (Wang *et al.* 2006; Schurigt *et al.* 2005; Schmidt *et al.* 2006).

In addition, certain MMPs are found to play a role in the shedding of cell surface proteins. Specifically, MT5-MMP has been shown to cleave cadherin (Monea *et al.* 2006), MMP7 has been shown to participate in the constitutive shedding of proTNF- $\alpha$  (Haro *et al.* 2000). MMP2 can cleave CCL7 producing an inactive fragment which becomes an antagonist of the receptor (McQuibban *et al.* 2000). MT1-MMP has been shown to participate in the shedding of the cell adhesion molecule CD44 (Nakamura *et al.* 2004) and the proTNF- $\alpha$  family member, TRANCE (Schlondorff *et al.* 2001). Recently, MT1-MMP mediated shedding of MUC1 was demonstrated (Thathiah and Carson 2004).

#### 1.3.2.2.1 Matrix metalloproteinase 9 (MMP9)

Among all MMPs, MMP9 is historically referred to as gelatinase B because of its ability to degrade gelatin (Stocker *et al.* 1995). Together with MMP2, MMP9 differs from other MMPs because it contains three fibronectin type II repeats that have high binding affinity for collagen. These repeats can mediate the binding of MMP9 and MMP2 to collagen (Bode *et al.* 1999). This binding interaction brings the catalytic pocket of the MMP proximal to collagen, thereby enhancing its rate of hydrolysis. MMP9 is capable of degrading type I, IV, V, VII, and XI collagens and laminin. In addition to ECM components, a growing body of evidence emerges to show that MMP-9 can directly accomplish cleavage of cell surface proteins including TGF- $\beta$  (Yu and Stamenkovic 2000), galectin-3 (Ochieng *et al.* 1994), IL-2R (Sheu *et al.* 2001) and ICAM-1 (Fiore *et al.* 2002).

## 2. Aim of the study

In summary, RAGE acts as a multi-ligand receptor to bind a range of ligands and therefore mediates various physiological and pathological effects. Based on its expression patterns, RAGE appears to play a major role in developmental processes. Of particular note is that RAGE is abnormally up-regulated in many situations and consequently contributes to these processes. Although the detailed molecular mechanisms underlying these RAGE-mediated disorders are far from being completely elucidated, widespread investigation by employing a variety of strategies and extensive data contributed by researchers from different disciplines have greatly advanced our understanding of RAGE (for example, see Bierhaus A et al. 2005). As a result, insightful views have emerged regarding the development of innovative diagnosis and therapy approaches against RAGE-mediated diseases. The identification and utilization of sRAGE is the most distinguished among these advances.

A growing body of evidence suggests the possibility of sRAGE as a biomarker for many RAGE-related diseases including coronary artery disease (Falcone *et al.* 2005), rheumatoid arthritis (Pullerits *et al.* 2005), Alzheimer disease (Emanuele et al. 2005), type 1 diabetes (Forbes et al. 2005) and hypertension (Geroldi et al. 2005). On the other hand, recombinant sRAGE has been used to alleviate RAGE-mediated diabetic atherosclerosis (Park et al. 1998) and diabetic late complications (Goova et al. 2001). Furthermore, it inhibits tumor metastasis and invasion (Taguchi et al. 2000) and blocks transport of A $\beta$  across the BBB (Deane et al. 2003). Therefore, sRAGE represents both a potential biomarker for RAGE-related diseases and a promising therapeutic tool for RAGE-mediated disorders. So it is desperately necessary to decipher the generation and pathophysiologic functions of sRAGE.

In fact, the source of naturally released human sRAGE is not well understood yet. Although most of present data strongly suggest that sRAGE is derived from alternative splicing of the RAGE mRNA, a recent paper (Hanford et al. 2004) reported purification of sRAGE from mouse lung by biochemical methods. In the same study, the investigators failed to detect splicing forms of mouse RAGE using either mouse lung RNA or a mouse lung cDNA library as template. Amino acid sequencing revealed that purified soluble mouse RAGE was ending after Gly (the 331 residue). The authors proposed that soluble RAGE was generated by proteolysis, but they failed to provide further evidence.

With regard to the above results on mouse sRAGE, considering that RAGE is type I membrane protein and growing members of type I membrane proteins undergo ectodomain shedding, in this thesis it was hypothesized that human RAGE also undergoes ectodomain shedding and as a result, soluble RAGE is generated by proteolysis in addition to alternative

splicing. In this study, I aimed to demonstrate the proteolytic processing of human RAGE, to identify the proteases responsible for ectodomain shedding of RAGE and to investigate possible mechanisms that regulate ectodomain shedding of RAGE.



### 3. Materials and Methods

#### 3.1 Materials

##### 3.1.1 Chemicals and Media

---

General laboratory chemicals	Roth, Karlsruhe Merck, Darmstadt Sigma, Deisenhofen
Agarose	Sigma, Deisenhofen
Acrylamid/Bisacrylamid (30 : 0.8)	Roth, Karlsruhe
Ampicillin (Sodium salt)	Roth, Karlsruhe
ATP	Pharmacia, Freiburg
Bactoagar	AppliChem, Darmstadt
Bacto-Trypton	AppliChem, Darmstadt
Blasticidine	Invitrogen, Karlsruhe
Bromphenol blue	Serva, Heidelberg
BSA	Roth, Karlsruhe
cAMP	Sigma, Deisenhofen
Chloroform	Roth, Karlsruhe
DEAE-Dextran	Pharmacia
Diethylether	Roth, Karlsruhe
DMEM	PAA, Linz, Österreich Sigma, Deisenhofen
DMSO	Merck, Darmstadt
DNA-Marker	MBI Fermentas, St. Leon-Rot
dNTPs	Sigma, Deisenhofen
DTT (Dithiothreitol)	Sigma, Taufkirchen
EDTA	Sigma, Deisenhofen
Ethidium bromid	Sigma, Deisenhofen
FCS (fetal calf serum)	PAA, Linz, Österreich
Formic acid	AppliChem, Darmstadt
Gelatin	Sigma, Deisenhofen
Geneticin (G418)	PAA, Linz, Österreich
Glucose	AppliChem, Darmstadt

---

---

L-Glutamin	PAA, Linz, Österreich
Glycerin	Roth, Karlsruhe
Isopropanol	Roth, Karlsruhe
I-Block	Applied Biosystems, Darmstadt
Lipofectamine 2000	Invitrogen, Karlsruhe
$\beta$ -Mercaptoethanol	Fluka, Buchs, Schweiz
Minimum Essential Medium (MEM)	Sigma, Deisenhofen
Penicillin	Sigma, Deisenhofen
Poly-L-Lysin	Sigma, Deisenhofen
RNaseA-solution	Sigma, Deisenhofen
RotiQuant Bradford reagent	Roth, Karlsruhe
SDS	BioRad, München
Serum Plus <sup>TM</sup>	JHR Bioscience, USA
Streptomycin	Sigma, Deisenhofen
Sulfo-NHS-Biotin	Pierce
TCA (Trichloroacetic acid)	AppliChem, Darmstadt
TEMED (N,N,N',N'-Tetra methyl ethylene diamine)	BioRad, München
Trypsin	PAA, Linz, Österreich
Triton X-100	Sigma, Deisenhofen
Tween-20	Serva, Heidelberg
Yeast extract	AppliChem, Darmstadt

---

### 3.1.2 Enzyme and Kit systems

---

Enzymes for molecular biology	NEB, Bad Schwalbach Amersham, Braunschweig Gibco BRL, Eggenstein MBI Fermentas, St. Leon-Rot
Plasmid Midi/Mini Kit	Qiagen GmbH, Hilden
QIAquick Spin Miniprep Kit	Qiagen GmbH, Hilden
QIAquick Gel Extraction Kit	Qiagen GmbH, Hilden
QIAquick PCR Purification Kit	Qiagen GmbH, Hilden

---

### 3.1.3 Laboratory instruments and accessories

---

Acryl half micro cuvettes	Sarstedt, Nürnberg
Analytical balance	Mettler-Toledo GMBH, Gießen
Bio-Imaging Analyzer BAS-1800 (Fuji)	Raytest Isotopenmessgeräte, Straubenhardt
Blot equipment	Biometra, Göttingen
Cell culture incubator	Heraeus, Hanau
Centrifuge rotor JA14 und JA20	Beckmann, München
Cooling centrifuge J2-21	Beckmann, München
DNA Thermal Cycler	Biometra, Göttingen
Double jet photometer Hitachi U-200	Colora Meßtechnik GmbH, Lorch
Flat bed gel equipment for DNA	home-made
Minigel-Electrophoresis	Biometra, Göttingen
Filter paper (3-MM)	Whatman, Springfield (UK)
Glass centrifuge tube	DuPont, Bad Homburg
Heating block	Scientific, Illkirch Cedex (F)
Hemocytometer	Neubauer-Zählkammer Roth, Karlsruhe
Incubation shaker	Infors GmbH, Einsbach
Plastic syringe (10 and 50 ml)	Braun, Melsungen
Plastic centrifuge tube(15 and 50ml)	Sarstedt, Nürnberg
Microfilter (0.2 and 0.4 µm)	Sarstedt, Nürnberg
Nunc CryoTubes	Nunc, Wiesbaden
nitrocellulose membranes	Amersham Pharmacia Biotech, Freiburg
PCR-tube (0.2ml)	Peq Lab, Erlangen
Petri plates	Sarstedt, Nürnberg
Microscope CK 2	Olympus, Hamburg
pH-Meter	WTW, Weilheim
Polystyrolcuvetten	Sarstedt, Nürnberg
PVDF-Membrane	Millipore, Eschborn
Reaction tube (1,5 und 2 ml)	Eppendorf, Hamburg
Scanner BAS-1800	Fujifilm, Düsseldorf
Vibration mixer	Laborfachhandel
Sterile work bench	Hera Safe HS 12 Heraeus, Hanau
Tissue culture dishes	Sarstedt, Nürnberg
Table centrifuge	Eppendorf 5415C Eppendorf, Hamburg

---

---

Vortexer	Janke und Kunkel, Heitersheim
VersaDoc imaging systems	Biorad, München
Water bath	BFL, Burgwedel

---

### 3.1.4 Solutions, buffers and media

<b>Antibiotic –stock solution</b>	100 mg/ml Ampicillin in H <sub>2</sub> O 20 mg/ml Chloramphenicol in 100% Ethanol Stored at -20°C
<b>Blocking buffer</b>	0.1% Tween 20 (w/v) 0.2% I-Block (w/v) in PBS
<b>DMEM-Complete medium</b>	DMEM supplemented with 2 mM L-Glutamine 100 U/ml Penicillin 100 mg/ml Streptomycin 10 % (v/v) FCS (fetal calf serum)
<b>DNA sample buffer</b>	50% (v/v) Glycerin 0.2% (v/v) SDS 0.05% Bromphenolblue 0.05% Xylencyanol 10 mM EDTA (Sigma, Deisenhofen)
<b>DEAE-Dextran Transfection solution (10X)</b>	125 mg DEAE-Dextran in 50ml of DMEM, sterile filtered.
<b>Ethidium bromide-Stock solution</b>	10 mg/ml Ethidium bromide and stored at 4°C in the dark
<b>LB-Medium pH7.4</b>	10 g/l Bacto-Trypton 5 g/l yeast extract 10 g/l NaCl in H <sub>2</sub> O, autoclaved (121°C, 20 min)
<b>LB-Medium with 20mM Glucose</b>	1 g Bacto-Trypton 0.5 g yeast extract 1 g NaCl

	98 ml H <sub>2</sub> O
	autoclaved, then add 2 ml 1 M Glucose solution
<b>LB/Amp-medium</b>	100 µg/ml Ampicillin in LB-medium
<b>LB/Amp-Agar-plates</b>	LB-Medium with 1.5% agar, 100 µg/ml Ampicillin
<b>MEM-Medium incomplete</b>	2 mM Glutamine
	7 % Serum Plus <sup>TM</sup>
	in MEM
<b>PBS</b>	8 g/l NaCl
	0.2 g/l KCl
	1.44 g/l Na <sub>2</sub> HPO <sub>4</sub>
	0.24 g/l KH <sub>2</sub> PO <sub>4</sub>
	in H <sub>2</sub> O
	adjusted to pH 7.4 with 2 M NaOH
<b>PBS-T</b>	PBS with 0.05% Tween 20
<b>PCI</b>	Phenol/Chloroform/Isoamylalcohol, 25:24:1 (v/v/v)
<b>STET-Buffer</b>	8 % (w/v) Saccharose
	5 % (w/v) Triton X-100
	50 mM EDTA
	50 mM Tris-HCl pH 8.0
<b>50x TAE-buffer</b>	2 M Tris
	1 M Acetic acid
	50 mM EDTA
	pH 8.4
<b>Trypsin/EDTA</b>	0.05 % (w/v) Trypsin
	0.54 mM EDTA
	in PBS
<b>Towbin-Puffer (modified)</b>	25 mM Tris pH 8,3
	192 mM Glycin
	20% (v/v) Methanol
	0.05% (w/v) SDS
<b>TBS</b>	20 mM Tris-HCl pH 7.5
	150 mM NaCl
<b>Buffers for Zymography</b>	

<b>Washing buffer</b>	2.5% Triton X-100 in H <sub>2</sub> O
<b>Assay buffer</b>	10mM CaCl <sub>2</sub> 100mM Tris-HCl pH 7.4
<b>Gel Coomassie blue staining solution</b>	25% Methanol 25% Roti-Blue R-250 in H <sub>2</sub> O
<b>Destaining solution</b>	25% Methanol in H <sub>2</sub> O
<b>Plasmid isolation buffers</b>	
<b>Suspension buffer (P1)</b>	50 mM Tris-HCl pH 8.0 10 mM EDTA
<b>Lysis buffer (P2)</b>	0.2 M NaOH 1 % SDS
<b>Neutralization buffer (P3)</b>	3 M potassium acetate pH 4.8
<b>Protein sample buffer</b>	
<b>Laemmli buffer</b>	3% (w/v) SDS 100 mM DTT 62.5 mM Tris-HCl pH 6.8 20% (w/v) Glycerin 0.01% (w/v) Bromphenol blue
<b>Nu-PAGE buffer</b>	50% Nu-PAGE-buffer (4x)(Invitrogen) 100 mM DTT
<b>Protein electrophoresis running buffer</b>	
<b>SDS-PAGEs</b>	25 mM Tris 192 mM Glycerin 0.1% SDS (w/v)
<b>Nu-PAGEs</b>	MES-buffer (Invitrogen)

### 3.1.5 Antibodies

#### Primary antibodies

<b>Name</b>	<b>description</b>	<b>Dilution</b>	<b>Source</b>
<b>9E10</b>	anti- <i>myc</i> Mouse-IgG	undiluted	Hybridoma culture

	(monoclonal)		medium of cell line MYC1-9E10.2 (ATCC)
<b>MAB5328</b>	Monoclonal antibody against the extracellular part of mouse RAGE. The antibody recognizes both natural and recombinant, as well as human RAGE	1:3000	Chemicon
<b>Anti-HA high affinity</b>	Rat anti-HA antibody	1:1000	Roche
<b>V5</b>	Mouse anti-V5 antibody	1:5000	Invitrogen

**Secondary antibodies**

<b>Name</b>	<b>dilution</b>	<b>source</b>
<b>Anti-mouse Peroxidase coupled antibody produced in goat</b>	1:5000	Sigma, Deisenhofen

### 3.1.6 Bacterial strains and cell lines

**E. coli DH5 $\alpha$** :  $\phi$ 80 $\delta$ (lacZ $\Delta$ M15), recA1, endA1, gyrA96, thi-1, hsdR17 (rk-mk +), supE44, relA1, deoR,  $\Delta$ (lacZYA-argFV169), F-,  $\lambda$ -; from Clontech, Heidelberg.

#### **9E10**

Hybridoma cell line for the 9E10 mouse anti-myc IgG. ATCC No. CRL-1729 (Evan et al., 1985).

#### **Flp-In-293** (Invitrogen, Catalog No. R750-07)

Derived from HEK 293, stably express the lacZ-Zeocin fusion gene and are designed for use with the Flp-In System (Catalog No. K6010-01 and K6010-02).

Each cell line contains a single integrated Flp Recombination Target (FRT) site from pFRT/lacZeo or pFRT/lacZeo2.

#### **COS-7**

African green monkey kidney fibroblast-like cell line. ATCC No. CRL-1651.

#### **myc-RAGE/V5/His-Flp-In-293 cell**

Single clone Flp-In-293 cell line transfected with plasmid pcDNA6-myc-RAGE/V5/His by Lipofectamine 2000, selected by blasticidine (4 mg/ml growth medium).

#### **RAGE-Flp-In-293 cell**

Mixed clone Flp-In-293 cell line transfected with plasmid pcDNA6-RAGE by Lipofectamine 2000, selected by blasticidine (4 mg/ml growth medium).

#### **myc-RAGE/V5/His-COS cell**

Mixed clone COS-7 cell line transfected with plasmid pcDNA6-myc-RAGE/V5/His by Lipofectamine 2000, selected by blasticidine (4 mg/ml growth medium).

#### **RAGE- $\Delta$ /V5/His-Flp-In-293 cell**

Mixed clone Flp-In-293 cell transfected with plasmid pcDNA6-RAGE- $\Delta$ C/V5/His by Lipofectamine 2000, selected by blasticidine (4 mg/ml growth medium).

#### **MMP9-COS**

Mixed clone COS-7 cell stably transfected with pIRESneo2-hMMP9, selected by G418.



### **3.1.7 Plasmids**

#### **pcDNA3**

Mammalian expression vector, Amp-resistance, Neo-resistance, CMV promoter, BGH poly A, high copy number plasmid, F1+ origin, selection on Geneticin (Invitrogen).

#### **pcDNA6/V5-HisB**

pcDNA6/V5-HisB is 5.1 kb vector designed for high-level expression in mammalian host cells, selection on blasticidin, Amp-resistance. It has the human cytomegalovirus immediate-early (CMV) promoter for high-level expression in a wide range of mammalian cells (Invitrogen).

#### **pIRESneo2**

Eukaryotic expression vector contains attenuated internal ribosome entry site (IRES) from encephalomyocarditis virus (ECMV), which permits the translation of two open reading frames from one messenger RNA, and a synthetic intron known to enhance the stability of the mRNA. The vector has a CMV promoter and an Amp resistance gene and a neomycin resistance gene.

#### **pSG5**

Eukaryotic expression vector contains the SV40 early promoter and the T7 bacteriophage promoter. High copy number yields large quantities of double-stranded DNA. Use for in vivo or in vitro expression. Amp resistance (Stratagene).

#### **pcDNA6-myc-RAGE/V5/His**

Vector pDNA-LIB-RAGE containing the human RAGE cDNA was used as initial template for construction of RAGE expression vectors. To insert an internal myc tag coding sequence immediately after the coding region for the signal peptide of human RAGE, PCR were performed of the N-terminal part of hRAGE with primer RAGE\_for and primer RAGE\_myc\_rev, furthermore the C-terminal part of hRAGE was amplified with primer RAGE\_myc\_for and primer RAGE\_rev respectively.

Then these two PCR products were combined into a single PCR with primer RAGE\_for and RAGE\_rev. The resulting PCR product was cut with KpnI and SacII and cloned into the expression vector pcDNA6/V5-HisB (Invitrogen), thus creating the hRAGE-cDNA expressing construct pcDNA6-mycRAGE/V5-His. By using this plasmid a N-terminal myc and C-terminal V5 and His tagged RAGE protein can be expressed.

#### **pcDNA6-RAGE**

The human RAGE cDNA was subcloned from the pDNA-LIB-RAGE into EcoRI/XbaI sites of plasmid pcDNA6/V5-HisB, thus creating construct pcDNA6-RAGE, which can be used for expression of an untagged human RAGE protein.

**pcDNA6-RAGE-ΔC**

The cytoplasmic domain deleted mutant RAGE-ΔCYT (367-404 amino acid) was generated from pcDNA6-RAGE by PCR using primer RAGE\_for and primer RAGE-ΔC. The PCR product was then subcloned into the pcDNA6/V5/HisB vector, thus creating pcDNA6-RAGE-ΔC, which can be used for expression of an untagged C-terminal truncated human RAGE protein.

**pcDNA6-RAGE-P328E**

The putative MMP9 cleavage consensus sequence PTAGS (Pro-X-X-Hydrophob-Ser/Thr) is mutated into ETAGS (point mutation).

With the plasmid pcDNA6-RAGE as template three PCRs were performed using primer pairs RAGE\_for and pcDNA3\_seq\_rev, RAGE\_P342E\_Down and pcDNA3\_seq\_rev, and RAGE\_for and RAGE\_P342E\_Up respectively. Three different PCR products of 1579 bp, 586 bp and 993 bp were purified from a gel. Then the 1579 bp product was used as template and the other two products (586 bp and 993 bp) were used as “Mega-primer” for a subsequent PCR. The newly generated PCR product (size is also 1579 bp) contained the mutation and a newly introduced PvuII site for screening of mutants. The 1579 bp PCR product was cut with Eco91I (cuts off a 582 bp fragment) and XhoI (cuts off a 140 bp fragment) and then the 857 bp fragment was purified from a gel and ligated with Eco91I/XhoI cut pcDNA6-RAGE vector to create construct pcDNA6-RAGE-P328E.

**pcDNA6-RAGE-ΔPTAGS**

The putative MMP9 cleavage consensus sequence PTAGS (Pro-X-X-Hydrophob-Ser/Thr) was mutated into AAGEG. With the plasmid pcDNA6-RAGE as template two PCRs were performed using primer pairs RAGE\_for and RAGE-dPTAGS-rev as well as pcDNA3\_seq\_rev, and RAGE\_for respectively. The two gel isolated PCR products were combined into a single PCR with primer pair RAGE\_for and pcDNA-Seq\_rev. The 1579 bp PCR product was cut with Eco91I (cuts off a 582 bp fragment) and XhoI (cuts off a 140 bp fragment) and the 857 bp fragment was purified from a gel and ligated with Eco91I/XhoI cut pcDNA6-RAGE vector to create construct pcDNA6-RAGE-ΔPTAGS.

**pSG5-bADAM10-HA**

From Kristina Endres, Institute for Biochemistry, Johannes Gutenberg-University, Mainz. The construct is used for expression of bovine ADAM10 with a hemagglutinin epitope tag at the C terminal end.

**pSG5-DN-bADAM10-HA**

From Annette Roth, Institute for Biochemistry, Johannes Gutenberg-University, Mainz. The construct can be used for expression of bovine ADAM10 with the E384A point mutation in the

Zinc-binding region of ADAM10 and with hemagglutinin epitope tag at the C terminal end.

#### **pSG5-mADAM17-HA**

From Kristina Endres, Institute for Biochemistry, Johannes Gutenberg-University, Mainz. The construct can be used for expression of murine ADAM17 with hemagglutinin epitope tag at C terminal end.

#### **pcDNA5/FRT-mTACE-HA**

Construct pcDNA5/FRT-mTACE-HA was subcloned from plasmid 162a.1 (from Rolf Postina) into the KpnI/ Bsp120I sites of the vector pcDNA5/FRT. It encodes the mouse TACE cDNA.

#### **pcDNA5/FRT-mTACE-DN-HA**

This is the putative dominant negative mutant E406A of mTACE.

With the plasmid pcDNA3-mTACE-HA as template two PCRs were performed using primer pairs pcDNA3\_seq and mTACE\_E406A\_rev as well as mTACE\_E406A\_for and mTACE-X828NruI\_R respectively. The two gel isolated PCR products were combined into a single PCR with primer pair pcDNA\_seq and mTACE-X828NruI\_R. The 2580 bp PCR product was cut with SmaI and ClaI and the 773 bp fragment was purified from a gel and ligated with the 6764bp ClaI/SmaI cut pcDNA5/FRT-mTACE-HA vector to create construct pcDNA5/FRT-mTACE-DN-HA.

#### **pIRESneo2-hMMP9**

Expression plasmid for human MMP9. The 2373bp fragment containing the MMP9 cDNA was subcloned from the human MMP9 containing plasmid pOTB7-MMP9 (RZPD clone IRALp962P0118Q) into the vector pIRESneo2 between BamHI and EcoRI sites.

#### **pSG5-hMMP9**

Expression plasmid for human MMP9. The human MMP9 cDNA was subcloned from the human MMP9 containing plasmid pOTB7-MMP9 (RZPD clone IRALp962P0118Q) into the vector pSG5 between BamHI and EcoRI sites.

#### **pIRESneo2-MMP2**

Expression plasmid for human MMP2. The human MMP2 cDNA was subcloned from the human MMP2 containing plasmid pOTB7-MMP2 (RZPD clone IRAUp969F048D) into the vector pIRESneo2 between BamHI and EcoRI sites.

#### **pCR3.1-MT1-MMP**

A gift from Prof. Stephen Weiss (University of Michigan Health System, USA). HA-tagged MT1-MMP cDNA, cloned into pCR3.1 vector (Invitrogen)

### 3.1.8 Oligonucleotides

The sequences of all oligonucleotides are in 5' - 3' direction as specified.

#### RAGE\_myc\_for

5'-GAAGAACAGAAGCT GATATCGAAGAAGATTTGTTA GGCGCCCAAACA

EcorV

NarI

TCACAGCCCGGATTGGCGAG-3'

#### RAGE\_myc\_rev

5'-GGCGCCTAACAAATCTTCTTCA GATATCAGCTTCTGTTCTTC GGCGCCTAC

NarI

EcorV

NarI

TACTGCCCCCACAGACTGAG-3'

#### RAGE\_for

5'-AAAGAA GGTACCATGGCAGCCGGAACAGCAGTTGGAGCCTG-3'

KpnI

#### RAGE\_rev

5'-CAACAA CCGCGGCCCTCCAGTACTACTCTCGCCTGC-3'

SacII

#### RAGE-delta C

5'-CACACCCTCAGGTAAACGCCTTTGCCACAAGATGACCCCAATG-3'

#### RAGE\_P342E\_Up

5'-GC CAGCTGT CTCCCCCTCCTCGCCTGG TTCGATG-3'

PvuII

#### RAGE\_P342E\_Down

5'-TCTGTGGGAGGATCAGGGCTGGGAACTCTA-3'

#### RAGE-dPTAGS\_rev

5'-CACTCCCTCTCCCGCGGCCCTCCTCGCCTGGTTCGATGATGC-3'

#### RAGE-dPTAGS\_for

5'-GGGGGCCGCGGGAGAGGGAGTGGGAGGATCAGGGCTGGG-3'

#### pcDNA3\_seq

5'-AGCAGAGCTCTCTGGCTA-3'

#### pcDNA3\_Seq\_rev

5'-ACTAGA AGGCACAGTCGAG-3'

**mTACE\_E406A\_for**

5'-GGTTACAACCTCACGCGTTGGGACACAATTTTGGAG-3'

**mTACE\_E406A\_rev**

5'-CTCCAAAATTGTGTCCCAACGCGTGAGTTGTAACC-3'

**MMP9 stealth RNAi oligonucleotide duplexes**

**RNAi-624**

5'-AAGAUGUUCACGUUGCAGGCAUCGU-3'

3'-UUCUACAAGUGCAACGUCCGUAGCA-5'

**RNAi-625**

5'-AAUACAGCUGGUUCCCAAUCUCCGC-3'

3'-UUAUGUCGACCAAGGGUUAGAGGCG-5'

**3.1.9 Inhibitors and Activators**

PMA (Phorbol-12-Myristat-13-Acetat)	Sigma, Deisenhofen
APMA (P-aminophenylmercuric acetate)	Sigma, Deisenhofen
E64	Calbiochem, San Diego, USA
Pefabloc-SC	Calbiochem, San Diego, USA
Pepstatin	Calbiochem, San Diego, USA
DL-thiophran	Calbiochem, San Diego, USA
GM6001	Calbiochem, San Diego, USA
GI254023X	Dr. I. Hussain, Glaxo SmithKline, Harlow (UK)
GW280264X	Dr. I. Hussain, Glaxo SmithKline, Harlow (UK)
PD98059	Sigma, Deisenhofen
Chelerythrine	Sigma, Deisenhofen
A23187 (calcimycin)	Calbiochem, San Diego, USA

## 3.2 Methods

### 3.2.1 Molecular biology

#### 3.2.1.1 Maintenance of bacterial strains

Strains were stored as glycerol stocks (LB-medium, 25% (v/v) glycerol) at  $-70^{\circ}\text{C}$ .

An aliquot of the stock was crossed out on LB-plate containing the appropriate antibiotics and incubated overnight at  $37^{\circ}\text{C}$ . Plates were stored up to 6 weeks at  $4^{\circ}\text{C}$ .

#### 3.2.1.2 Preparation of competent bacteria

##### Calcium chlorid-method (Dagert and Ehrlich 1979)

A single colony was inoculated into 2 ml LB medium and incubated overnight on a shaker at  $37^{\circ}\text{C}$ . 1 ml overnight culture was inoculated into 400 ml of LB medium and incubated on a shaker at  $37^{\circ}\text{C}$  for 3-4 hours until  $\text{OD}_{600}=0.4-0.6$ . The culture was transferred to sterile centrifuge tubes and centrifuged 5000 rpm (Rotor JA-14), 10 min at  $4^{\circ}\text{C}$ . The supernatant was poured off and the cells were kept on ice. Then the cell pellet was resuspended in 100 ml of ice cold sterile 50 mM  $\text{CaCl}_2$  and incubated for 15 min on ice. After centrifugation 6000 rpm (Rotor JA-14), 10 min at  $4^{\circ}\text{C}$  the cells were resuspended in 20 ml of ice cold 50 mM  $\text{CaCl}_2$  containing 10% Glycerol. Aliquot of 100  $\mu\text{l}$  were incubated in microrcentrifuge tubes for 2 h on ice. Subsequently, the suspension was frozen in liquid nitrogen and stored at  $-70^{\circ}\text{C}$ .

#### 3.2.1.3 Transformation of *E. coli*

To 100  $\mu\text{l}$  of competent DH5 $\alpha$  cells either 50-100 ng of plasmid DNA or 10  $\mu\text{l}$  of ligation mixture were added and incubated for 20 min on ice. After a heat shock (1.5 min,  $42^{\circ}\text{C}$ ) and successive incubation on ice (3 min), 800  $\mu\text{l}$  of LB-medium with 20 mM glucose were added to the bacteria and incubated at  $37^{\circ}\text{C}$  for 60 min with gently shaking. Cells were plated on LB plates containing the appropriate antibiotics. Plates were incubated at  $37^{\circ}\text{C}$  overnight.

#### 3.2.1.4 Plasmid Miniprep

##### 3.2.1.4.1 Isolation of plasmid DNA from *E. coli* by the rapid boiling method

A single colony was inoculated into 3-5 ml of LB media in a 15 ml sterile culture tube with appropriate antibiotics and incubated at  $37^{\circ}\text{C}$  overnight. After centrifugation and removal of the supernatant, the cells were resuspended in 0.35 ml of STET buffer by vortexing. Then 25  $\mu\text{l}$  of 20 mg/ml lysozyme were added and incubated at room temperature for 5 min. Then samples were boiled for 50 seconds and then centrifuged (14000 rpm for 20 min). After removal of the pellet,

38 µl of 3 M potassium acetate were added to each sample, and after mixing by inversion, 400 µl of isopropanol were added. The sample was centrifuged at 14000 rpm for 15 min at room temperature. After removal of the supernatant and washing with 75% ethanol the nucleic acids were dried at room temperature. Subsequently the DNA was dissolved in 50 µl of H<sub>2</sub>O.

#### 3.2.1.4.2 Isolation of plasmid DNA from E.coli by Silica columns

To obtain high purity and quality plasmid DNA for cloning, transfection and sequencing, QIAprep Spin Miniprep Kit (Qiagen, Germany) was used for preparation of small scales of plasmid DNA (Miniprep) according to the manufacture's protocol.

#### ***3.2.1.5 Plasmid Maxiprep***

A single colony was inoculated in 2 ml of LB/amp (100 µg ampicillin/ml LB) medium and grown at 37°C for 8 h with constant agitation. Afterwards, this culture was added to 400 ml of LB/amp medium and the culture was incubated at 37°C with constant agitation overnight. Cells were pelleted in a Beckmann centrifuge (4000 rpm, 10 min, and 4 °C) and suspended with 8 ml of buffer P1 and incubated for 5 min at room temperature. Then 8 ml of buffer P2 was added, mixed thoroughly and incubated for 7 min at room temperature. Then 8 ml of buffer P3 was added, mixed thoroughly and incubated on ice for 5 min. After centrifugation (15000 rpm, 30 min, 4°C), the supernatant was transferred to a fresh centrifuge tube, mixed thoroughly with 17 ml isopropanol and incubated for 10 min at room temperature. Then after centrifugation (15000 rpm, 20 min, 4°C), the supernatant was removed and 3 ml 75% ethanol was added. After centrifugation (15000 rpm, 5 min, 4°C), the ethanol was removed and the pellet was dissolved in 6 ml H<sub>2</sub>O. Then 5 ml of 10 M NH<sub>4</sub>AC was added, mixed thoroughly and incubated on ice for 20 min. After centrifugation (15000 rpm, 20 min, 4°C), the supernatant was transferred into a fresh glass centrifuge tube and 7 ml of isopropanol were added, mixed thoroughly and incubated on ice for 20 min. The supernatant was removed after centrifugation (11000 rpm, 20 min, 4°C) and 3 ml 75% ethanol was added to wash the pellet. The ethanol was removed after centrifugation (11000 rpm, 5 min, 4°C) and the pellet was dried under laminar air flow.

Then the nucleic acid pellet was dissolved in 800 µl H<sub>2</sub>O and transferred into a 2 ml Eppendorf tube. 6 µl RNaseA were added and incubated at 37 °C for 30 min. Then 800 µl PEG-solution were added, mixed and incubated on ice for 20 min. After centrifugation (7000 rpm, 20 min, room temperature), the supernatant was removed and 1 ml 75% ethanol was added to wash the DNA pellet. The ethanol was removed after centrifugation (14000 rpm, 5 min, room temperature) and then the pellet was dried.

Then the DNA pellet was dissolved with 500  $\mu$ l H<sub>2</sub>O. Proteins were extracted from the plasmid DNA with 1X 600  $\mu$ l Phenol (pH 7.5) and 4X 600  $\mu$ l PCI (phenol/chloroform/isoamyl alcohol) by centrifugation (14000 rpm, 3 min, room temperature). After each centrifugation, the upper aqueous layer containing the plasmid DNA was transferred carefully into a fresh Eppendorf tube. Finally the DNA solution was extracted twice with 1 ml diethylether. After centrifugation (14000 rpm, 3 min, room temperature) and the upper ether phase was removed. Then the rest of ether in this DNA solution was evaporated under the sterile bench for 10 min.

The DNA was mixed with 50  $\mu$ l 3 M potassium acetate (pH 4.8), then 1500  $\mu$ l 100% ethanol were added, mixed and incubated at -20 °C for 1h. After centrifugation (14000 rpm, 20 min, room temperature) the supernatant was removed and 1 ml 75% ethanol was added. The supernatant was removed after centrifugation (14000 rpm, 5 min, room temperature) and the DNA pellet was dried at room temperature.

Finally the DNA pellet was dissolved in 1000  $\mu$ l H<sub>2</sub>O. This is the final stock of plasmid DNA which is suitable for transfection and long term storage. The concentration of the plasmid DNA was determined photometrically.

### ***3.2.1.6 Enzymatic modification of DNA***

#### **3.2.1.6.1 Digestion of DNA by restriction endonucleases**

For digestion, the DNA was incubated with the recommended amount of appropriate enzymes in the recommended buffer for 2 h at recommended temperature according to the manufacturer's protocol. The DNA was purified between the two digestions using the QIAquick PCR Purification Kit.

#### **3.2.1.6.2 Generation of blunt-end DNA fragments**

A reaction mixture was made containing DNA, 1  $\times$  T4 DNA polymerase reaction buffer and 20  $\mu$ M of each dNTP. Then 1 unit of T4 DNA polymerase was added and incubated at 15 °C for 30 min. Then the reaction was stopped by heating at 75 °C for 10 min.

#### **3.2.1.6.3 Dephosphorylation of plasmid DNA**

Alkaline phosphatases (AP) catalyze the removal of 5' phosphate groups from DNA, RNA, ribo- and deoxyribonucleoside triphosphates. So AP can remove 5' phosphates from plasmid vectors that have been cut with a restriction enzyme. In subsequent ligation reactions, this treatment prevents self-ligation of the vector and thereby greatly facilitates ligation of other DNA fragments into the vector. After restriction the plasmid DNA was purified by using the QIAquick PCR



purification kit. Then SAP buffer (Boehringer Ingelheim) and 1 unit of SAP (saccharic alkaline phosphatase) per 100 ng plasmid DNA were added. The reaction was incubated at 37 °C for 2 h and terminated by incubation at 70 °C for 10 min. The plasmid DNA was used for ligation without further purification.

#### 3.2.1.6.4 Ligation of DNA fragments

Ligation of DNA fragments was performed by mixing 50 ng vector DNA with fivefold to eightfold molar excess of insert DNA. 1 µl of T4 DNA ligase (5 Weiss unit/µl) and 2 µl of 10x ligation buffer (both from MBI Fermentas) were added and the reaction mix was brought to a final volume of 20 µl. The reaction was incubated for overnight at 12 °C. The reaction mixture was used directly for transformation without any further purification.

#### ***3.2.1.7 DNA electrophoresis***

DNA fragments were separated in horizontal electrophoresis chambers using agarose gels. Depending on the size of DNA fragments, agarose gels were prepared by heating 1-1.5 % (w/v) agarose (Gibco) in 1x TAE buffer. After agarose was dissolved completely, ethidium bromide was added. The gel was covered with 1x TAE buffer and the DNA samples were mixed with sample buffer and pipetted in the sample pockets. The gel was run at constant voltage (10 V/cm gel length) until the bromophenol blue dye had reached the end of the gel. Finally gels were documented using a UV-light imaging system.

### **3.2.1.8 DNA purification**

#### 3.2.1.8.1 Purification of DNA fragments

For purification of DNA fragments the QIAquick PCR Purification Kit (Qiagen GmbH, Germany) was used according to the manufacturer's protocol.

#### 3.2.1.8.2 Extraction of DNA fragments from agarose gels

The QIAquick Gel Extraction Kit (Qiagen GmbH, Germany) was used for isolation and purification of DNA fragments from agarose gels. Ethidium bromide-stained gels were illuminated with UV-light and the appropriate DNA band was excised from the gel with a clean scalpel and transferred into an Eppendorf tube. The DNA fragment was purified following the manufacturer's protocol.

#### 3.2.1.8.3 Determination of DNA concentration

DNA concentration was determined spectroscopically using a photometer from Eppendorf. DNA samples were usually diluted 1:20 with water. Concentration was determined by measuring the absorbance at 260 nm, 280 nm and 320 nm. Absorbance at 260 nm should be higher than 0.1 but less than 0.6 for reliable determinations. A ratio of  $A_{260}/A_{280}$  between 1.8 and 2 monitored a sufficient purity of the DNA preparation.

### **3.2.1.9 DNA Sequencing**

DNA sequencing was performed by the Genterprise company (Genterprise, Mainz, Germany).

#### **3.2.1.10 Polymerase Chain Reaction (PCR)**

Polymerase chain reaction (PCR) employs multiple cycles of template denaturation, primer annealing, and primer elongation to amplify DNA. PCR is an exponential process and a highly sensitive technique for DNA amplification. Plasmid DNA was used as template. Several reaction components are incorporated in PCR (Table 5). The template can be genomic or plasmid DNA. The primers determine the sequence and the length of the amplified product. The most frequently used thermostable polymerase is Taq DNA Polymerase. This enzyme is appropriate for routine applications, but the use of other thermostable proof-reading DNA polymerases can improve products of PCR.

**Table 5. Reaction Components of PCR**

<b>Component</b>	<b>Final Concentration</b>
Template	10-100 ng plamid DNA or cDNA
Primer forward	0.1–0.5 $\mu$ M
Primer reverse	0.1–0.5 $\mu$ M
10x Reaction buffer	1x
Magnesium	1.0–3.0 mM
dNTP mix	200 $\mu$ M each dNTP
Thermostable DNA polymerase	1 unit/100 $\mu$ l reaction

PCR was carried out using an automated thermal cycler (Biometra). The following standard protocol was adjusted to each specific application:

3 min 95°C (initial denaturation)

30 cycles:

1 min 95°C (denaturation)

1 min 46-70°C (annealing)

1.5 min/kb 72°C (extension)

10 min 72°C (final extension)

PCR products were either separated by agarose gel electrophoresis, excised and subsequently purified with the QIAquick Gel Extraction kit or directly purified with the PCR Purification Kit. Purified PCR products were ready to use for downstream work.

### 3.2.2 Protein biochemical methods

#### 3.2.2.1 Determination of protein concentration (Bradford assay)

To determine the total protein concentration of e.g. cell lysates, the Bradford assay (Bradford, 1976) was used. The assay is based on the observation that the absorbance maximum for an acidic solution of Coomassie Brilliant Blue G-250 shifts from 465 nm to 595 nm when binding to protein occurs. Both hydrophobic and ionic interactions stabilize the anionic form of the dye, causing a visible color change. Within the linear range of the assay (~5-25 µg/ml), the more protein present, the more Coomassie binds.

The BSA standard dilution series as described in Table 6 was prepared in a 1.5 ml Eppendorf tube and 50 µl of 100% formic acid were added. Then the unknown sample was diluted in 50% formic acid to an appropriate concentration to be within the linear range of the BSA standard line. To 100 µl BSA standard or 100 µl diluted sample (each in 50% formic acid) 900 µl Roti-Quant (Roth) which was previously diluted 1:5 with water were added. After being mixed by inverting and incubation for 20 min at RT, the samples were measured at 595 nm.

**Table 6. Preparation of BSA standard series**

BSA (0.5 mg/ml)	H <sub>2</sub> O	Concentration
0 µl	50 µl	0 µg/ml
4 µl	46 µl	2 µg/ml
8 µl	42 µl	4 µg/ml
12 µl	38 µl	6 µg/ml
16 µl	34 µl	8 µg/ml
20 µl	30 µl	10 µg/ml

#### 3.2.2.2 TCA precipitation of proteins

TCA precipitation was used to concentrate proteins from cell supernatants for further analysis. Supernatants were collected and centrifuged at 1500 rpm for 10 min to remove cell debris, and then subjected to TCA precipitation. Briefly, samples were mixed with 11.11% volumes of 6.1 M TCA (the final TCA concentration is 10%), incubated on ice for 2 min, centrifuged at 13,000 g for 5 min, and then supernatants were carefully removed. The pellets were washed twice with ice-cold acetone by centrifugation at 13,000 g for 5 min, subsequently dried, and then dissolved in SDS-PAGE loading buffer and heated at 95°C for 10 min.

### ***3.2.2.3 Chloroform-Methanol precipitation of proteins***

The method can be used to purify proteins from lipids, detergents and salts.

400  $\mu$ l methanol was added to 50  $\mu$ l solubilized protein and mixed by vortexing. Then 100  $\mu$ l chloroform was added and mixed by vortexing. Next, 300  $\mu$ l H<sub>2</sub>O was added and mixed.

Subsequently the samples were centrifuged at 14,000 rpm (2 min, room temperature); proteins accumulate at the border-line, between the water phase and the organic phase. After that, the supernatant was removed completely without losing any protein, and then 400  $\mu$ l methanol was added and mixed by vortexing.

By centrifugation at 14,000 rpm (2 min, RT), the proteins were precipitated. After removal of the supernatant the protein pellet was dried and could be used for gel electrophoresis or for protein quantification.

If gel electrophoresis should be carried out, the pellet was dissolved in an appropriate protein sample buffer.

If the amount of proteins should be determined, the protein pellet was dissolved in formic acid and subjected to the Bradford assay.

### ***3.2.2.4 SDS-polyacrylamide gel electrophoresis***

Separation of proteins was performed by means of the discontinuous SDS-polyacrylamide gel electrophoresis (SDS-PAGE) using the Mini-Protean III system (BioRad). The size of the running and stacking gel was as follows:

Separation gel: height ~8 cm, thickness 1 mm

10 % (v/v) acrylamide

Stacking gel: height ~2 cm, thickness 1 mm

5% (v/v) acrylamide

10 or 15-well combs

After complete polymerization of the gel, the chamber was assembled as described by the manufacture's protocol. Samples were loaded in the pockets and the gel was run at constant current at 10 mA for the stacking gel and then for the separation gel at 20 mA. The gel run was stopped when the bromphenol blue dye had reached the end of the gel. Gels were then either stained or subjected to Western Blotting.

### **3.2.2.5 Western Blot**

#### 3.2.2.5.1 Electrophoretic transfer

Proteins were transferred from the SDS-gel onto a nitrocellulose membrane (Amersham) using a Semi-Dry-Blot instrument (Biometra, Göttingen). After equilibration of the nitrocellulose membrane in blot buffer for 5 min, the blotting sandwich was assembled as described in the manufacturer's protocol. Proteins were transferred at room temperature at constant voltage (10 V for 30 min). The prestained marker See Blue plus (Invitrogen) was used as molecular weight marker and to monitor the transfer.

#### 3.2.2.5.2 Immunological detection of proteins on nitrocellulose membranes

After electrophoretic transfer, the membranes were removed from the sandwich and placed protein-binding side up in plastic dishes. Membranes were washed once in PBS-T and then incubated in blocking buffer for 1 h at room temperature with gently shaking. Afterwards, the primary antibody was added in an appropriate dilution and incubated either for 1 h at RT or overnight at 4°C. The primary antibody was removed and the membrane was washed 3x 5 min then 2x 10 min with PBS-T. The appropriate secondary antibody was then applied for 1 h at RT. The membrane was washed again 3x 5 min with PBS-T followed by two short washing steps with PBS. And then immunoreactive proteins were visualized using the enhanced chemiluminescence detection reagent (ECL).

#### 3.2.2.5.3 Immunological detection using enhanced chemiluminescence

The antibody bound to the membrane was detected by using the enhanced chemiluminescence detection reagent (100 mM Tris/HCl pH 8.5; 1.25 mM Luminol; 0.2 mM p-Cumaric acid; 0.01 % (v/v) H<sub>2</sub>O<sub>2</sub>).

The membrane was incubated for 5 min in detection reagent. Then the solution was removed and the blot was dried and placed between two saran warp foils. The membrane was either exposed to X-ray film (Biomax-MR, Kodak) for several time periods, starting with a 5 min exposure, or signals were detected and quantified with the VersaDoc imaging systems (Model 3000, Biorad, München) by the quantity one program.

### ***3.2.2.6 Coomassie staining of polyacrylamide gels***

The colloidal Coomassie staining of polyacrylamide gels was performed with the Roti-Blue kit (Carl Roth GmbH). After SDS-PAGE, the gels were incubated with Roti-Blue staining solution for 2-15 h with constant agitation. The gels were then incubated in destaining solution until the background of the gels appeared nearly transparent.

### ***3.2.2.7 Biotinylation of cell surface proteins***

Cell surface proteins were biotinylated using the water soluble cell membrane-imperviable biotinylation reagent Sulfo-NHS-Biotin (Pierce) following manufacture's instruction.

#### **3.2.2.7.1 Biotin labeling and induction of shedding**

The adherent cells were washed twice with 3 ml of PBS, and then 1 ml PBS was added to each well. Sulfo-NHS-LC-Biotin was equilibrated to room temperature. Immediately before use, a 10 mM Sulfo-NHS-LC-Biotin solution was prepared by adding 1.65 mg to 300  $\mu$ l of ultrapure water. Then this solution was transferred completely into 15 ml PBS and mixed carefully. Then, 1 ml of the Sulfo-NHS-LC-Biotin/PBS solution was added to each well and mixed carefully followed by incubation at room temperature for 30 min. After incubation, cells were washed once with about 4 ml of TBS pH 7.4. Then 1.5 ml of preheated secretion medium (DMEM with 2 mM glutamine and 10  $\mu$ g/ml fatty acid-free BSA) was added together with either 1  $\mu$ M PMA, 142  $\mu$ M AMPA or DMSO (negative control). The cells were then incubated with PMA and DMSO for 1.5h but were incubated with AMPA only for 15 min.

Then the supernatant was collected by transferring the secretion medium (1.5 ml) into a 1.5 ml Eppendorf tube. After centrifugation for 5 min at 2500 rpm, 1.3 ml supernatant was transferred into a fresh 1.5 ml Eppendorf tube. The samples were then frozen at -20°C before the biotinylated proteins were captured.

At the same time the cells were collected and solubilized with 300  $\mu$ l 5% SDS (dissolved in water). The samples were then frozen at -20°C before denaturation at 95°C for 10 min. During the denaturation step the samples were vortexed vigorously every 2 min.

#### **3.2.2.7.2 Capturing of biotinylated proteins**

After the frozen supernatant being thawed, 26  $\mu$ l of 5% SDS was added to 1.3 ml of supernatant (secretion medium) and then 35  $\mu$ l of well mixed NeutrAvidin Biotin binding agarose (Pierce) was added. After denaturation, 1274  $\mu$ l of PBS was added to 26  $\mu$ l of SDS-solubilized cells and then 35  $\mu$ l of well mixed NeutrAvidin Biotin binding agarose (Pierce) was added.

Subsequently, all samples were incubated by rotating for 1.5-2 h at 4°C. After incubation, the agarose beads were spun down by centrifugation at 2500 g (7 min, RT). Next, the agarose beads were washed at least 2 times with 0.8 ml PBS/0.1% SDS followed by rotating for 3 min for mixing, and then the agarose beads were spun down at 2500 g (7 min and RT). After that, the final wash was removed and 30 µl of 2x Laemmli buffer including 100 mM DTT were added and then the samples were boiled for 10 min at 85°C with frequent vortexing. After denaturation the samples were incubated for 10 min at RT followed by centrifugation at 6000 rpm (10 min, RT). Then 20 µl of the supernatant was transferred very carefully into a fresh Eppendorf tube for Western blot analysis.

### ***3.2.2.8 Gelatin zymography assay***

MMP9 activity was analyzed by 10% SDS-PAGE containing 0.1% gelatin as described (Woessner, Jr. 1995). Briefly, after electrophoresis, gels were washed in 2.5% Triton X-100 at room temperature for 1 h and then incubated for 16 h at 37°C in reaction buffer (100 mM Tris-HCl pH 7.5, 10 mM CaCl<sub>2</sub>). The gels were then stained with Coomassie Brilliant Blue R250 for 2-12 h followed by washing with 25% methanol overnight. The clear bands represented gelatinase activity.

## **3.2.3 Cell biology methods**

### ***3.2.3.1 Cell culture***

All culture incubations were performed in a humidified 37°C, 5% CO<sub>2</sub> incubator unless otherwise specified. Flp-In 293 cells and COS-7 cells were cultured in Dulbecco's modified Eagle's medium (DMEM) supplemented with 10% fetal calf serum, 2 mM glutamine, 100 U/ml penicillin and 100 mg/ml streptomycin.

### ***3.2.3.2 Trypsinizing adhesive cells***

All medium from cultured cells was removed with a sterile Pasteur pipette. Adhering cells were washed once with 5 ml PBS then 5 ml Trypsin/EDTA solution was added to cover the cell layer. The cells were released from the bottom of the culture dish using a 5 ml pipette. The cells were pipetted gently up and down to disrupt cell clumps and then transferred into a sterile 15 ml centrifuge tube filled with 5 ml DMEM-Complete medium. The cells were spun down by centrifugation at 1000 rpm for 5 min. After aspiration of the supernatant the cell pellet can be used as required.



### ***3.2.3.3 Subculture adhesive cells***

After harvesting the cells by trypsinization (3.3.3.2), the cells were resuspended in an appropriate volume of prewarmed growth medium (DMEM-Complete medium) and plated on cell culture dishes.

### ***3.2.3.4 Freezing cells***

After harvesting the cells by trypsinization (3.3.3.2), the cells were resuspended in an appropriate volume of freezing medium (DMEM-Complete medium with 10% DMSO) at a density of  $3-5 \times 10^6$  cells/ml. 1.5 ml of cell suspension was transferred into each freezing vial. Then the vials were put on ice in a closed styropor box, incubated at  $-80^{\circ}\text{C}$  overnight and then stored in liquid nitrogen.

### ***3.2.3.5 Thawing cells***

Prewarmed growth medium was added to an appropriately sized cell culture dish. Then a vial of frozen cells was removed from liquid nitrogen. Subsequently, the thawed cell suspension was transferred into a cell culture dish containing prewarmed growth medium.

### ***3.2.3.6 Transfection of cells with lipofectamine 2000***

The day before transfection, the cells were plated in 5 ml of growth medium containing serum but no antibiotics in 35 mm dishes so that they were 90-95% confluent on the day of transfection. For each plate of cells to be transfected, 10  $\mu\text{g}$  of DNA was diluted in 300  $\mu\text{l}$  of MEM-medium (without serum etc.) and 25  $\mu\text{l}$  of Lipofectamine 2000 (LF2000 for abbreviation) reagent was diluted in 300  $\mu\text{l}$  MEM-Medium (without serum etc.). Then the diluted LF2000 was incubated for 5 min at room temperature. Once the LF2000 reagent is diluted, it must be combined with the DNA within 30 min and then incubated at room temperature for 20 min to allow DNA-LF2000 reagent complexes to form.

While the DNA-LF2000 reagent complexes were incubated, the cells were washed once carefully with MEM-medium (without serum etc.). Then the DNA-LF2000 reagent complexes (600  $\mu\text{l}$ ) were added directly to each plate and mixed gently by rocking the plate. After that, the cells were incubated at  $37^{\circ}\text{C}$  in a  $\text{CO}_2$  incubator for 4-6 h. Then growth medium was added and incubation proceeded until the cells were used for further experiments.

### ***3.2.3.7 Transfection of cells with DEAE-Dextran reagent***

#### ***3.2.3.7.1 Prepare transfection mixtures***

Immediately before transfection, transfection mixtures were prepared as following (indicated volumes are sufficient for one 10 cm cell culture dish):

400  $\mu$ l DEAE-Dextran (10x Stock) and 5  $\mu$ l Chloroquine (1000x Stock) were added to 4.6 ml DMEM-Incomplete (DMEM containing 7% Serum Plus<sup>TM</sup>, 2 mM glutamine) and mixed by shaking. Then 10  $\mu$ g of plasmid DNA was added and mixed.

#### ***3.2.3.7.2 Transfection***

The day before the transfection, COS cells were plated on 10 cm plates so that they were 70% confluent on the next day. Then the culture medium was soaked off and the cells were washed carefully once with 6 ml DMEM (without serum etc.). Subsequently, 5 ml of transfection mixtures were added to each plate and the cells were incubated for 4.5 h at 37°C/5% CO<sub>2</sub>. After that, the transfection mixtures were soaked off and 6 ml of PBS/10% DMSO was added to the cells and incubated for 3 min at RT. Then the PBS/DMSO solution was soaked off and the cells were washed carefully once with 6 ml of DMEM. Finally the DMEM was soaked off and 10 ml of DMEM complete medium was added and then the cells were incubated for 2-3 additional days.

### ***3.2.3.8 Selection of stably transfected cells***

Cells were transfected with plasmid containing the gene of interest by Lipofectamine 2000 in 35 mm cell culture dishes. 24 h after transfection, the cells were subcultured in 60 mm cell culture dishes without antibiotic selection. The next day the medium was exchanged against selection medium with appropriate antibiotics. The cells grown during 2-3 weeks in selection medium, which was changed every 2-3 days, were considered as stably transfected cells. Individual cell clones were isolated by seeding different dilutions of cells on 96 well plates.

## **3.2.4 Methods for analysis of ectodomain shedding**

### ***3.2.4.1 General procedures***

Cells were seeded on poly-L-Lysin coated cell culture dishes and incubated at 37°C overnight so that the next day the cells were 90-95% confluent. The cells were then washed carefully twice with washing medium (serum free DMEM), then secretion medium (serum free DMEM with 2 mM glutamine) containing different chemicals was added and the cells were incubated at 37 °C for indicated time points according to individual experiments. For experiment with protease inhibitors or other inhibitors, the cells were preincubated with growth medium containing

indicated concentration of inhibitors for 30 min and then the medium was replaced by secretion medium containing the same concentration of fresh inhibitors followed by incubation at 37°C for indicated periods according to individual experiments. All information about the chemicals used and incubation times in different experiments is summarized in Table 7.

**Table 7. Summary of inhibitors and activators used for analysis of shedding of RAGE**

Chemical	Character	Final concentration	Preincubation time	Incubation time
PMA (Phorbol-12-Myristat-13-Acetat)	phorbol ester	1 $\mu$ M	No	1.5-4 hours
APMA (P-aminophenylmercuric acetate)	mercuric metalloproteinase activator	70-350 $\mu$ M	No	15 minutes
E64	Cysteinproteases inhibitor	1.4 $\mu$ M	30 minutes	1.5 hours
Pefabloc-SC	Serinproteases	1 mM	30 minutes	1.5 hours
Pepstatin	Aspartatproteases	1.4 $\mu$ M	30 minutes	1.5 hours
DL-thiophran	Neprylisin inhibitor	1 mM	30 minutes	1.5 hours
GM6001	Metalloproteinases inhibitor	10 $\mu$ M or 50 $\mu$ M	30 minutes	1.5 hours
GI254023X	Metalloproteinases inhibitor	10 $\mu$ M	30 minutes	1.5 hours
GW280264X	Metalloproteinases inhibitor	10 $\mu$ M	30 minutes	1.5 hours
PD98059	MEK inhibitor	25 $\mu$ M	30 minutes	1.5 hours
Chelerythrine	PKC inhibitor	5 $\mu$ M	30 minutes	1.5 hours
A23187 (calcimycin)	Calcium ionophore	2 $\mu$ M	No	1.5 hours or 4 hours

#### ***3.2.4.2 Handling of the secretion medium***

After incubation for indicated periods, secretion medium was collected and centrifuged at 1500 rpm for 10 min to remove cell debris. Proteins in secretion medium were precipitated with 10% TCA as described in 3.2.2.2.

#### ***3.2.4.3 Handling of cells***

Cells were washed with PBS and were dissolved with protein sample buffer (Laemmli buffer or NuPAGE buffer). Then the cell lysates were stored at -20°C until use.

### **3.3 Data analysis**

The western blot analysis was quantified with the VersaDoc imaging software Quantity one (Biorad, München).

The software Sigmaplot 9.0 (Systat Software Inc., USA) was used for statistical analysis. All data are present as mean  $\pm$  SD. The unpaired one-tailed student's t-test was used for comparison of differences between two groups. Results were termed significance for  $p < 0.05$ .

## 4. Result

### 4.1 Overexpression of myc-RAGE or wild-type RAGE in Flp-In 293 cells as well as COS-7 cells

The human RAGE receptor gene encodes a protein of 404 amino acids with an expected molecular weight about 55 kDa. Both wild-type and myc-tagged human RAGE cDNAs were cloned into the pcDNA6/V5/HisB vector. The obtained pcDNA6-RAGE and pcDNA6-myc-RAGE/V5/His constructs were stably transfected into Flp-In 293 cells. In addition, pcDNA6-myc-RAGE/V5/His was also stably transfected into COS-7 cells. To confirm that both constructs are expressed, western blot analysis was performed with lysates from myc-RAGE/V5/His-Flp-In 293 cells, RAGE-Flp-In 293 cells and myc-RAGE/V5/His-COS-7 cells. A monoclonal anti-RAGE N-terminal antibody was used as primary antibody for wild-type RAGE and an anti-myc antibody (9E10) was used as primary antibody for myc-tagged RAGE. A 55 kDa band was detected in lysates from all three cell lines, while no signal was detected in mock transfected control Flp-In 293 cells (Figure 7). Furthermore, the myc-tagged RAGE protein showed no significant difference from wild-type RAGE in its molecular weight.

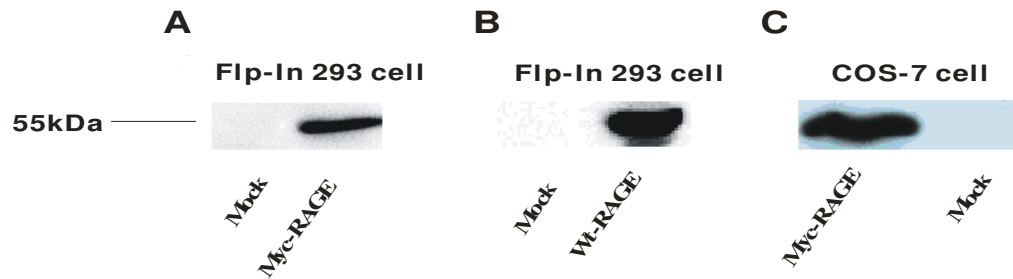


**Figure 7. Expression of either myc-tagged RAGE or wild-type RAGE in Flp-In 293 cells and COS-7 cells.**

Cell lysates of Flp-In 293 cells or COS-7 cells stably expressing myc-tagged RAGE or wild-type RAGE were separated by SDS-PAGE and blotted onto nitrocellulose membranes. The proteins were detected with mouse anti-myc antibody (9E10) and monoclonal anti-RAGE N-terminal antibody respectively. Myc-RAGE: myc-tagged RAGE. wtRAGE: wild-type RAGE. Mock: control vector. (A) and (B): Flp-In-293 cells. (C): COS-7 cells.

## 4.2 Human soluble RAGE is released from the cell membrane

### 4.2.1 Cleavage products of full-length RAGE

To investigate whether the extracellular domain of full-length RAGE is released from the cell membrane into the cell culture medium, myc-RAGE/V5/His-Flp-In 293 cell were grown to 95% confluence and incubated with serum-free DMEM containing 1% Glutamine (Secretion medium, SM) for 4 hours, the cell lysates as well as the precipitated protein from SM were analyzed by immunoblots as described in “Materials and Methods”.

As shown in Figure 8A lane 1, two close bands of about 48 kDa and 45 kDa were detected in SM by the 9E10 antibody, while an antibody against the C-terminal part of RAGE detected a 14 kDa fragment in cell lysates in addition to full-length RAGE (Figure 8B Lane 1). These data indicated that RAGE undergoes proteolytic cleavage.

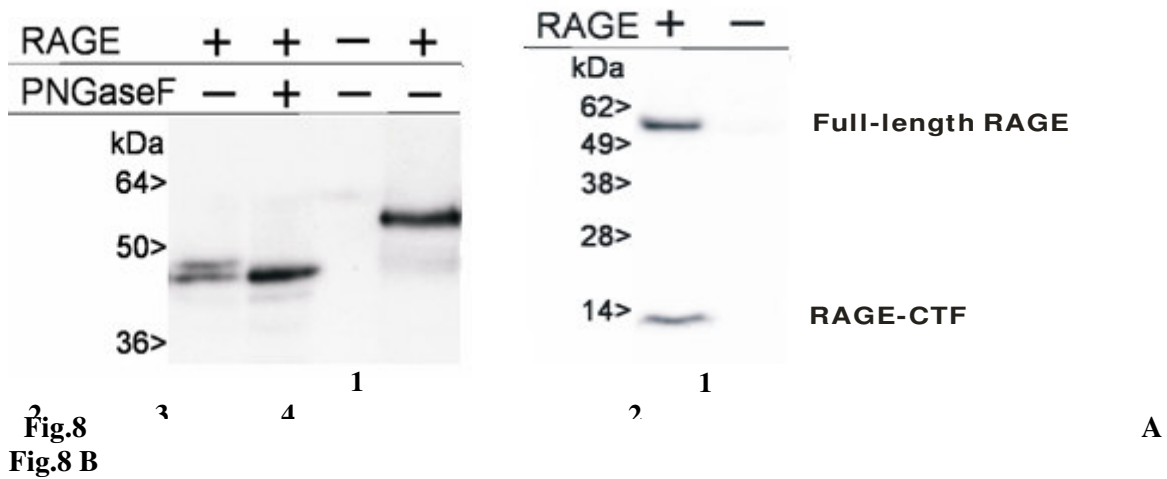


**Figure 8. Cleavage of epitope-tagged RAGE and glycosylation of sRAGE.**

Flp-In 293 cells stably expressing myc-tagged RAGE were incubated at 37°C for 4 hours with SM. Proteins in SM were precipitated with 10% TCA and cells were lysed in 2X Laemmli buffer. The cell lysates and the precipitated SM proteins were subjected to western blot analysis. Mouse anti-myc antibody (9E10) and mouse anti-V5 antibody were used as primary antibody for proteins in SM and cell lysates respectively. (A) Lane 1: sRAGE of about 48 kDa and 45 kDa detected in SM are N-terminal cleavage product of RAGE. Lane 2: unglycosylated sRAGE resulting from PNGaseF treatment. Lane 3: SM from mock transfected controls. Lane 4: full-length RAGE from cell lysates. (B) Lane 1: full-length (upper band) and cleaved C-terminal fragment (CTF, lower band) of myc-RAGE/V5/His in cell lysate. Lane 2: cell lysate from mock-transfected control cells.

#### 4.2.2 Glycosylation of secreted RAGE (sRAGE)

Furthermore, to examine whether the two detected isoforms of secreted RAGE are either differently glycosylated or result from two distinct proteolytic steps, we treated SM from myc-RAGE/V5/His -Flp-In 293 cells with PNGase F and then detected only the low molecular weight band (Figure 8A lane 2). This demonstrates that the two forms of sRAGE result from different glycosylation rather than from different proteolytic cleavage. In fact, it has been suggested that the first Ig-like domain of RAGE (V-domain) contains two potential N-linked glycosylation sites (Neeper *et al.* 1992). The importance of RAGE glycosylation has been demonstrated recently (Srikrishna *et al.* 2002). Presumably, N-linked glycosylation of sRAGE is of importance because sRAGE has the same ligand specificity as full-length RAGE. Actually, it was recently reported that sRAGE purified from mouse lung contains two potential N-glycosylation sites (Hanford *et al.* 2004). Thus the finding that human RAGE secreted from cultured cells appears as two different N-glycosylated forms is consistent with results of other reports.

#### 4.2.3 Full-length human RAGE is cell surface associated and the cleavage of RAGE occurs at the plasma membrane

Cell surface biotinylation has been considered as an important method to study the expression and regulation of receptors and transporters, and for differentiation of plasma membrane proteins from those localized to organelle membranes (Daniels and Amara 1998). The specificity of the Sulfo-NHS-Biotin reagents for cell surface labeling has been demonstrated in these applications (Liaw *et al.* 2001; Borroto *et al.* 2003). Because these molecules cannot penetrate the cell membrane, as long as the cell remains intact, only primary amines exposed on the cell surface will be biotinylated with the Sulfo-NHS-Biotin reagents.

To confirm the membrane localization of overexpressed RAGE in Flp-In-293 cells, cell surface biotinylation was performed as described in “Materials and Methods”. For biotinylation, cells were washed carefully twice with PBS and then incubated with 5mM Sulfo-NHS-Biotin reagents at room temperature for 30 min. Then cells were washed with TBS to stop the biotinylation. After washing, cells were incubated with SM containing either 1  $\mu$ M PMA, or 142  $\mu$ M APMA or equal amounts of DMSO for indicated time points (Figure 9). SM and cells were collected respectively and the biotinylated proteins were isolated with streptavidin-agarose beads. Biotinylated proteins in SM and cell lysates were analyzed by western blotting with the anti-RAGE N-terminal antibody. The results showed that full-length RAGE in cell lysates and secreted RAGE in SM

were biotinylated. In conclusion, this demonstrates that the RAGE receptor is located on the cell plasma membrane and moreover, that the cleavage of RAGE occurs at the plasma membrane (Figure 9).

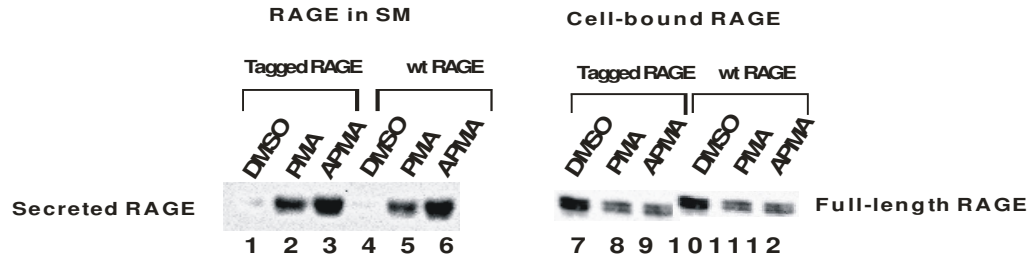


**Figure 9. RAGE is cell surface associated and the cleavage of RAGE occurs at the plasma membrane.**

myc-RAGE/V5/His-Flp-In-293 cells (lanes 1-3 and lanes 7-9) or RAGE-Flp-In-293 cells (lanes 4-6 and lanes 10-12) were biotinylated. After washing, cells were incubated with SM containing either 1  $\mu$ M PMA or equal amounts of DMSO for 2 hours, or 142  $\mu$ M APMA for 15 min. SM and cells were collected respectively and the biotinylated proteins were isolated with streptavidin-agarose beads. Biotinylated proteins in SM (lanes 1-6) and cell lysates (lanes 7-12) were analyzed by western blotting with the anti-RAGE N-terminal antibody.

### 4.3 Proteolysis of RAGE is both constitutive and regulated

Ectodomain shedding by proteolysis occurs in a constitutive as well as a regulated way. The most widely studied inducer of shedding is phorbol 12-myristate 13-acetate (PMA), which activates protein kinase C (PKC) (Schlondorff and Blobel 1999). Calcium ionophores, cytokines, growth factors and chemotactic peptides also induce shedding (Hooper *et al.* 1997). To test whether proteolysis of RAGE is also regulated, myc-RAGE/V5/His-Flp-In 293 cells or RAGE-Flp-In 293 cells were incubated with SM containing: PMA, calcium ionophore A23187, PKC inhibitor chelerythrin chloride, MAP kinase (MAPK) inhibitor PD98059, APMA or equal volumes of DMSO as control for indicated time as described in “Materials and Methods”.



### 4.3.1 Constitutive and PMA stimulated shedding of RAGE

In myc-RAGE/V5/His-Flp-In 293 cells and RAGE-Flp-In 293 cells, there was a certain level of constitutive shedding, which was increased upon stimulation with PMA (1  $\mu$ M) for 2 hours (Figure 10A). Similar experiments were performed with COS-7 cells transiently transfected with myc-tagged RAGE or wild-type RAGE expression constructs. Also in COS-7 cells shedding of RAGE was constitutive and PMA-inducible (Figure 10B).

Based on these results, one can conclude that shedding of RAGE is both constitutive and stimulated, which is common to most reported shedding events.

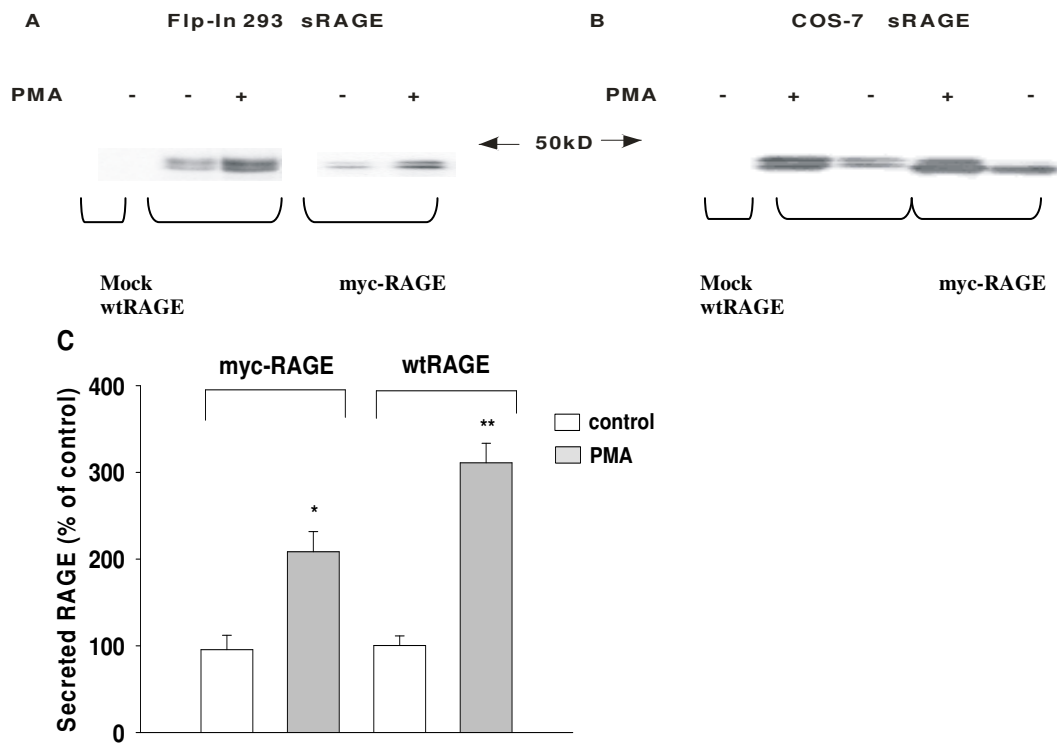


**Figure 10. Constitutive and PMA-stimulated shedding of RAGE.**

(A) myc-RAGE/V5/His-Flp-In 293 cells or RAGE-Flp-In 293 cells were incubated with 1  $\mu$ M PMA or an equal volume of DMSO for 2 hours. Proteins in secretion medium were precipitated with 10% TCA and then subjected to 10% SDS-PAGE followed by immunoblotting. The proteins were detected with either the mouse anti-myc antibody (9E10) or monoclonal anti-RAGE N-terminal antibody respectively. myc-RAGE: myc-tagged human RAGE. wtRAGE: wild type RAGE. Mock: negative control. (B) COS-7 cells transiently transfected with myc-tagged RAGE or wild-type RAGE were incubated with SM containing 1  $\mu$ M PMA or an equal volume of DMSO for 2 hours. Secreted RAGE in secretion medium was detected in the same way as in (A). (C) Graphic representation of density evaluation of immunoblotting from experiments showed in (A). The experiments were performed in triplicates for 3 times. The mean effect  $\pm$  SD were shown here and analyzed by unpaired student's t-Test: \*  $p < 0.05$ , \*\*  $p < 0.01$ .

### 4.3.2 APMA stimulated shedding of RAGE

P-aminophenylmercuric acetate (APMA), a mercuric metalloproteinase activator, is known to activate MMPs as well as ADAMs (Tsakadze *et al.* 2006). APMA can activate latent metalloproteinases by inducing the removal of the enzyme propeptide inhibitory region. To examine whether APMA can stimulate shedding of RAGE, myc-RAGE/V5/His-COS-7 cells were incubated with secretion medium containing different concentration of APMA up to 350  $\mu$ M for 15 min. secreted RAGE was analyzed in secretion medium by immunoblotting. As shown in Figure 11, APMA up-regulated the cleavage of RAGE. The increase of secreted RAGE in secretion medium corresponded to the gradient increase of APMA concentration. However, the amount of secreted RAGE in secretion medium reached to a maximum when 142  $\mu$ M APMA were added to secretion medium..

In conclusion, APMA could stimulate shedding of RAGE which suggests that shedding of RAGE may be mediated by metalloproteinases.

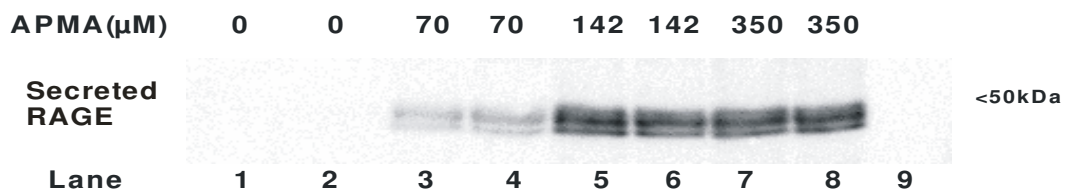


**Figure 11. Shedding of RAGE stimulated by APMA.**

Myc-RAGE/V5/His-COS-7 cells were incubated with secretion medium containing DMSO or indicated concentration of APMA for 15 min. Proteins in secretion medium were precipitated with 10% TCA and then subjected to 10% SDS-PAGE followed by immunoblotting. The proteins were detected with the mouse anti-myc antibody (9E10). Lanes 1-8: myc-RAGE/V5/His-COS-7 cell supernatant. Lane 9: supernatant of COS-7 cell transfected with the control vector pcDNA6/V5/HisB. This experiment was done with duplicates and repeated for at least 3 times.

### 4.3.3 Calcium ionophore stimulated shedding of RAGE

Calcium ionophores such as calcimycin (A23187) lead to a calcium influx into cells, resulting in the activation of a variety of cell signaling pathways that can be involved in shedding activation (Sanderson *et al.* 2005). To investigate whether A23187 have similar stimulatory effects as PMA on shedding of RAGE, RAGE-Flp-In 293 cells seeded in triplicate on poly-lysine coated 6-well plates. On the next day the cells were incubated with secretion medium containing either 2  $\mu$ M A23187 or 1  $\mu$ M PMA for 1.5 hours and 4 hours respectively, equal volumes of DMSO was used as negative control. sRAGE was analyzed in secretion medium by immunoblotting. Similar to

PMA, treatment with A23187 increased the level of sRAGE in secretion medium (Figure 12). Therefore calcium ionophores also stimulated shedding of RAGE, which suggests that calcium is implicated in the regulation of shedding of RAGE.

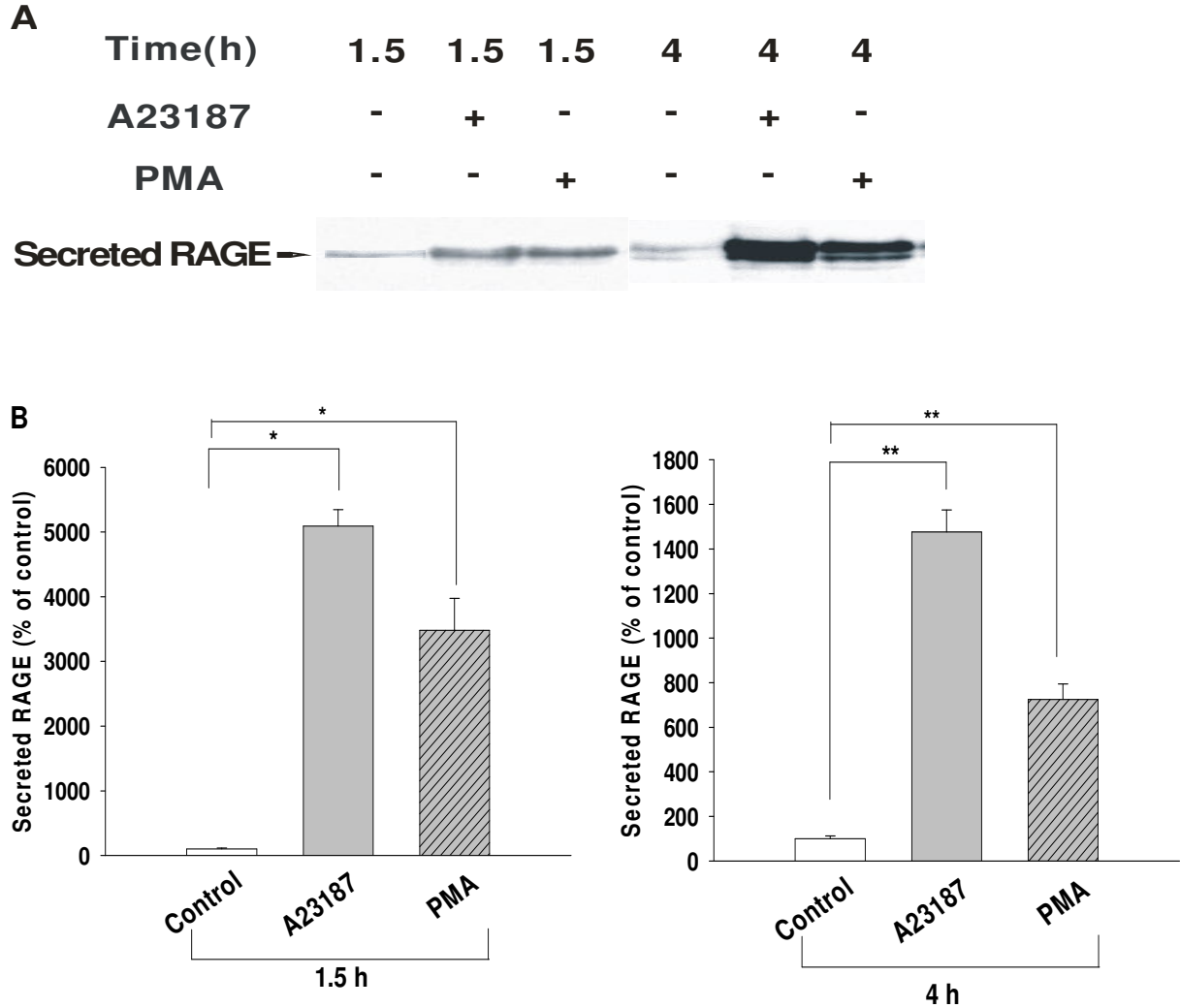


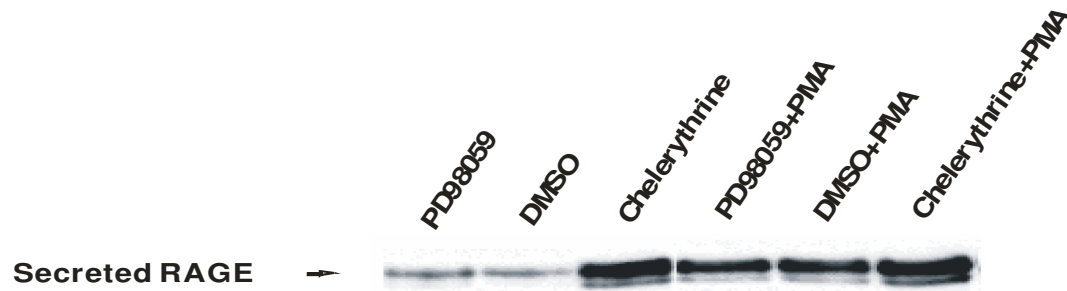
**Figure 12. Shedding of RAGE stimulated by a calcium ionophore.**

(A) RAGE-Flp-In 293 cells were incubated with secretion medium containing either 2  $\mu$ M of A23187 or 1  $\mu$ M PMA for indicated periods. Proteins in secretion medium were precipitated with 10% TCA and then subjected to 10% SDS-PAGE followed by immunoblotting. sRAGE in secretion medium was detected with the mouse anti-RAGE N-terminal antibody. (B) Graphic representation of density evaluation of immunoblotting from experiments showed in (A). The experiments were performed in triplicates for 3 times. The mean effect  $\pm$  SD were shown here and analyzed by unpaired student's t-Test: \*  $p < 0.01$ , \*\*  $p < 0.001$ .

#### 4.3.4 PD98059 does not affect shedding of RAGE whereas Chelerythrine enhances shedding of RAGE

The mechanism by which PMA stimulates shedding of transmembrane proteins remains largely unclear. Several reports have shown that PMA activated shedding is PKC-dependent (Hahn *et al.* 2003; Le Gall *et al.* 2003) while others have controversial results (Racchi *et al.* 1999). To test whether PKC or MAPK signaling pathways are involved in shedding of RAGE, RAGE-Flp-In 293 cells were treated with either chelerythrine (PKC inhibitor), or PD98059 (MEK inhibitor that blocks the MAPK/ERK pathway) alone or together with PMA as described in “Material and Methods”. Both inhibitors had no inhibitory effect on constitutive and PMA stimulated shedding of RAGE. On the contrary, to our surprise, chelerythrine enhanced the release of sRAGE in secretion medium under both constitutive and PMA stimulated conditions (Figure 13).

**A**



**B**

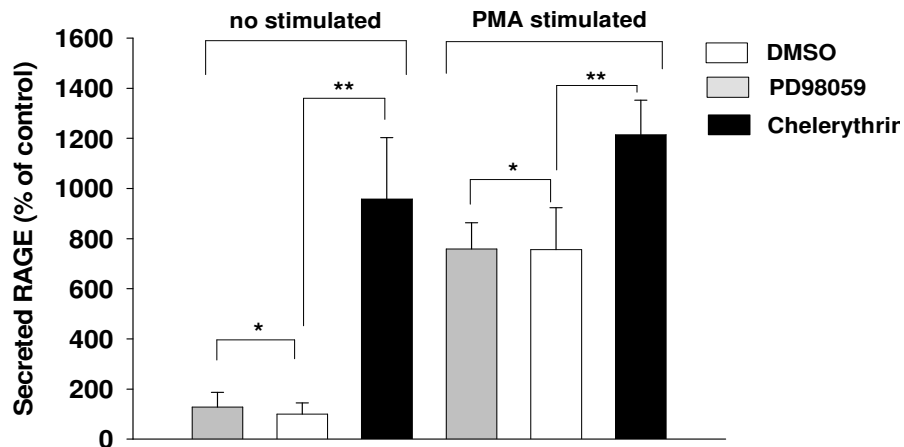


**Figure 13. Effects of chelerythrine and PD98059 on RAGE shedding.**

(A) RAGE-Flp-In 293 cells were treated with either chelerythrine (5  $\mu$ M), or PD98059 (25  $\mu$ M) alone or together with PMA for 1.5 hours. Proteins in secretion medium were precipitated with 10% TCA and then subjected to 10% SDS-PAGE followed by immunoblotting. Secreted RAGE in secretion medium was detected with the mouse anti-RAGE N-terminal antibody. (B) Graphic representation of density evaluation of immunoblotting from experiments showed in (A). The experiments were performed in triplicates for 3 times. The mean effect  $\pm$  SD were shown here and analyzed by Student's t-test. Since the MAPK pathway inhibitor PD98059 (25  $\mu$ M) had no effects on constitutive and

stimulated shedding of RAGE, the MAPK pathway is unlikely to play a role in shedding of RAGE. Based on the data that the PKC inhibitor chelerythrine could not inhibit PMA-stimulated shedding, one can assume that PMA-stimulated shedding can take place independently from activation of PKC. Interestingly, chelerythrine induced shedding has been demonstrated in a recent report where chelerythrine stimulated proteolytic processing of HB-EGF through a reactive oxygen species (ROS) dependent way (Kim *et al.* 2005). In this line, although chelerythrine is a potent PKC inhibitor, it was shown to induce intracellular ROS (Yu *et al.* 2000). The mechanism by which chelerythrine induces shedding of RAGE remains to be investigated, but it is likely that ROS induced by chelerythrine are involved in regulation of RAGE shedding.

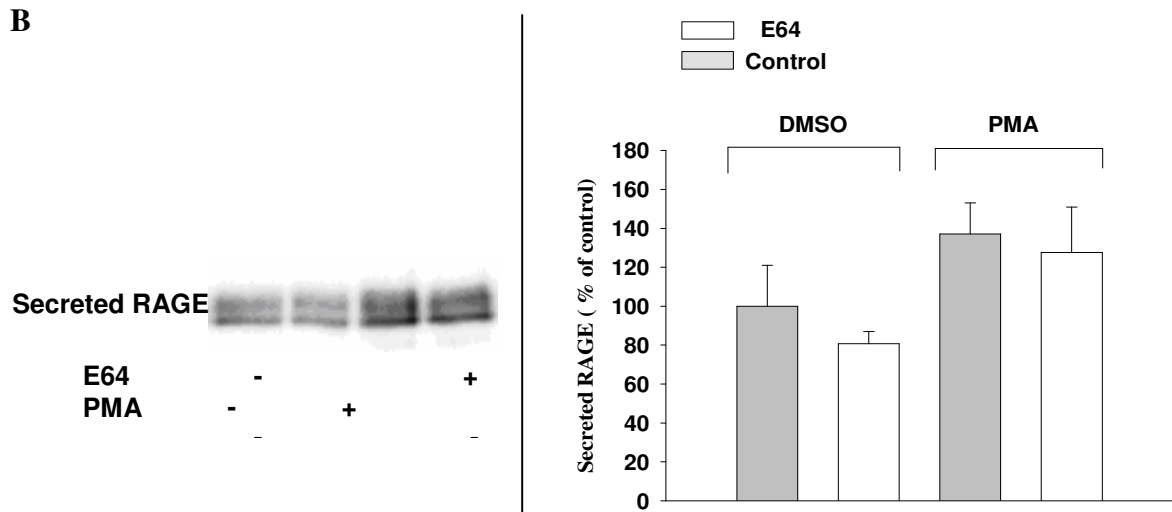
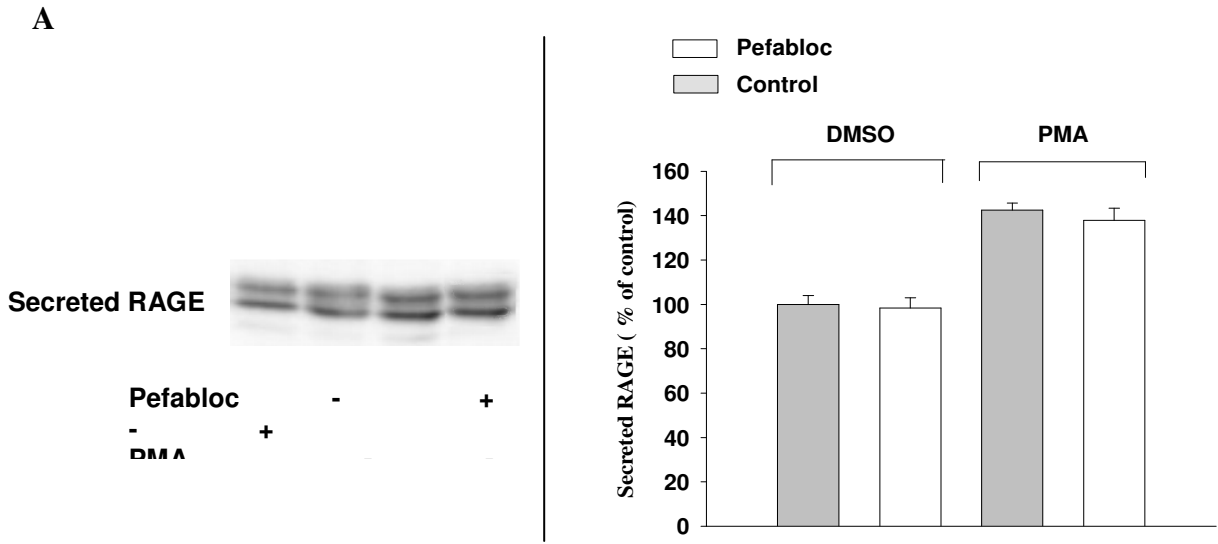
#### **4.4 The cleavage of RAGE is unaffected by several different proteases inhibitors**

To characterize which class of protease(s) might be involved in proteolysis of RAGE, the effects of various protease inhibitors were analyzed. The protease inhibitors used in the experiments are listed in Table 8.

**Table 8. Protease inhibitors, inhibition profile and experimental concentration**

<b>Name</b>	<b>Specificity</b>	<b>Concentration</b>
E-64	Cysteine Proteases	1.4 $\mu$ M
DL-Thiorphan	Nepilysin	1 mM
Pepstatin	Aspartic Proteases	1.4 $\mu$ M
Pefabloc SC	Serine Proteases	1 mM

RAGE-Flp-In 293 cells were preincubated with growth medium containing indicated inhibitors for 30 min and then the medium was change to secretion medium containing indicated concentration of different inhibitors. After 1.5 hours secretion medium was collected. The amount of secreted RAGE was measured by Western blot analysis with the mouse anti-RAGE N-terminal antibody (Figure 14 A-D). None of the inhibitors employed here had significant inhibitory effect on constitutive and PMA-stimulated cleavage of RAGE. Correspondingly, proteases inhibited by these inhibitors were excluded to be responsible for shedding of RAGE. These proteases include aspartic proteases, cysteine proteases, serine proteases and nepilysin.



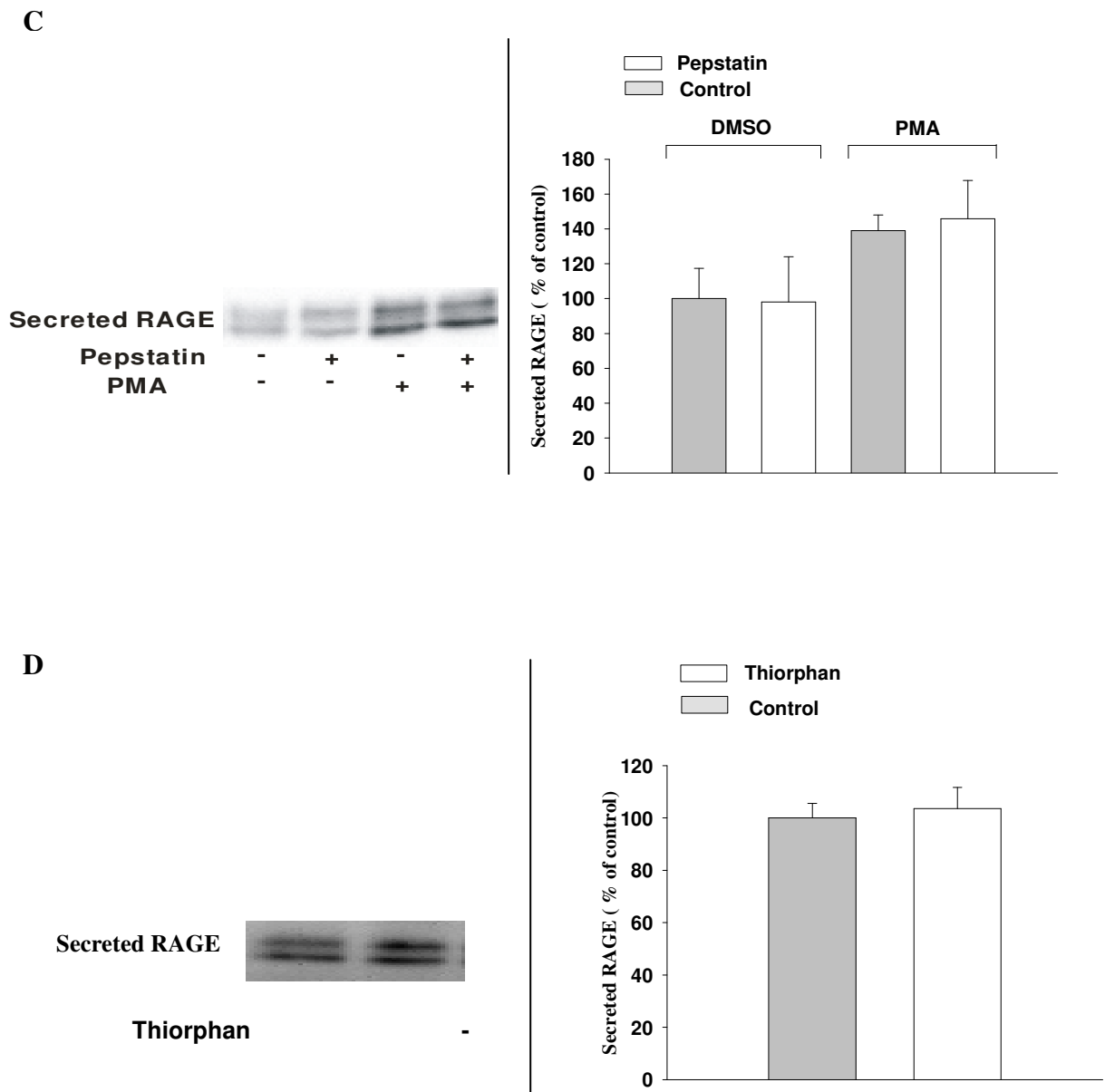


**Figure 14. Proteolysis of RAGE is unaffected by several protease inhibitors.**

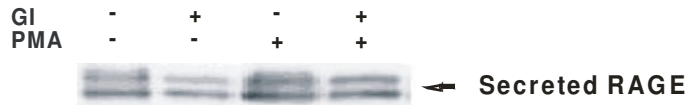
RAGE-Flp-In 293 cells were preincubated with growth medium containing indicated inhibitors for 30 min and then treated with secretion medium containing indicated inhibitors for 90 min at 37°C. Secretion medium was analyzed by immunoblotting with the anti-RAGE N-terminal antibody. **(A)** 1 mM Pefabloc with or without PMA (1  $\mu$ M). **(B)** 1.4  $\mu$ M E64 with or without PMA (1  $\mu$ M). **(C)** 1.4  $\mu$ M Pepstatin with or without PMA. **(D)** 1 mM DL-Thiorphan. Graphic representations of density evaluation from immunoblotting presented here are shown in the right. The experiments were performed in triplicates for 3 times. The mean effect  $\pm$  SD were shown here and analyzed by unpaired student's t-Test. All inhibitors presented here showed no effect on cleavage of RAGE.

#### 4.5 Shedding of RAGE is inhibited by metalloproteinase inhibitors

The majority of the shedding events are mediated by metalloproteinase including MMPs and ADAMs. Hydroxamic acid-based inhibitors, which bind the essential zinc ion at the active site of the protease, were originally designed as inhibitors of zinc-dependent matrix metalloproteinase. In addition, these inhibitors have been shown to inhibit protein ectodomain shedding of several different types of membrane proteins such as pro-EGF (Le Gall *et al.* 2003), pro-TGF- $\alpha$  (Arribas and Massague 1995), betacellulin (Sanderson *et al.* 2005), Fas ligand (Ethell *et al.* 2002), ACE2 (Lambert *et al.* 2005), and APP (Arribas *et al.* 1996; Parkin *et al.* 2002).

In order to identify which protease is involved in the cleavage of RAGE, the effects of three different hydroxamic acid-based metalloproteinase inhibitors were investigated as described in “Materials and Methods”. The amount of sRAGE in secretion medium was measured by western blot analysis. As shown in Figures 15-17, all three inhibitors GM6001, GW280264X, and GI254023X exhibited strong inhibitory effects on constitutive and stimulated shedding of RAGE without obvious differences among the three inhibitors at a concentration of 10  $\mu$ M.

**A**



**B**

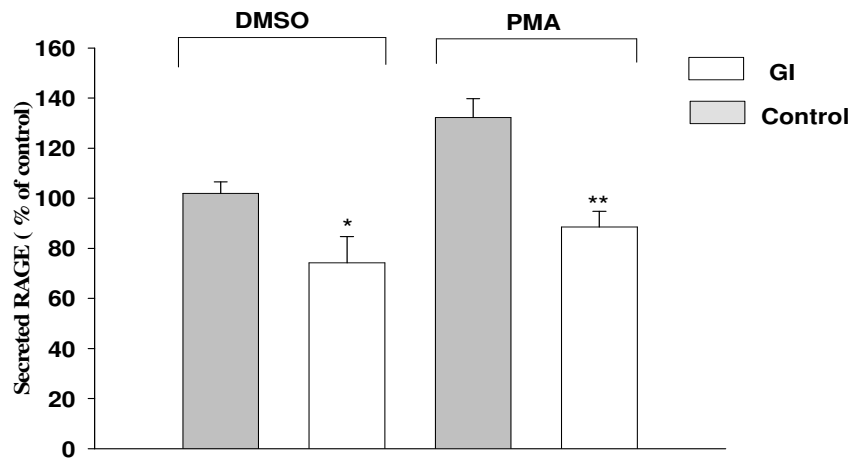


**Figure 15. Shedding of RAGE inhibited by the metalloproteinase inhibitor GI254023X.**

(A) myc-RAGE/V5/His-Flp-In-293 cells were preincubated with 10  $\mu$ M GI254023X or control solvent DMSO at 37°C for 30 min, then the medium was changed to secretion medium containing fresh 10  $\mu$ M GI254023X alone or together with PMA (1  $\mu$ M) or control solvent. Subsequently the samples were incubated at 37°C for 1.5 hour and then the release of secreted RAGE was detected by western blot analysis with the mouse anti-myc antibody (9E10). (B) Graphic representation of density evaluation from immunoblotting shown in (A). The experiments were performed in triplicates for 3 times. The mean effect  $\pm$  SD were shown here and analyzed by unpaired student's t-Test: \*  $p < 0.05$ , \*\*  $p < 0.01$ .



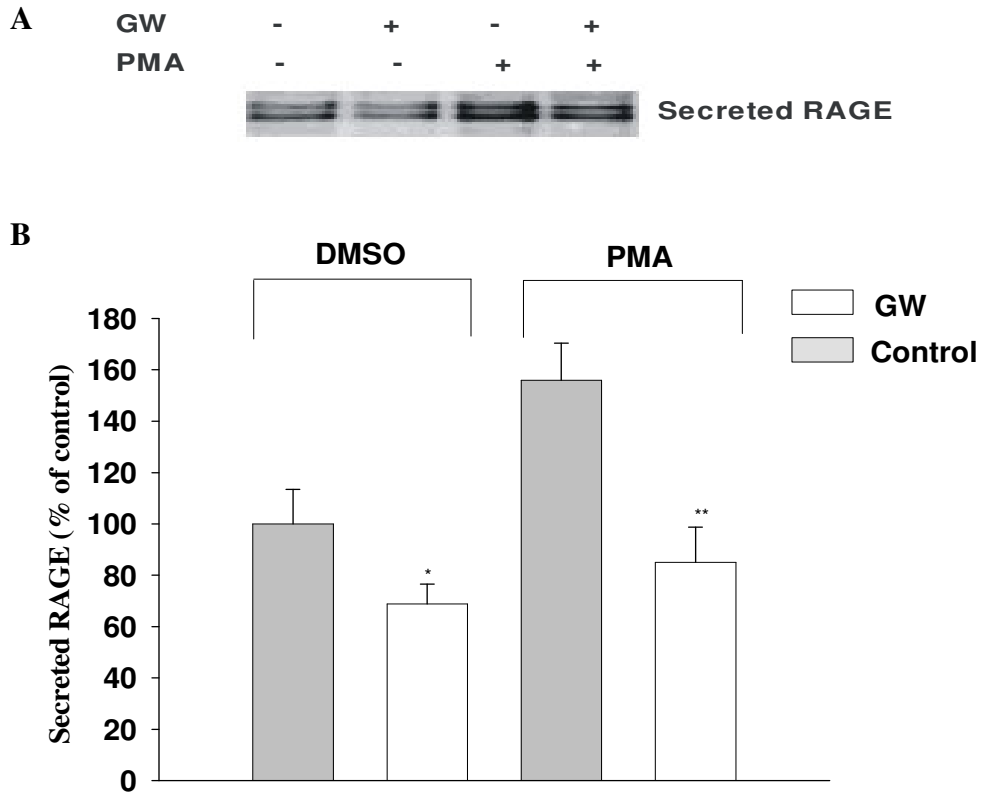


**Figure 16. Shedding of RAGE inhibited by the metalloproteinase inhibitor GW280264X.**

(A) myc-RAGE/V5/His-Flp-In-293 cells were preincubated with 10  $\mu$ M GW280264X or control solvent DMSO at 37°C for 30 min, then the medium was changed to secretion medium containing fresh 10  $\mu$ M GW280264X alone or together with PMA (1  $\mu$ M) or control solvent. Subsequently the samples were incubated at 37°C for 1.5 hour and then the release of sRAGE was detected by western blot analysis with the mouse anti-myc antibody (9E10). (B) Graphic representation of density evaluation from immunoblotting shown in (A). The experiments were performed in triplicates for 3 times. The mean effect  $\pm$ SD were shown here and analyzed by unpaired student's t-Test: \*  $p < 0.05$ , \*\*  $p < 0.01$ .

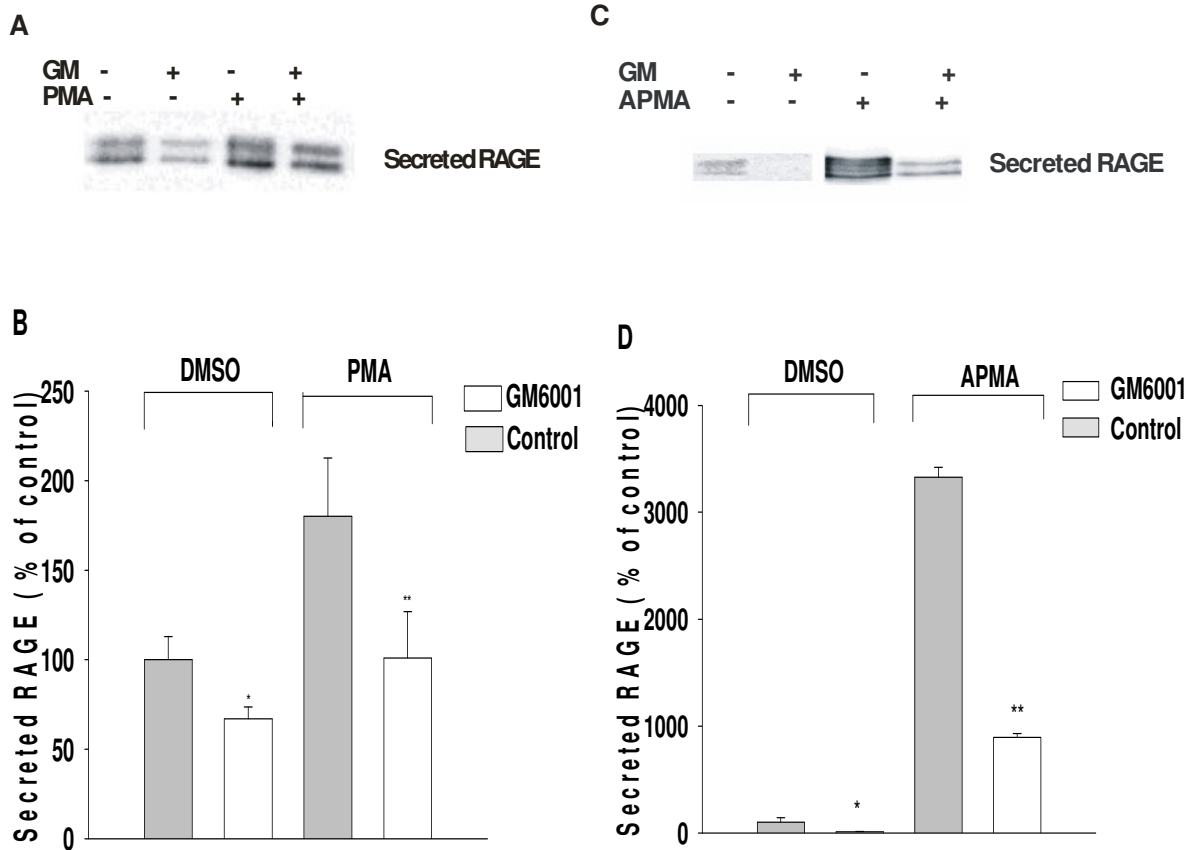


**Figure 17. Shedding of RAGE inhibited by the metalloproteinase inhibitor GM6001.**

(A) myc-RAGE/V5/His-Flp-In-293 cells were preincubated with 10  $\mu$ M GM6001 or control solvent DMSO at 37°C for 30 min, then the medium was changed to secretion medium containing fresh 10  $\mu$ M GM6001 alone or together with PMA or control solvent. Subsequently the samples were incubated at 37°C for 1.5 hours and then the release of sRAGE was detected by western blot analysis with the mouse anti-myc antibody (9E10). (B) Graphic representation of density evaluation from immunoblotting shown in (A). The experiments were performed in triplicates for 3 times. The mean effect  $\pm$  SD were shown here and analyzed by unpaired student's t-Test: \*  $p < 0.01$ , \*\*  $p < 0.05$ . (C) myc-RAGE/V5/His-Flp-In 293 cells were preincubated with 50  $\mu$ M GM6001 or control solvent DMSO at 37°C for 30 min, then the medium was changed to secretion medium containing fresh 50  $\mu$ M GM6001 alone or together with 142  $\mu$ M APMA or control solvent. Subsequently the samples were incubated at 37°C for 1.5 hours and then the release of sRAGE in secretion medium was detected by western blot analysis with the mouse anti-myc antibody (9E10). (D) Graphic representation of density evaluation from immunoblotting shown in (C). The experiments were performed in triplicates for 3 times. The mean effect  $\pm$  SD were shown here and analyzed by unpaired student's t-Test: \*  $p < 0.05$ , \*\*  $p < 0.001$ .

shown in Figure 17C, at higher concentration, GM6001 (50  $\mu$ M) completely inhibited the release of RAGE into the secretion medium, and furthermore, APMA-stimulated shedding of RAGE was almost completely inhibited.

Among the tested inhibitors, GM6001 inhibits a broad spectrum of MMPs as well as ADAMs, while GW280264X and GI254023X differ in their ability to inhibit TACE and ADAM10.

GW280264X blocks both TACE and ADAM10, whereas GI2254023X has potent ADAM10 inhibitory activity with minimal activity on TACE. In addition to TACE and ADAM10, GW280264X and GI254023X also have potent inhibitory effect on other MMPs such as MMP1, MMP3, MMP9 and MMP13. The IC<sub>50</sub> values (Table 9) for GW280264X and GI2254023X were recently tested (Ludwig *et al.* 2005).

**Table 9. IC<sub>50</sub> values of two metalloproteinase inhibitors for recombinant metalloproteinases**

Compound	MMP1	MMP3	MMP9	MMP13	ADAM10	ADAM17
GW280264X	94*	17	10	4	12	8
GI2254023X	108	187	2.5	1.1	5.3	541

\* The inhibitor concentration required for half maximal inhibition was calculated from the inhibition kinetics and are given in nM. (Adapted from Ludwig *et al.*, 2005)

The above data provide strong evidence that the cleavage of RAGE is mediated by metalloproteinase. However, as all three inhibitors used here have similar inhibition effect on shedding of RAGE, it remains to be determined which metalloproteinases mediate the cleavage of RAGE.

#### **4.6 ADAM10 and ADAM17 are not essential for constitutive or stimulated shedding of RAGE**

Two related ADAMs termed ADAM10 and ADAM17 have been implicated in a number of shedding events. ADAM17 (also known as TACE) was the first protease shown to be responsible for shedding of pro-TNF- $\alpha$  (Black *et al.* 1997). Furthermore, numerous reports indicated that ADAM17 is a common protease required for the shedding of many more proteins (Moss and Lambert 2002; Zheng *et al.* 2004). ADAM10 shares higher homology in the catalytic domain to ADAM17 than to any other protease of the ADAM family. ADAM10 was first to be confirmed as  $\alpha$ -secretase of APP (Lammich *et al.* 1999). Later on, several other membrane proteins were found to be cleaved by ADAM10 (Schafer *et al.* 2004; Gough *et al.* 2004; Yan *et al.* 2002; Matthews *et al.* 2003).

To determine whether ADAM10 or ADAM17 is involved in shedding of RAGE, a gain of function approach was used to examine whether overexpression of either ADAM10 or ADAM17 leads to increased shedding of RAGE. To this end, COS-7 cells were transiently co-transfected with pcDNA6-myc-RAGE-V5/His and HA-tagged ADAM10 or ADAM17 expression vectors. 48 hours after transfection, cells were incubated with secretion medium containing DMSO or PMA

at 37°C for indicated periods (See Figures 18-19). The amount of secreted RAGE in secretion medium was detected by western blot analysis with the anti-myc antibody. The expression of ADAMs was analyzed in cell lysates with an anti-HA antibody respectively (refer to “Materials and Methods”).

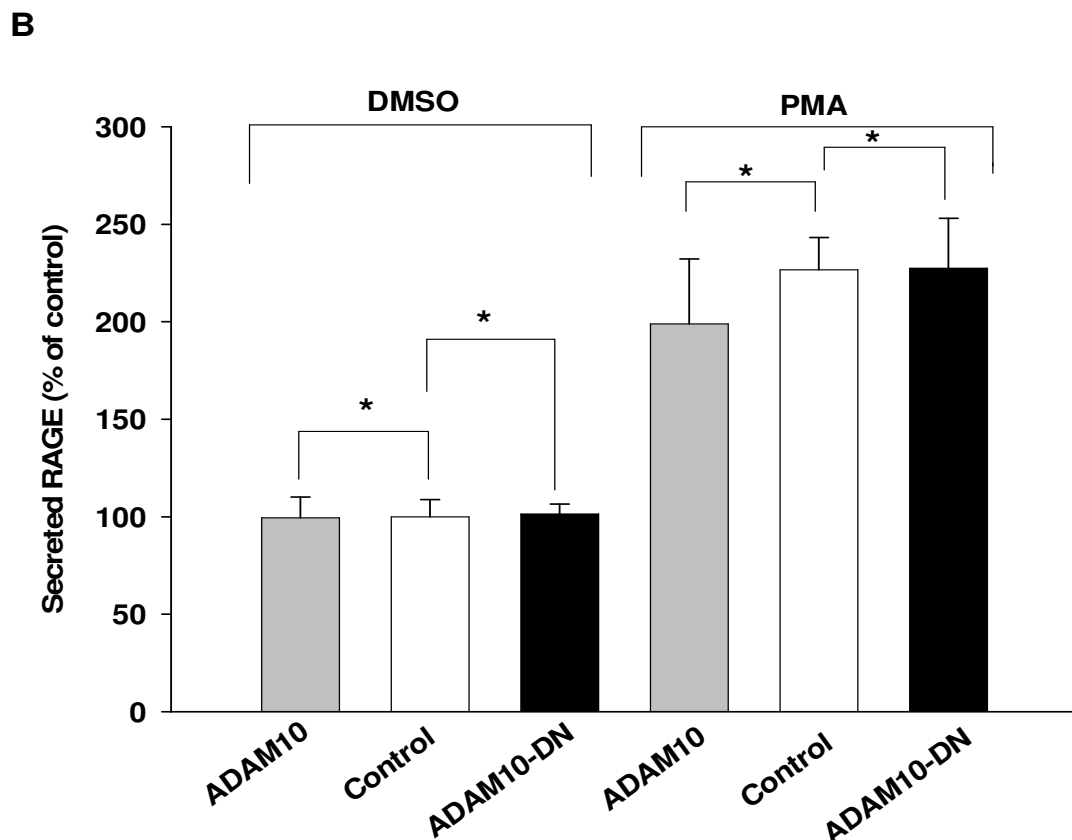
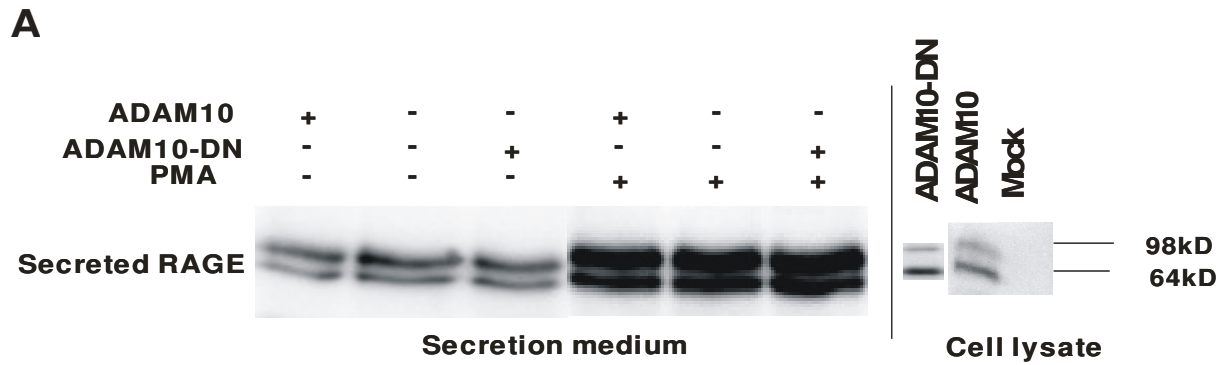


**Figure 16. Shedding of RAGE is unaffected by ADAM10.**

(A) COS-7 cells were transiently co-transfected with RAGE and ADAM10 or dominant negative ADAM10 (ADAM10-DN) expression vectors. 48 hours post-transfection, cells were incubated with secretion medium for 4 hours or with secretion medium containing 1  $\mu$ M PMA for 2 hours. Proteins in secretion medium were precipitated with 10% TCA and cells were harvested as described in Materials and Methods. Secreted RAGE in secretion medium was detected by western blotting with the mouse anti-myc antibody (9E10). The expression of ADAM10 and ADAM10-DN was detected in cell lysates with an anti-HA antibody. (B) Graphic representation of density evaluation from such experiments presented in (A). The experiments were performed in triplicates for 3 times. The mean effect  $\pm$  SD were shown here and analyzed by unpaired student's t-Test: \*  $P > 0.05$

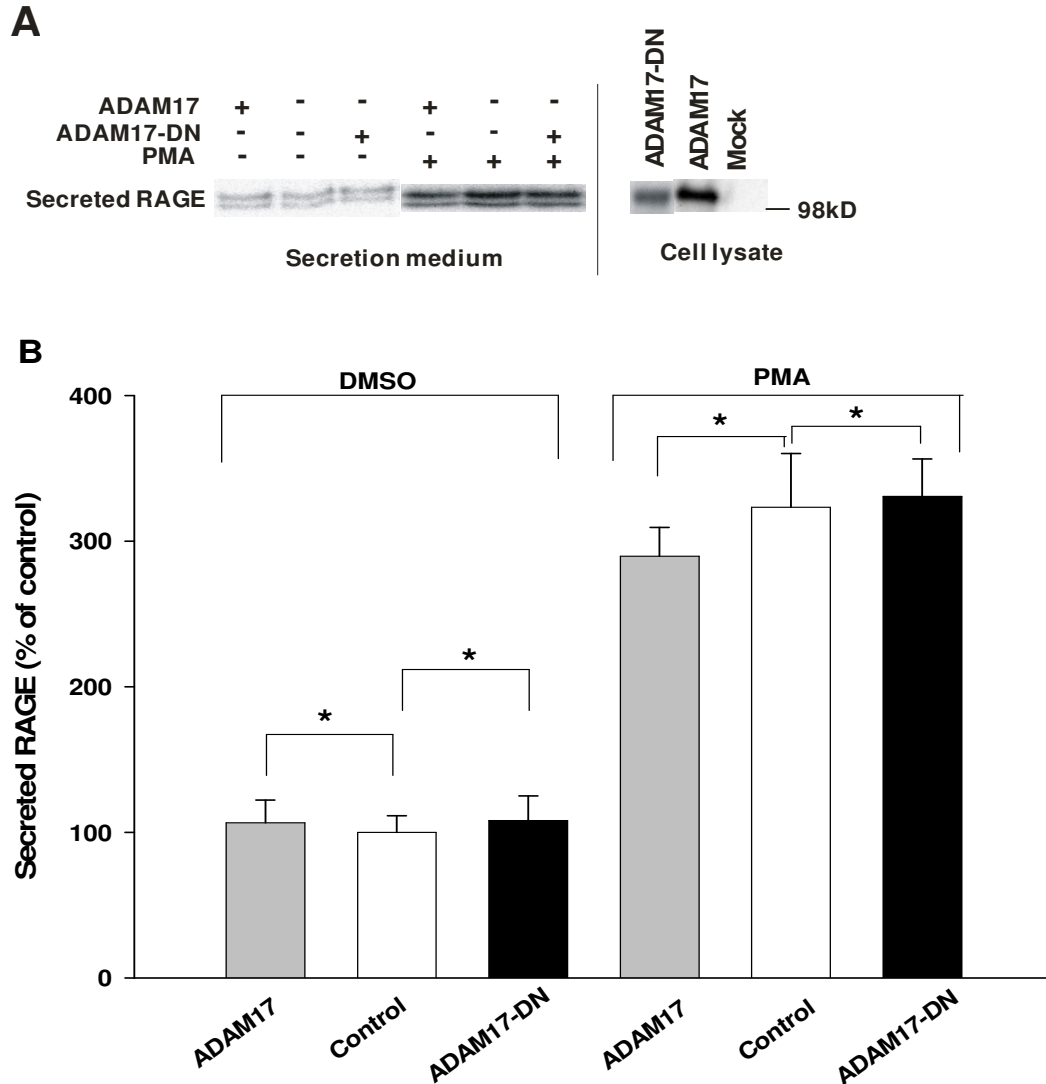


**Figure 19. Shedding of RAGE is unaffected by ADAM17.**

COS-7 cells were transiently co-transfected with RAGE and ADAM17 or putative dominant negative ADAM17 (ADAM17-DN) expression vectors. 48 hours post-transfection, cells were incubated with secretion medium for 4 hours or with secretion medium containing 1  $\mu$ M PMA for 2 hours. (A) Proteins in secretion medium were precipitated with 10% TCA and cells were harvested as described in Materials and Methods. Secreted RAGE in secretion medium was detected by western blotting with the mouse anti-myc antibody (9E10). The expression of ADAM17 and ADAM17-DN was detected in cell lysates with anti-HA antibody. (B) Graphic representation of density evaluation from such experiments presented in (A). The experiments were performed in triplicates for 3 times. The mean effect  $\pm$  SD were shown here and analyzed by unpaired student's t-Test: \*  $P > 0.05$

As shown in Figure 18, ADAM10 was expressed well in COS-7 cells. However, no significant difference in the amount of secreted RAGE derived from constitutive shedding or PMA stimulated shedding in secretion medium from cells overexpressing both RAGE and ADAM10 compared to that of cells overexpressing only RAGE was observed. Similarly, ADAM17 was expressed (Figure 19) and also had no observable effects on the amount of secreted RAGE

derived from either constitutive shedding or PMA stimulated shedding. Based on these data, it is likely to conclude that neither ADAM10 nor ADAM17 have any effects on constitutive and stimulated shedding of RAGE.

To further confirm this conclusion, dominant negative (DN) mutants of ADAM10 or ADAM17 were used to block endogenous ADAM10 or ADAM17 activity. If ADAM10 or ADAM17 indeed is involved in shedding of RAGE, then their dominant negative mutants should inhibit shedding of RAGE. Therefore, COS-7 cells were transiently co-transfected with pcDNA6-myc-RAGE-V5/His and ADAM10-DN (catalytically inactive by mutation of its 384th residue from Glu to Ala) or ADAM17-DN (catalytically inactive by mutation of its 406th residue from Glu to Ala) expression vectors. 48 hours after transfection, cells were incubated with secretion medium containing DMSO or PMA at 37° C for indicated periods. The amount of secreted RAGE in secretion medium was detected by western blot with anti-myc antibody.

ADAM10-DN and ADAM17-DN had no detectable effects on the amount of secreted RAGE derived from constitutive and PMA stimulated shedding. Thus neither ADAM10-DN nor ADAM17-DN has an effect on shedding of RAGE. However, the ADAM17-DN mutant does not act in a dominant negative way on shedding of APP (personal information from Kristina Endres). Therefore the results obtained with ADAM17-DN and RAGE have to be considered with caution. In the case of ADAM10 a specific knockdown of ADAM10 with siRNA had no effect on shedding of RAGE (see results part 4.8.3.2, Figure 26.)

Taken together, the results from two complementary experimental approaches strongly support the argument that ADAM10 and ADAM17 are not essential for constitutive or stimulated shedding of RAGE.

#### 4.7 Overexpression of MT1-MMP does not affect constitutive and stimulated shedding of RAGE

Membrane-type metalloproteinase, MT1-MMP (also known as MMP14) is responsible for cleavage of several transmembrane proteins such as CD44 (Kajita *et al.* 2001), TRANCE (Schlondorff *et al.* 2001), TGF- $\beta$  (Karsdal *et al.* 2002; Mu *et al.* 2002), syndecan-1 (Endo *et al.* 2003). Most recently, MT1-MMP was reported to mediate shedding of MUC1, a transmembrane mucin (Thathiah and Carson 2004). To address whether MT1-MMP plays a role in cleavage of RAGE, COS-7 cells were transiently co-transfected with pcDNA6-RAGE/V5/His and a vector encoding HA-tagged MT1-MMP. 48 hours after transfection, cells were incubated with secretion medium containing 1  $\mu$ M PMA for 2 hours or an equal volume of DMSO for 4 hours at 37° C. Secreted RAGE was detected by western blot analysis with the anti-RAGE N-terminal antibody and the expression of MT1-MMP was analyzed in cell lysates with an anti-HA antibody.

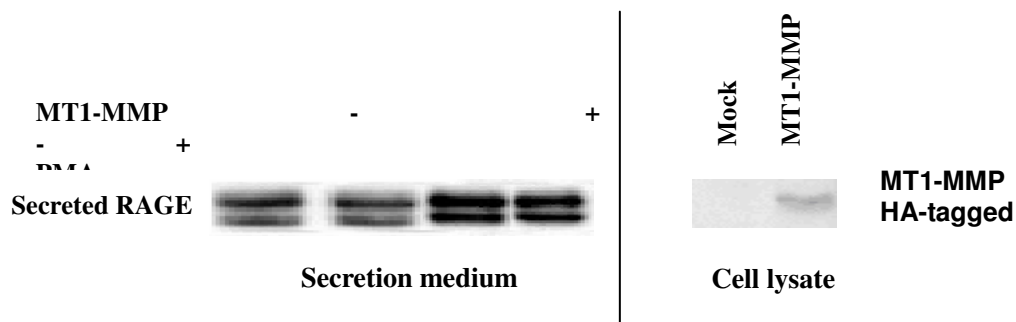


**Figure 20. Overexpression of MT1-MMP does not influence shedding of RAGE.**

COS-7 cells were transiently co-transfected with expression vectors encoding RAGE and MT1-MMP. 48 hours post-transfection, cells were incubated with secretion medium for 4 hours or with 1  $\mu$ M PMA for 2 hours. (A) Proteins in secretion medium were precipitated with 10% TCA, and then separated by SDS-PAGE. Subsequently, western blot analysis for detection of secreted RAGE with the anti-RAGE N-terminal antibody was performed. (B) Cells were harvested and lysed. Expression of MT1-MMP was detected in cell lysates with an anti-HA antibody.

As shown in Figure 20, the data gave no evidence that overexpression of MT1-MMP has an impact on constitutive and PMA stimulated shedding of RAGE.



## 4.8 Shedding of RAGE by MMP9

Having excluded ADAM10, ADAM17 and MT1-MMP as metalloproteinases responsible for shedding of RAGE, other metalloproteinase candidates were considered. Recent evidence indicated that soluble RAGE purified from mouse lung may be generated as the result of protein cleavage instead of mRNA splicing (Hanford *et al.* 2004). In this line, it is interesting to note that MMP9 has been suggested to cause murine pulmonary epithelial cells to shed RAGE into the culture medium (Devaux *et al.* 2004). Therefore, it was investigated whether human MMP9 is indeed involved in cleavage of human RAGE. To achieve this, suitable cell models for MMP9 expression were established and furthermore, methods to assess the activity of expressed MMP9 were optimized.

### 4.8.1 MMP9 zymography assay

COS cells serve as an ideal model to study MMPs because these cells constitutively express only small amounts of endogenous MMPs while express high level of proteins in response to transfection with cDNAs (Cao *et al.* 2005). To assess if MMP9 is a specific metalloproteinase responsible for the shedding of human RAGE, firstly a COS-7 cell line stably overexpressing human MMP9 was established (designated as MMP9-COS cells). To this end, COS-7 cells were transfected with plasmid pIRESneo2-hMMP9 and subsequently selected by G418 to get a stable cell line overexpressing human MMP9 (see “Materials and Methods”). The MMP9-COS cells were grown to 90% confluence and then the growth medium was replaced by secretion medium followed by incubation for 18 hours at 37° C. At the end of incubation, secretion medium was collected and centrifuged to sediment the cell debris. MMP9 expression as well as activity in secretion medium was analyzed by gelatine zymography as described in “Materials and Methods”. After staining the gel with Coomassie Brilliant Blue R250, clear areas represent gelatinase activity of MMP9 (Figure 21 lanes 1, 3-6). In addition, the shedding activators PMA (Figure 21 lanes 3-4) and APMA (Figure 21 lanes 5-6) were tested for their possible effects on expression and/or activity of MMP9 with similar methods.

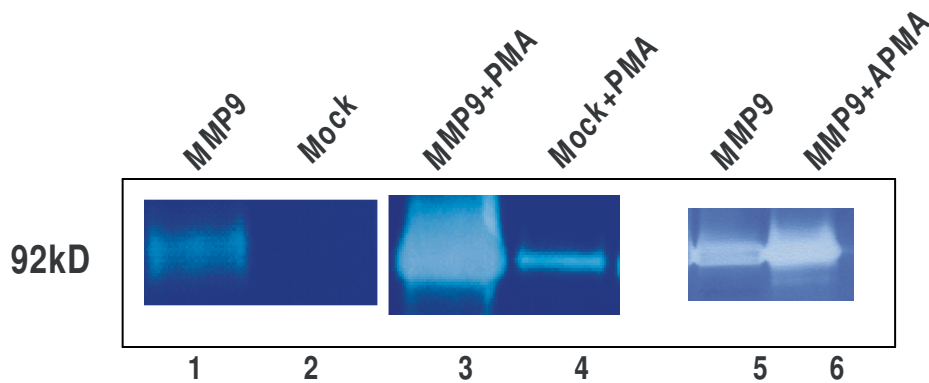


**Figure 21. Expression and activity of human MMP9 in secretion medium from COS-7 cells.**

**Lane 1-2:** Secretion medium from MMP9-COS cells was tested by gelatine zymography assay. COS-7 cells stably transfected with control vector pIRESneo2 were used as negative control. **Lane 3-4:** MMP9-COS cells and control cells were incubated with secretion medium containing 1  $\mu$ M PMA for 18 hours. Secretion medium was collected and subjected to gelatine zymography assay. **Lane 5-6:** MMP9-COS cells were incubated with secretion medium for 18 hours. Then APMA to a final concentration of 142  $\mu$ M or a same volume of DMSO was added and incubated for another 30 min. Secretion medium was collected and subjected to the gelatine zymography assay.

As expected, a 92 kDa clear band was revealed in MMP9-COS cells (Figure 21 lane 1). In contrast, there was no detectable MMP9 activity in control COS-7 cells (Figure 21 lane 2). Under unstimulated conditions, secretion medium from MMP9-COS cells had higher gelatinase activity compared to control COS-7 cells which had nearly no gelatinase activity (compare Figure 21 lane 1 to lane 2). Importantly, under PMA stimulation, the MMP9 gelatinase activity could be observed even in control COS-7 cells and was significantly increased in MMP9-COS cells (Figure 21 Lanes 3-4).

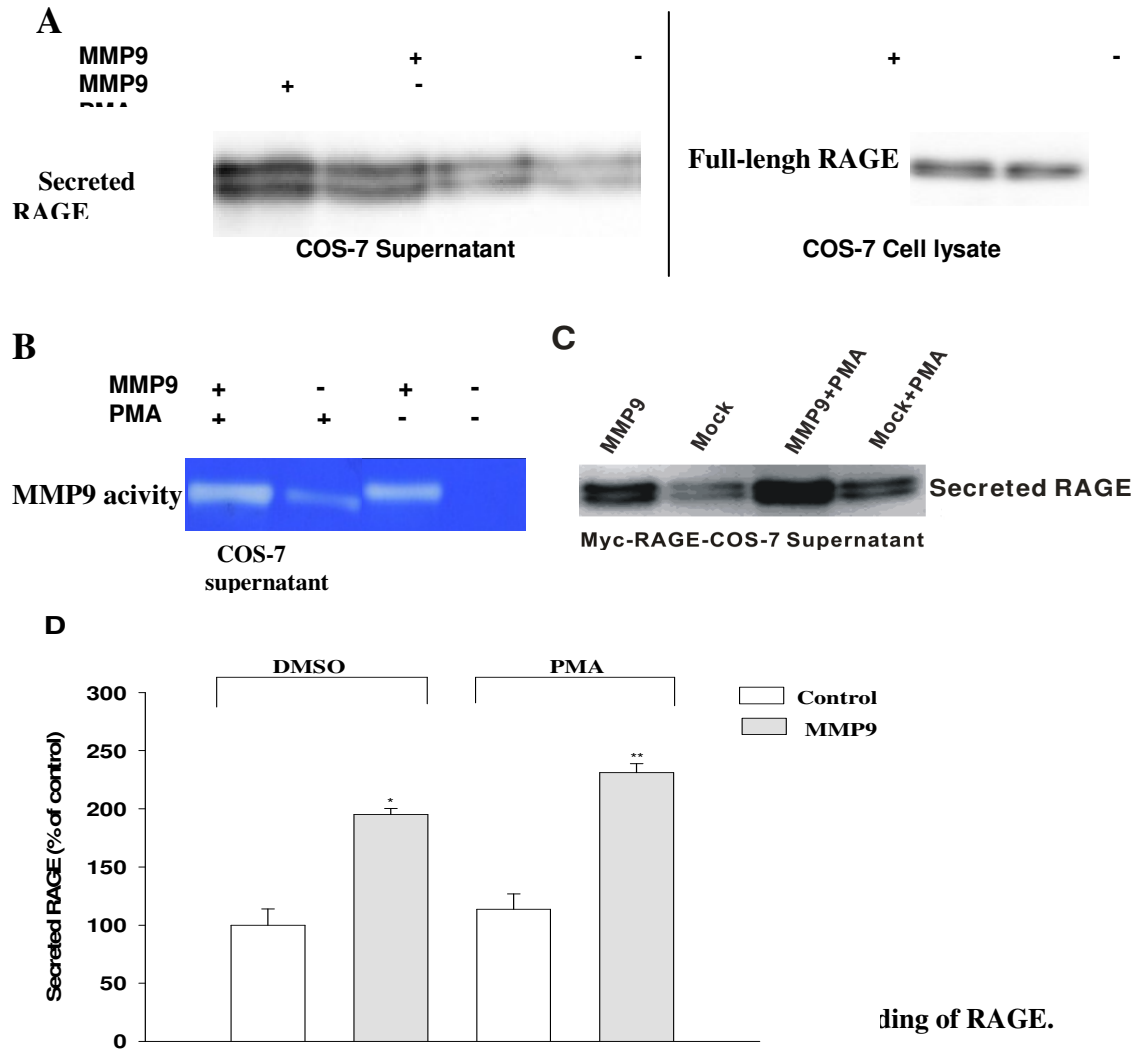
How can PMA increase endogenous MMP9 activity? Up to now, several mechanisms have been postulated on the regulation of MMP9 activity: (1) MMP9 gene transcription; (2) MMP9 proenzyme activation and (3) inhibition by endogenous inhibitor such as tissue inhibitors of metalloproteinase (TIMPs) (Chakraborti *et al.* 2003). Inducers of MMP9 gene transcription range from oncogenic proteins, cytokines, mitogens to phorbol esters (Woo *et al.* 2005). Indeed, it has been reported that PMA can trigger two independent signaling pathways in endothelial cells leading to MMP9 expression, one being the PKC/Raf/MEK/ERK cascade, and the other involving Ras but not ending in ERK activation (Genersch *et al.* 2000). So it is likely that PMA induces MMP9 mRNA transcription resulting in an increase of MMP9 activity as observed here. Moreover, APMA increased gelatinase activity of secretion medium from MMP9-COS cells

(Figure 21 lanes 5-6). APMA causes the cysteine of the MMP9 prodomain to become dissociated from the zinc ion of the catalytic core; consequently, the proteinase undergoes autocatalytic cleavage resulting in activation of the enzyme. This is called as “cysteine switch” mechanism for activation (Springman *et al.* 1990). Therefore the “cysteine switch” mechanism may explain the observation that APMA increases MMP9 activity.

#### **4.8.2 Enhancement of shedding of RAGE via overexpression of MMP9**

To further examine the involvement of MMP9 in RAGE shedding, COS-7 cells were transiently co-transfected with MMP9 and wild-type RAGE expression plasmids. Successful overexpression of MMP9 was confirmed by the gelatine zymography assay with secretion medium from MMP9 overexpressing cells. 48 hours after transfection, cells were treated with secretion medium with or without PMA for indicated periods (See Figure 22). Then secretion medium and cells were collected and secretion medium was subjected to 10% TCA precipitation followed by 10% SDS-PAGE. Analysis of secreted RAGE in secretion medium by western blot analysis with anti-RAGE N-terminal antibody revealed that overexpression of MMP9 increased constitutive and PMA simulated shedding of RAGE compared to mock transfected cells (Figure 22A left). All overexpression experiments were repeated at least 3 times and each time in triplicate. A representative result is shown here. Obviously, overexpression of MMP9 could increase secreted RAGE levels in secretion medium compare to mock transfected cells. Furthermore, the increased shedding of RAGE corresponded well with the increased activity of MMP9 in secretion medium as revealed by gelatine zymography (Figure 22B). Cell lysates were also analyzed to confirm that overexpression of MMP9 had no effect on expression levels of full-length RAGE (Figure 22A right).

In additional experiments, myc-RAGE/V5/His-COS cells were treated with conditioned medium (CM) collected from stable MMP9-COS cells in the presence or absence of PMA (1  $\mu$ M) as described in “Materials and Methods”, and then secreted RAGE in secretion medium from myc-RAGE/V5/His-COS-7 cells was analyzed. As expected, compared with CM from pIRESneo2-COS cells (negative control), CM from MMP9-COS cells increased secretion of secreted RAGE from myc-RAGE/V5/His-COS-7 cells (Figure 22C). Taken together, these results clearly show that MMP9 increases both constitutive and PMA-stimulated shedding of RAGE.



- (A) in lysates from COS-7 cells transiently co-transfected with expression vectors encoding RAGE and MMP9. 48 hours post-transfection, cells were incubated with secretion medium containing 1  $\mu$ M PMA or an equal volume of DMSO for 4 hours. Proteins in secretion medium were precipitated with 10% TCA and cells were harvested as described in Materials and Methods. Proteins in secretion medium or cell lysates were separated by SDS-PAGE and followed by western blot analysis for detection of secreted RAGE or full-length RAGE.
- (B) MMP9 activity in secretion medium from COS-7 cells transiently co-transfected with expression vectors encoding RAGE and MMP9. 48 hours post-transfection, cells were incubated with secretion medium for 18 hours and then 1  $\mu$ M PMA or an equal volume of DMSO was added and incubated for further 4 hours. Secretion medium was then collected for gelatin-substrate zymography.
- (C) myc-RAGE-COS-7 cells were treated with conditioned medium collected from stable MMP9-COS cells or pIRESneo2 transfected COS-7 cells in the presence or absent of PMA. Proteins in secretion medium were precipitated with 10% TCA followed by western blot analysis for detection of secreted RAGE.
- (D) Graphic representation of density evaluation from immunoblotting presented in (C). The experiments were performed in triplicates for 3 times. The mean effect  $\pm$  SD were shown here and analyzed by unpaired student's t-Test: \*  $p < 0.05$ , \*\*  $p < 0.01$ .

### 4.8.3 Knockdown of MMP9 expression by RNAi reduces constitutive and PMA-stimulated shedding of RAGE

RNA interference (RNAi) is a sequence-specific, post-transcriptional gene silencing (PTGS) process, which is mediated by double-stranded RNA (dsRNA) that is homologous in sequence to the silenced gene (Hannon 2002). The small interfering RNAs (siRNAs) mediated RNAi pathway is demonstrated in Figure 17. RNAi is triggered by the RNase III like nuclease Dicer, which promotes the cleavage of long dsRNAs into 21-23-bp small interfering RNAs (siRNAs). Subsequently, the siRNAs are incorporated into an RNA-induced silencing complex (RISC), then the active complex recognizes and destroys the target mRNA, thereby selectively inhibiting the expression of the target gene (Hammond *et al.* 2001). Recently, it has been demonstrated that short synthetic sequence-specific siRNAs can also mediate efficient gene silencing in mammalian cells without evoking non-specific effects (Elbashir *et al.* 2001). Thus RNAi represents a powerful tool to directly evaluate the effects of a loss of function of specific genes in mammalian cells.

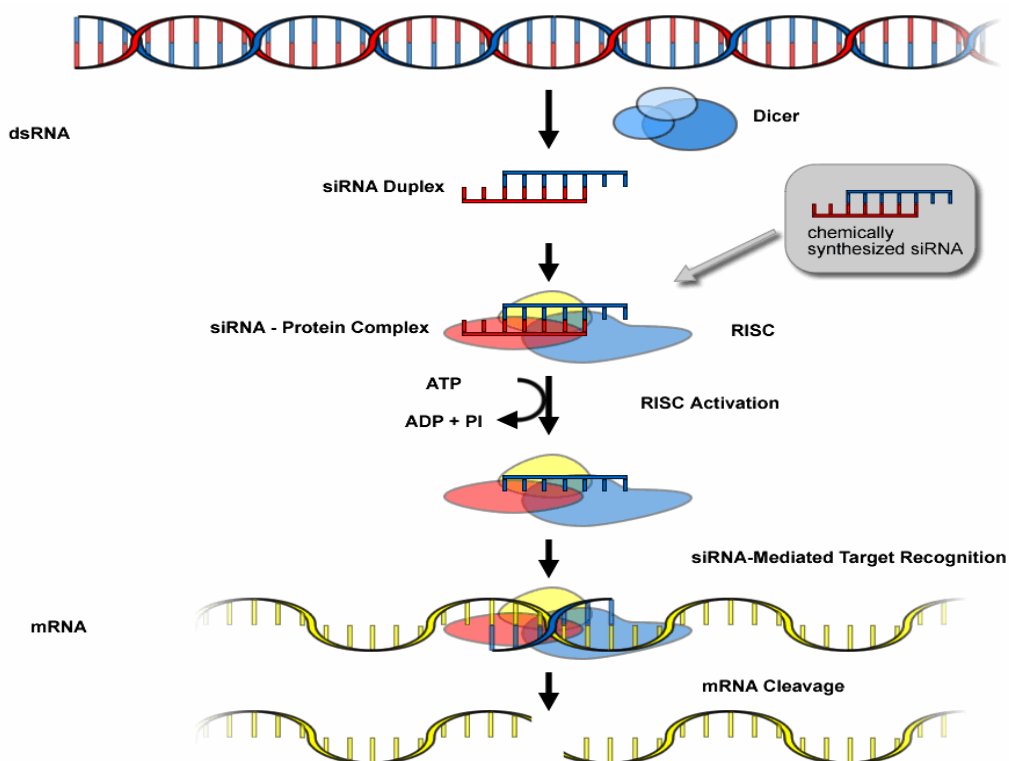


**Figure 23.** Scheme of the RNAi Pathway.

First, the dsRNA is degraded by a highly conserved cellular RNase named Dicer into small oligoribonucleotides with a length of about 21-23 bp, including 2-nucleotide long 3'-overhangs. This type of small dsRNA is called small interfering RNA or siRNA. In a second step, siRNA binds to a multimolecular protein complex consisting of several proteins named RISC (RNA Induced Silencing Complex). The double-stranded siRNA molecule is unwound resulting in a ribonucleoprotein particle consisting of the RISC proteins and one siRNA strand. If a mRNA with a sequence complementary to the siRNA moiety is encountered by this complex, the mRNA is cleaved by an RNase named Slicer and thereby rendered inactive (Adapted from <https://www.roche-applied-science.com>).

with RNAi to suppress expression of MMP9 in myc-RAGE/V5/His-Flp-In 293 cells was employed and the impact on shedding of RAGE was evaluated.

#### ***4.8.3.1 Efficient suppression of MMP9 expression in MMP9-COS-7 cells as well as in myc-RAGE-Flp-In 293 cells by a RNAi strategy***

So called “Stealth RNAi” (Invitrogen) which represents modified synthetic RNA duplex with high knockdown specificity and efficacy as well as enhanced long term stability were chosen for the experiment. The siRNA sequence targeting human MMP9 used here had no homology with other members of the MMP family. To examine their ability to suppress MMP9, Stealth RNAi was first tested on MMP9-COS cell. An ineffective siRNA sequence was used as negative control. MMP9-COS cells were transfected with 20 pmol Stealth RNAi per well in a 24-well plate (refer to “Material and Methods”). 48 hours post-transfection, growth medium was changed to secretion medium containing 1  $\mu$ M PMA or an equal volume of DMSO and incubated overnight. Zymography analysis of secretion medium from cells transfected with MMP9 specific Stealth RNAi revealed barely constitutive gelatinase B activity at 92 kDa compared to control transfected cells (Figure 24A left). Moreover, the MMP9 specific Stealth RNAi also displayed a high knockdown efficiency on PMA-simulated MMP9 activity (Figure 24A right).

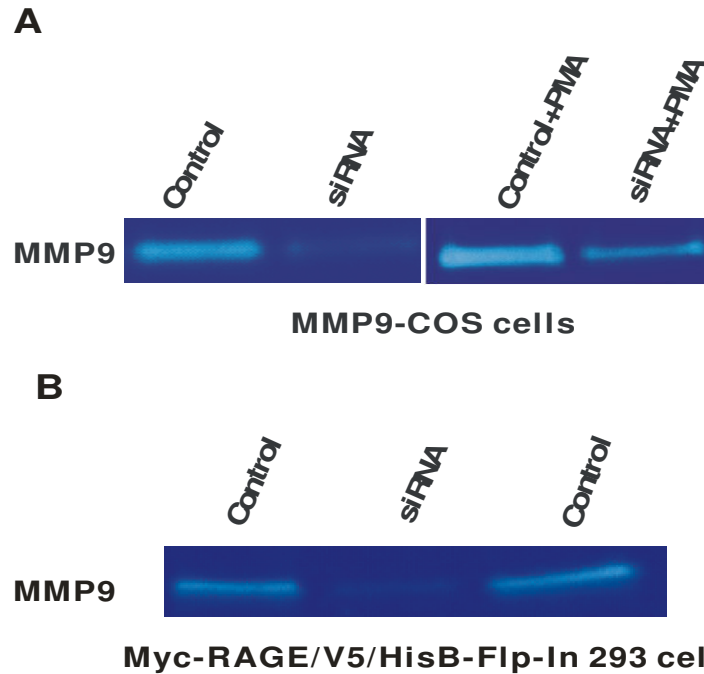


**Figure 24. Activity of human MMP9 inhibited by MMP9 Stealth RNAi.**

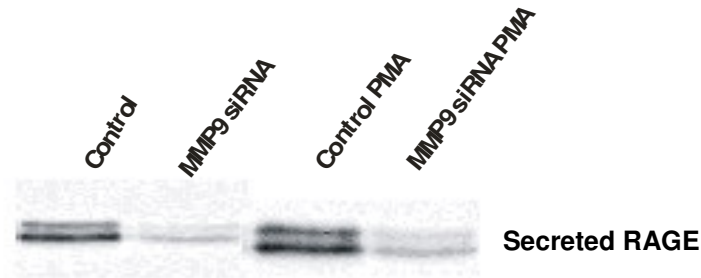
(A) MMP9-COS cells; (B) Myc-RAGE/V5/His-Flp-In 293 cells were transfected with MMP9 stealth RNAi or control RNAi. 48 hours post-transfection, the medium was replaced by secretion medium containing 1  $\mu$ M PMA or an equal amount of DMSO. Secretion medium was collected after incubation for 18 hours and subjected to gelatin zymography assay.

NEXT, it was tested whether myc-RAGE/V5/His-Flp-In 293 cells have constitutive MMP9 activity and whether MMP9 stealth RNAi is able to deplete MMP9 in these cells. Zymography analysis showed that there was a low level of constitutive MMP9 activity in myc-RAGE/V5/His-Flp-In 293 cells and similar to MMP9-COS cells, MMP9 stealth RNAi successfully suppressed constitutive MMP9 activity in Myc-RAGE/V5/His-Flp-In 293 cells (Figure 24B). Together, these findings indicated that MMP9 stealth RNAi efficiently inhibits MMP9 activity via suppressing MMP9 gene expression.

#### **4.8.3.2 MMP9 silencing severely reduces shedding of RAGE**

To further characterize the consequence of MMP9 gene silencing on shedding of RAGE, Myc-RAGE/V5/His-Flp-In 293 cells were transfected with MMP9 stealth RNAi. 48 hours post-transfection, cells were incubated in secretion medium containing 1  $\mu$ M PMA or an equal volume of DMSO for 2 hours. Then secretion medium and cells were collected and secreted RAGE was analyzed by western blot analysis with the anti-myc antibody. Compared to control oligonucleotides, MMP9 specific stealth RNAi reduced constitutive and PMA simulated shedding of RAGE significantly (Figure 25).

A



B

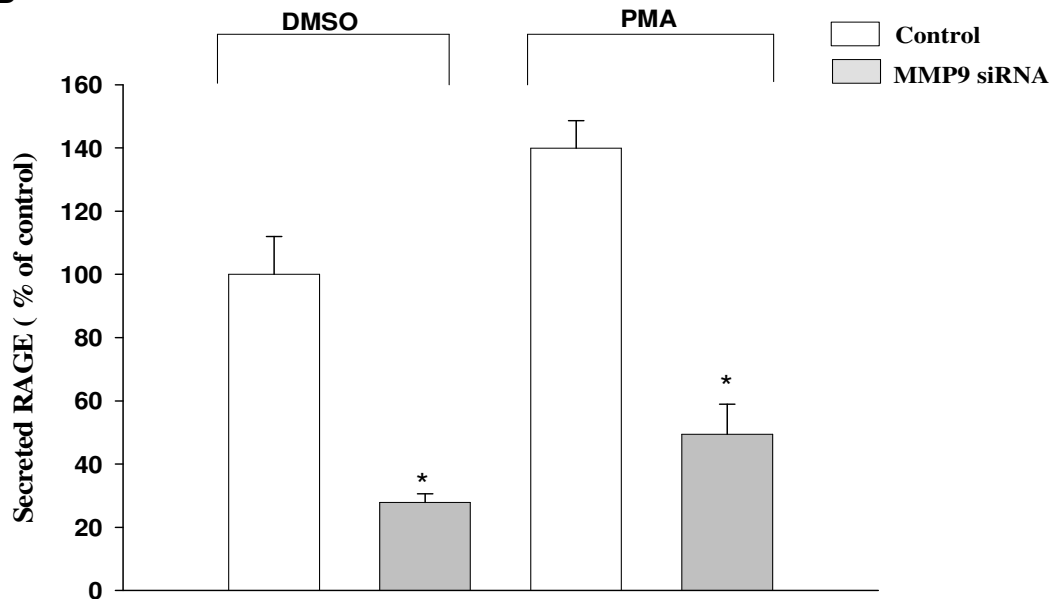


**Figure 25. Shedding of RAGE decreased by MMP9 knockdown.**

(A) myc-RAGE/V5/His-Flp-In 293 cells (50% confluent) were transfected with MMP9 stealth RNAi oligos or a negative control sequence. 48 hours post-transfection, the medium was replaced by secretion medium containing 1  $\mu$ M PMA or an equal amount of DMSO and incubated for 2 hours. After incubation, SM was analyzed by western blotting with the mouse anti-myc antibody for detection of secreted RAGE. (B) Graphic representation of density evaluation from immunoblotting shown in (A). The experiments were performed in triplicates for 3 times. The mean effect  $\pm$ SD were shown here and analyzed by unpaired student's t-Test: \*  $p < 0.001$ .

In another separate experiment, myc-RAGE/V5/His-Flp-In 293 cells were transfected either with MMP9 stealth RNAi or ADAM10 stealth RNAi as well as a negative control sequence. 48 hours post-transfection, the cells were incubated with secretion medium for 4 hours. Then secretion medium and cells were collected and sRAGE in secretion medium was analyzed by western blot analysis with the anti-RAGE N-terminal antibody. Compared to control oligonucleotides, MMP9 specific stealth RNAi significantly reduced the amount of secreted RAGE in secretion medium



(Figure 26B Lane 3), while the ADAM10 specific RNAi had no influence on shedding of RAGE (Figure 26B Lane 1). As described in Material and Methods, the cells were subjected to a membrane protein preparation, and after performing protein quantification same amounts of membrane proteins were analyzed by western blotting with an anti-ADAM10 antibody to confirm the efficiency of ADAM10 gene silencing (as shown in Figure 26A).

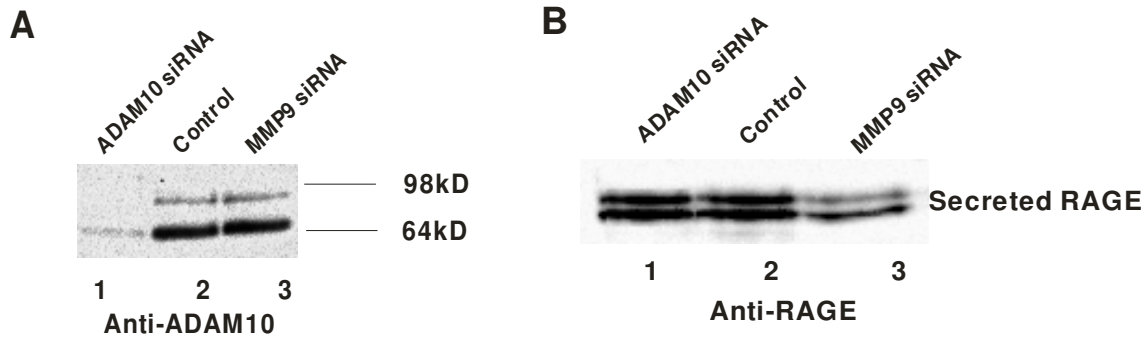


**Figure 26. Shedding of RAGE is decreased by MMP9 but not ADAM10 knockdown.**

Myc-RAGE/V5/His-Flp-In 293 cells (50% confluence) were transfected with MMP9 or ADAM10 stealth RNAi oligos or a negative control sequence. 48 hours post-transfection, the medium was replaced with secretion medium and incubated for 4 hours. **(A)** The same amount of protein from membrane preparation was analyzed to confirm the efficiency of ADAM10 gene silencing. **(B)** Secretion medium was analyzed by western blot analysis for detection of sRAGE.

Taken together, the results evidently demonstrate the special requirement for MMP9 but not ADAM10 in shedding of RAGE.

## **4.9 The cytoplasmic domain of RAGE is not essential for constitutive and PMA stimulated shedding of RAGE**

The cytoplasmic domains of transmembrane receptors play important roles in signal transduction (Vinogradova *et al.* 2002; Urena *et al.* 1999). In addition, cytoplasmic domains have been shown to play a role in ectodomain shedding of various transmembrane proteins such as ectoenzymes, adhesion molecules and receptors. For instance, Arg747 in the cytoplasmic domain of APP is essential for  $\alpha$ -secretase cleavage of the ectodomain (Tomita *et al.* 1998). Deletion of the cytoplasmic domain increases basal shedding of angiotensin-converting enzyme (Chubb *et al.* 2004). Nevertheless, in other cases, deletion or modification of the cytoplasmic domain has no effects on ectodomain shedding (Brakebusch *et al.* 1994; Gutwein *et al.* 2000).

### ***4.9.1 Deletion of cytoplasmic domain does not abrogate ectodomain shedding of RAGE***

In order to investigate whether the cytoplasmic domain of RAGE is necessary for shedding of its ectodomain, the cytoplasmic domain (367-404 amino acids) deletion mutant pcDNA6-RAGE- $\Delta$ C was constructed. Construct pcDNA6 -RAGE- $\Delta$ C was transfected into Flp-In 293 cells to establish a stable cell line expressing RAGE- $\Delta$ C. RAGE- $\Delta$ C-Flp-In 293 cells were incubated in secretion medium containing 1  $\mu$ M PMA or an equal amount of DMSO for 2 hours, and secreted RAGE in secretion medium was determined by immunoblotting with the anti-RAGE N-terminal antibody. As shown in Figure 27, deletion of cytoplasmic domain of RAGE did not abrogate the release of the ectodomain of RAGE in both constitutive and PMA stimulated conditions. The expression of RAGE- $\Delta$ C was confirmed in cell lysates from RAGE- $\Delta$ C-Flp-In 293 cells. Western blot analysis using the anti-RAGE N-terminal antibody showed a clear band of about 50 kDa representing RAGE- $\Delta$ C, which is smaller than full-length RAGE as expected.

Secreted RAGE released from RAGE- $\Delta$ C-Flp-In 293 cells had a molecular weight of approximately 48 kDa, which is the same size as fully glycosylated secreted RAGE released from RAGE-Flp-In 293 cells. Therefore, it is most likely that the cleavage occurs at the same site in both RAGE and RAGE- $\Delta$ C. Furthermore, the data indicated that the cytoplasmic domain of RAGE is not essential for constitutive and PMA stimulated shedding of RAGE. Nevertheless, whether the cytoplasmic domain of RAGE has any regulatory effects on shedding of RAGE remains to be elucidated.

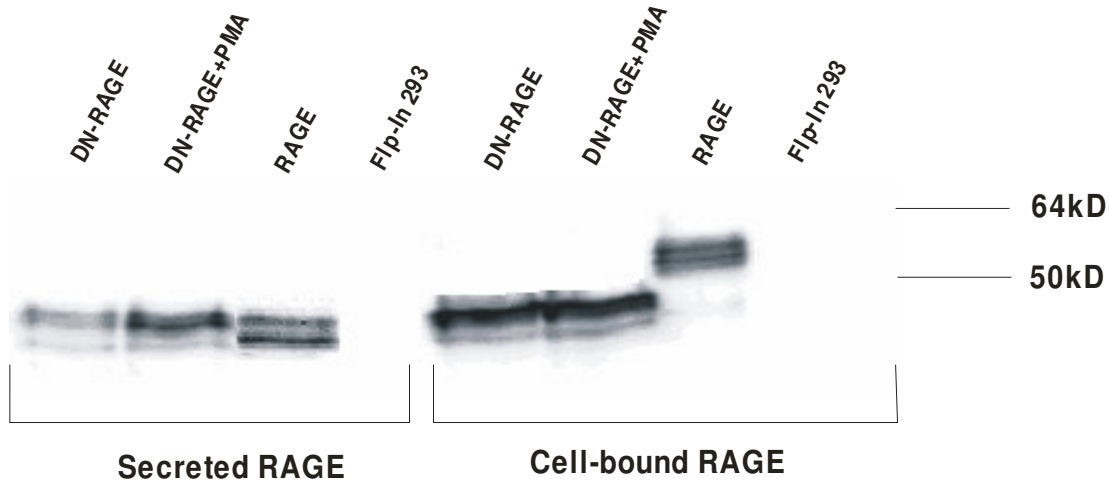


**Figure 27. Deletion of its cytoplasmic domain does not abrogate ectodomain shedding of RAGE.**

RAGE- $\Delta$ C-Flp-In 293 cells were incubated in secretion medium containing 1  $\mu$ M PMA or an equal amount of DMSO for 2 hours. Proteins in secretion medium were precipitated with 10% TCA and cells were lysed in 2X Laemmli buffer. The cell lysates and the precipitated proteins from secretion medium were subjected to western blot analysis. RAGE proteins were detected with the mouse anti-RAGE N-terminal antibody.

In another independent experiment, RAGE- $\Delta$ C-Flp-In 293 cells were incubated in secretion medium containing 142  $\mu$ M APMA or an equal amount of DMSO for 15 min, secreted RAGE in secretion medium were determined by immunoblotting with the anti-RAGE N-terminal antibody. As shown in Figure 28, after 15 min incubation, there was no detectable secreted RAGE in secretion medium under constitutive condition, whereas APMA strongly enhanced shedding of RAGE- $\Delta$ C. These results provide further support for the conclusion that the cytoplasmic domain of RAGE is not essential for shedding of RAGE.



**Figure 28. Deletion of its cytoplasmic domain does not abrogate APMA-stimulated shedding of RAGE.**

RAGE- $\Delta$ C-Flp-In 293 cells were incubated in secretion medium containing 142  $\mu$ M APMA or an equal amount of DMSO for 15 min. Proteins in secretion medium were precipitated with 10% TCA and subjected to western blot analysis. Secreted RAGE was detected with the mouse anti-RAGE N-terminal antibody.

#### ***4.9.2 RAGE deleted of its cytoplasmic domain is membrane-anchored and proteolysed***

***at the cell surface***

The cytoplasmic domain of some transmembrane proteins is essential for protein trafficking and maturation (Urena *et al.* 1999), thus truncation of cytoplasmic domains probably severely impairs the transport of proteins to the cell surface and subsequently impairs ectodomain shedding. So it is possible that the RAGE- $\Delta$ C protein expressed in RAGE- $\Delta$ C-Flp-In 293 cells is incorrectly folded and not transported to the plasma membrane. Due to the lack of the cytoplasmic domain it may be processed by the proteasome to yield protein fragments with similar size to secreted RAGE, which is then released to the medium by some unknown mechanisms like cell death or leakage. To exclude this possibility and prove whether secreted RAGE as detected above is derived from ectodomain shedding of membrane-bound RAGE- $\Delta$ C, cell surface biotinylation experiments were performed to demonstrate that the expressed RAGE- $\Delta$ C protein is cell membrane-anchored.

RAGE- $\Delta$ C-Flp-In 293 cells were washed carefully twice with PBS and then incubated with 5 mM of the Sulfo-NHS-Biotin reagent at room temperature for 30 min. Then cells were washed with TBS to stop the biotinylation. After washing, cells were incubated in secretion medium containing either 1  $\mu$ M PMA, or 142  $\mu$ M APMA or equal amounts of DMSO for indicated periods (See Figure 29). Secretion medium and cells were collected respectively and the biotinylated proteins were isolated with streptavidin-agarose beads. Biotinylated proteins in secretion medium and cell lysates were analyzed by western blotting with the anti-RAGE N-terminal antibody. Biotinylation experiments showed that both RAGE- $\Delta$ C in cell lysates and secreted RAGE in secretion medium were biotinylated (Figure 29).

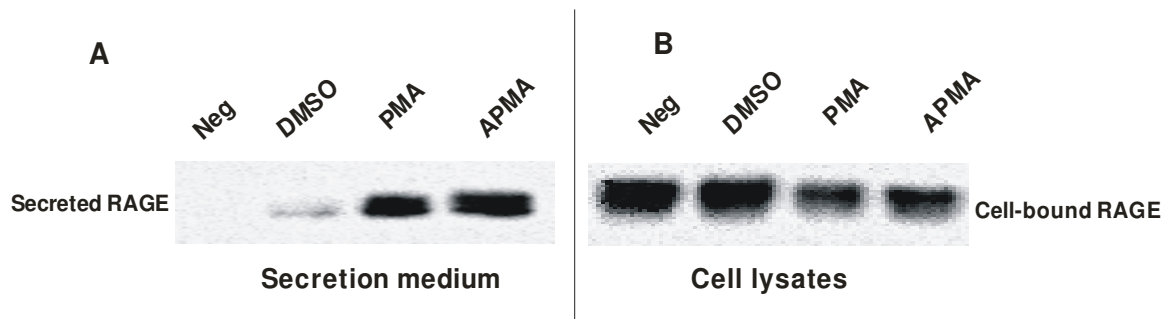


**Figure 29. RAGE- $\Delta$ C is present and cleaved at the cell surface.**

RAGE- $\Delta$ C-Flp-In 293 cells were washed twice with PBS and then incubated with 5 mM Sulfo-NHS-Biotin reagents at room temperature for 30 min. Then cells were washed with TBS to stop the biotinylation. After washing, cells were incubated with secretion medium containing either 1  $\mu$ M PMA, or an equal amount of DMSO for 2 hours or 142  $\mu$ M APMA for 15 min. Secretion medium and cells were collected respectively and the biotinylated proteins were isolated with streptavidin-agarose beads. Biotinylated proteins in secretion medium (A) and cell lysates (B) were analyzed by western blotting with the anti-RAGE N-terminal antibody. Neg: negative control in which the secretion medium was not incubated on cells.

Therefore, the results demonstrate that the RAGE- $\Delta$ C receptor is located on the plasma membrane and suggest that delivery of RAGE to the plasma membrane is independent of its cytoplasmic domain. Furthermore, secreted RAGE is released from the cell surface by proteolysis of RAGE- $\Delta$ C. In summary, the biotinylation experiment proved that shedding of RAGE is independent of its cytoplasmic domain.

#### 4.10 Analysis of the RAGE cleavage site

Recently, an unbiased phage display strategy was applied to define the substrate recognition specificity of MMP9 (Kridel *et al.* 2001) and it was found that the most prevalent motif contains the sequence Pro-X-X-Hy-(Ser/Thr) ( here X represent any residue, and Hy is a hydrophobic residue). A sequence consistent with this motif, P-T-A-G-S, is present in the proximal ectodomain of RAGE (Figure 30), and there is some evidence that the mouse RAGE protein is proteolytically processed within this region (Hanford *et al.* 2004). Since the data provided so far indicate that MMP9 mediates shedding of RAGE, the sequence P-T-A-G-S may serve as the putative cleavage site in RAGE. Therefore, a point mutation replacing the proline (328th residue) against glutamic acid was generated (RAGE-P328E) and analyzed.

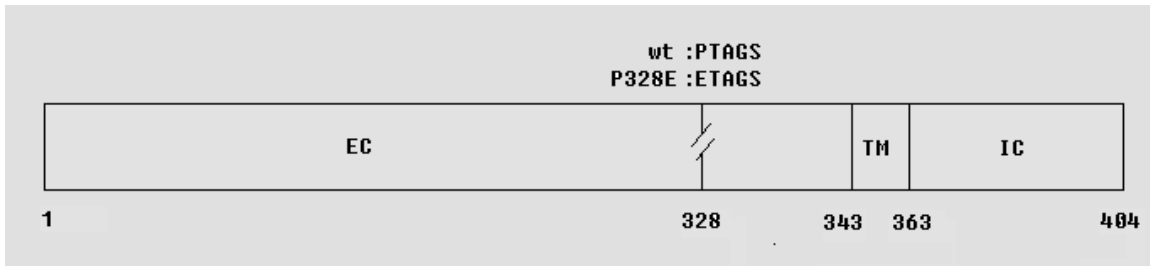


**Figure 30. Schematic representation of the putative cleavage sequence of RAGE and the P328E mutation.**

EC: extracellular domain. TM: transmembrane domain. IC: intracellular domain. When COS-7 cells were transiently transfected with the RAGE-P328E expression vector, secreted RAGE released into secretion medium could still be detected in both constitutive and PMA stimulated conditions (Figure 31A). Furthermore, another mutant where the putative cleavage sequence PTAGS was replaced by AAGEG (RAGE- $\Delta$ PTAGS) was analyzed. This mutation also did not abrogate shedding of RAGE in COS-7 cells (Figure 31A). After testing these mutant constructs in Flp-in 293 cells, the same results were obtained (Figure 31B). Thus the data argue that shedding of RAGE is not sequence specific. In contrast, it is indicated that a strict sequence specificity may not be required for the shedding machinery of RAGE.

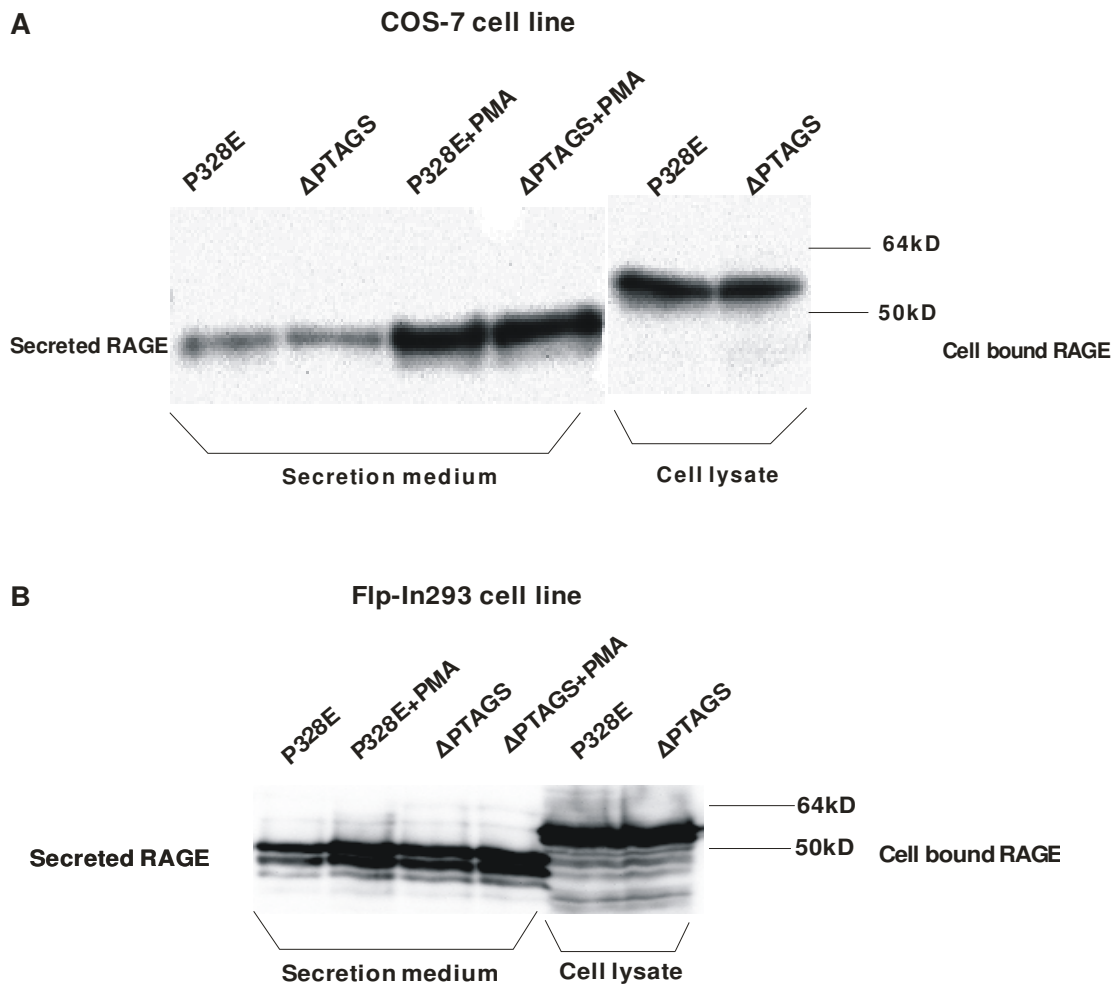


**Figure 31. Mutation or deletion of the P-T-A-G-S motif does not abrogate ectodomain shedding of RAGE.**

COS-7 cells (**A**) or Flp-in-293 cells (**B**) were transiently transfected with RAGE-P328E or RAGE- $\Delta$ PTAGS expression vectors. Proteins in secretion medium were precipitated with 10% TCA and cells were lysed in 2X Laemmli buffer. The cell lysates and the precipitated proteins were subjected to western blot analysis. The RAGE proteins were detected with the mouse anti-RAGE N-terminal antibody. P328 E: mutation RAGE-P328E.  $\Delta$ PTAGS: mutation: RAGE $\Delta$ PTAGS.

## 5. Discussion

### 5.1 Human soluble RAGE is glycosylated and is generated by proteolysis

Soluble isoforms of RAGE have been detected in a variety of human cells and tissues such as fetal lung (Malherbe *et al.* 1999), human lymphnode, myometrium, fibroblasts, breast cancer cells (Schlueter *et al.* 2003), endothelium cells, pericytes (Yonekura *et al.* 2003) and brain (Ding and Keller 2005b). Furthermore, the presence of soluble RAGE has been detected in human plasma. The plasma levels of soluble RAGE have been reported to be reduced in patients with some diseases including hypertension (Geroldi *et al.* 2005), Alzheimer's disease (Emanuele *et al.* 2005), rheumatoid arthritis (Pullerits *et al.* 2005) and coronary artery disease (Falcone *et al.* 2005). Therefore, investigation of mechanisms underlying the generation of soluble RAGE is of particular importance. To date, many lines of evidence have demonstrated that soluble RAGE is produced through alternative splicing of the RAGE gene product (Malherbe *et al.* 1999; Schlueter *et al.* 2003; Yonekura *et al.* 2003; Ding and Keller 2005b). By alternative splicing, the exon that encodes the transmembrane and cytoplasmic domains of RAGE is excised and the resultant mRNA is translated into proteins that only retains the ectodomain of RAGE and therefore can be released to the extracellular space. Nevertheless, up to date, it is unknown whether a soluble isoform of RAGE can also be released by ectodomain shedding mediated by proteases.

To determine whether soluble RAGE can be generated through ectodomain shedding of the full-length protein, Flp-In 293 cell lines which overexpress exclusively the human cDNA for either full-length or epitope tagged RAGE were engineered. Two cellular RAGE forms were identified in cell lysates. A low molecular mass form (14 kDa) was detected only with the anti-V5 antibody directed against the C-terminus of recombinant RAGE, indicating that it represents the membrane anchored cytoplasmic remnant fragment generated following ectodomain shedding. While the high molecular mass cellular RAGE form (48 kDa) could be detected with antibodies directed either against the C-terminus or the N-terminus. This 48 kDa isoform represents the full-length transmembrane protein that may undergo shedding to generate the soluble ectodomains. Accordingly, a soluble form of RAGE was detected in cell culture medium with a specific anti-N-terminal RAGE antibody. Collectively, the results show for the first time that soluble RAGE can be released as a consequence of proteolysis.

Generation of soluble forms of cell surface receptors via two diverse pathways including ectodomain shedding and alternative splicing has been reported. A classic example of such events

is the generation of soluble growth hormone receptors by proteolytic cleavage in rabbit and human and by alternative splicing in mouse and rat (Baumbach et al. 1989; Wang et al. 2002). Other examples include syndecan-4 (Xing et al. 2003) and Granulocyte-macrophage colony-stimulating factor receptor alpha (Prevost et al. 2002). Previous studies have shown that human soluble RAGE is derived from alternative splicing of RAGE mRNA. However, the present study provides evidence that human soluble RAGE can also be derived from ectodomain shedding, a mechanism completely different from alternative splicing. This observation is consistent with a recent study indicating that soluble RAGE in mice may be generated as the result of protein cleavage instead of splicing (Hanford et al. 2004). Whether the circulating soluble RAGE found in human biological fluids such as serum and cerebral spinal fluid is derived from mRNA splicing or ectodomain shedding is indistinguishable because specific antibodies are not available at present. Interestingly, a novel mechanism for secretion of a receptor has recently been identified for the full-length 55 kDa TNF receptor 1 which is released to extracellular compartments in exosome-like vesicles (Hawari et al. 2004). However, in this exosome-mediated release model, a full-length membrane-bound receptor but not a receptor ectodomain is released. So it remains unclear whether exosome-like particles may also mediate the release of human soluble RAGE to extracellular compartment. But from our data based on cells overexpressing RAGE, it is unlikely since full-length RAGE could not be detected in cell culture medium.

Full-length RAGE has two potential N-linked glycosylation sites, and its alternatively spliced and secreted isoforms from human lung and brain have additional sites (Neeper et al. 1992; Malherbe et al. 1999). The two N-linked sites on mature RAGE are within the Ig-like V-domain principally responsible for ligand-binding (Kislinger et al. 1999). The data obtained in the present study indicate that via proteolysis secreted soluble RAGE is also N-linked glycosylated, although the exact glycosylation sites remain to be determined. The fact that soluble RAGE is glycosylated is consistent with previous observations (Hanford et al. 2004; Srikrishna et al. 2002). The importance of glycosylation for the ability of RAGE to bind its ligands has been demonstrated (Srikrishna et al. 2002). It is highly likely that glycosylation is of the same importance for soluble RAGE to bind its ligand. As full-length as well as shedded RAGE possess the same glycosylation pattern, ligand binding should be indistinguishable between these two isoforms. Thus, soluble RAGE produced in a bacterial expression system should be used extremely carefully because the lack of glycosylation might decrease or prevent ligand binding by sRAGE and therefore impair the ability of sRAGE to compete with full-length RAGE for ligand binding.



In addition, by cell surface protein biotinylation experiments, it was demonstrated that RAGE is expressed as a full-length receptor at the cell surface of intact Flp-In 293 cells and that secreted RAGE is also biotinylated. This experiment provides further evidence that RAGE is cleaved at the cell surface resulting in the release of a soluble form of the RAGE receptor.

Taken together, our data clearly showed that full-length RAGE is properly glycosylated and targeted to the cell membrane. Furthermore, it is processed at the cell surface by proteolysis by which its ectodomain is released from the cell.

## **5.2 Several stimuli can stimulate the release of soluble RAGE**

Similar to other shedding events, several lines of evidence presented here suggest that soluble RAGE is released by proteolysis in both constitutive (under normal cell culture conditions) and stimulated (under certain stimulated conditions) ways. Furthermore, various stimuli employed here can stimulate RAGE shedding.

It has been documented that a range of proteins are released from the cell surface after stimulation with PMA, a potent activator of PKC, by triggering a metalloproteinase-dependent ectodomain sheddase machinery. This pathway seems to be highly conserved among multiple cell types. PMA stimulation leads to the rapid cleavage of cell surface RAGE and the release of soluble RAGE into the cell culture medium. In addition to RAGE, several other proteins known to be shed from the cell surface display both constitutive and PMA-stimulated shedding, for example APP (Lammich *et al.* 1999), LDL-R (low density lipoprotein receptor) (Begg *et al.* 2004), fractalkine (Garton *et al.* 2001) and others. Currently, the mechanism of PMA-stimulated ectodomain shedding is poorly understood. Although some reports indicated that PMA-stimulated shedding is PKC-dependent (Hahn *et al.* 2003; Le Gall *et al.* 2003), others have controversial results (Racchi *et al.* 1999).

APMA has been previously used to activate ectodomain shedding of transmembrane proteins including TGF $\alpha$  and HB-EGF (Merlos-Suarez *et al.* 2001), ACE (Allinson *et al.* 2004) and ICAM-1 (Tsakadze *et al.* 2006). The mercurial compound APMA has been extensively used to activate recombinant MMPs *in vitro*. These metalloproteinases are synthesized as zymogens in which an unpaired cysteine residue of the prodomain binds to the active site zinc ion. *In vitro* APMA reacts with the free thiol group of the zymogen and stabilizes an active form of the enzyme that leads to autoproteolytic processing of the propeptide (Birkedal-Hansen 1995).

Although in the present work the mechanisms by which APMA enhances RAGE shedding was not addressed, the known ability of APMA to activate the removal of prodomains from metalloproteinase opens the possibility that prodomains could play a role in the regulation of the RAGE sheddase in cells.

Ionophore-induced shedding has been observed for TGF $\alpha$  (Pandiella and Massague 1991), HB-EGF (Dethlefsen *et al.* 1998), amphiregulin (Brown *et al.* 2001) and the betacellulin precursor (Sanderson *et al.* 2005). The calcium ionophore A23187 increased RAGE shedding within 1.5 hours of treatment and more significantly after 4 hours treatment of RAGE expressing cells. Therefore, A23187 activated RAGE shedding might be dependent on extracellular calcium levels. Calcium ionophors can activate a range of cell signaling pathways including PKC (Eguchi *et al.* 1998; Franklin *et al.* 2000), which may lead to activation of metalloproteinases. However, at present, possible pathways downstream of A23187 and their role in metalloproteinase activation and RAGE shedding are poorly understood.

In conclusion, shedding of RAGE occurs constitutively and can be stimulated by several known molecules that activate ectodomain shedding, thus providing further support that sRAGE we observed in secretion medium is generated by ectodomain shedding.

### **5.3 RAGE shedding seems to be PKC and MAPK independent**

The release of a large number of secreted proteins derived from integral plasma membrane proteins is enhanced by treatment of cells with phorbol esters such as PMA, presumably through activating PKC, indicating common mechanisms. PKC is a cytoplasmic protein that becomes membrane associated after activation and rapidly phosphorylates intracellular target proteins (Hug and Sarre 1993). PMA is thought to activate some PKC isoenzymes (Nishizuka 1984; Nishizuka 1986) by substituting the endogenous ligand 1,2-diacylglycerol in its binding domain or by binding simultaneously to the C1 region of the kinase (Slater *et al.* 1994; Zhang *et al.* 1995). PMA-induced shedding of several membrane proteins can be reduced by PKC inhibitors (Hahn *et al.* 2003; Thabard *et al.* 2001) and therefore it is presumed that PMA activates ectodomain shedding in a PKC-dependent manner.

Surprisingly, the specific PKC inhibitor chelerythrine did not inhibit the shedding of RAGE; instead it enhances RAGE shedding under both constitutive and PMA-stimulated conditions. This finding is in accordance with a recent study which reported chelerythrine stimulated shedding of

HB-EGF in a ROS (reactive oxygen species) dependent manner (Kim *et al.* 2005). In this line, although chelerythrine is a potent PKC inhibitor, it was shown to induce intracellular ROS (Yu *et al.* 2000), suggesting the involvement of intracellular peroxides in the regulated ectodomain shedding of some cell surface proteins. To investigate whether ROS induced by chelerythrine are indeed involved in regulation of RAGE shedding, it will be indispensable in further study to test the effects of ROS blockers or scavengers on chelerythrine-stimulated RAGE shedding. Furthermore, the effect of other PKC inhibitors on RAGE shedding should be analyzed to clarify the role of PKC in processing of RAGE.

In addition to PKC, multiple signaling pathways including MAP kinase activation have been implicated in the PMA stimulated shedding mechanism, and in some cases these pathways are independent of each other (Dethlefsen *et al.* 1998). The activation of MAP kinase by PMA can be blocked by pretreating cells with the specific MAP kinase kinase (MEK) inhibitor PD98059 (Phong *et al.* 2003; Gechtman *et al.* 1999). The blockade of MEK pathway by PD98059 has no effect on either constitutive or PMA-stimulated RAGE shedding. Therefore, it is unlikely that this particular MAPK pathway is involved in RAGE shedding. In further studies JNK and p38 MAP kinase pathways may be investigated.

#### **5.4 The cleavage of RAGE is mediated by a metalloproteinase**

Metalloproteinases of the ADAM and MMP families are involved in ectodomain shedding of transmembrane proteins. ADAM17 has been implicated in the shedding of TGF $\alpha$  (Peschon *et al.* 1998), neuregulin-1 (Montero *et al.* 2000), HB-EGF (Sunnarborg *et al.* 2002) and APLP2 (APP like protein 2) (Endres *et al.* 2005), while MMP family members have been shown to mediate the shedding of E-cadherin (Perl *et al.* 1998), proTNF- $\alpha$  (Haro *et al.* 2000), CD44 (Nakamura *et al.* 2004) and others.

Here several lines of evidence for the role of metalloproteinases in constitutive and stimulated shedding of RAGE are provided. By using metalloproteinase inhibitors, it was demonstrated that MMPs and/or ADAMs are potential sheddases for RAGE in Flp-in 293 cells. Three different metalloproteinases inhibitors GM6001, GI254023X and GW280264X blocked constitutive and PMA stimulated shedding of RAGE. In addition, GM6001 blocked APMA stimulated RAGE shedding. Some other kinds of protease inhibitors were also included in this study, but contrary to metalloproteinases inhibitors, these inhibitors had no significant effects on RAGE shedding, thus excluding the role of cysteine proteases, aspartic proteases, serine proteases and neprilysin in the

cleavage of RAGE. Both gain of function and loss of function experiments rule out the involvement of ADAM10 as candidate sheddase for RAGE. In addition, overexpression of either ADAM17 or MT1-MMP did not enhance RAGE shedding. In contrast, overexpression of MMP9 enhanced RAGE shedding while silencing MMP9 by RNAi reduced RAGE shedding. Taken together, the data suggest MMP9 as RAGE sheddase. Therefore, RAGE is a novel substrate for MMP9.

The fact that some sRAGE was still detectable in the secretion medium of MMP9 siRNA transfected cells is likely caused by an incomplete knockdown. However, it may also argue for an involvement of other proteases in shedding of RAGE. Thus the results obtained do not exclude the possibility that metalloproteinases other than MMP9 are also involved in the proteolytic cleavage of RAGE. Other MMPs including MMP2 might represent possible candidate sheddases which share the ability together with MMP9 to cleave RAGE. Since the activation of proMMP9 to catalytic active MMP9 involves many MMPs including MMP1, MMP2, MMP7 and MMP13, a potential role of these MMPs in regulating the shedding of RAGE needs further investigation.

In addition to RAGE, MMP9 has been showed to be involved in direct cleavage of cell surface proteins such as TGF- $\alpha$  (Yu and Stamenkovic 2000), galectin-3 (Ochieng *et al.* 1994), IL-2R (Sheu *et al.* 2001) and ICAM-1 (Fiore *et al.* 2002). Furthermore, it has been postulated that the proteolytic activity of MMP9 is most effective when MMP9 is localized to the cell surface (Fiore *et al.* 2002; Toth *et al.* 1997; Yu and Stamenkovic 2000). In this aspect, it is interesting to note that the cell surface localization of proteolytic activities has been observed for a variety of secreted MMPs including MMP1, MMP2 and MMP7. Indeed, there is evidence that the cell surface may provide a privileged microenvironment for the preservation of MMP9 activity from natural inhibitors including the tissue inhibitors of metalloproteinases (TIMPs) that block the activity of soluble MMPs (Yu and Stamenkovic 1999). So regulation of MMP9 localization to the cell surface seems to be important for the shedding events mediated by MMP9. In future work, one may figure out whether RAGE provides cell surface docking site for MMP9 and whether cell surface localization is important for MMP9 to cleave RAGE.

As working hypothesis it was presumed that shedding of RAGE may be important to prevent the progression of Alzheimer's disease because the amount of membrane-bound RAGE is elevated in the brain vasculature of AD patients, therefore promoting A $\beta$  uptake from serum into the brain (Deane *et al.* 2003). Now evidence is provided here that RAGE is cleaved by MMP9 to generate soluble RAGE. Interestingly, MMP9 is synthesized in neurons (Backstrom *et al.* 1996) and levels

of soluble RAGE are significantly reduced in the plasma of AD patients compared with controls (Emanuele *et al.* 2005). Taken together, it is conceivable that elevated levels of membrane-bound RAGE in the brain vasculature and accumulation of A $\beta$  in brain as well as the decrease of circulating soluble RAGE in the plasma may be due to the disturbance of either MMP9 expression or its activation in AD patients. In this context, the level of circulating MMP9 in AD patient's plasma has been studied by several different research groups. Although one group detected an increased level of plasma MMP9 in AD patients (Lorenzl *et al.* 2003), others found no significant difference between AD patients and normal controls. On the other hand, increased MMP9 expression levels have been observed in AD brains but MMP9 was predominantly found in the latent or proenzyme form in the proximity of extracellular amyloid plaques (Backstrom *et al.* 1996). It was proposed by the authors that the lack of MMP9 activation contributes to the accumulation of insoluble A $\beta$  peptides in plaques.

In the context of RAGE shedding, whether a lack of MMP9 activation contributes to decreased levels of soluble RAGE in the plasma and corresponding elevated amounts of membrane-bound RAGE in the brain vasculature in AD need to be addressed in future studies.

The functional interaction between MMP9 and RAGE is highly reasonable in view of several aspects. First, both molecules are expressed in human endothelial cells, neurons, astrocytes, and microglia, thus giving the chance to interact with each other. Secondly, increased expression of both MMP9 (Backstrom *et al.* 1996) and RAGE (Yan *et al.* 1996) are found in A $\beta$  rich tissues. Thirdly, overexpression of both molecules is involved in inflammation, tumor growth and migration, atherosclerosis, multiple sclerosis (MS) and neurodegenerative disorders such as AD. All these coincidences between MMP9 and RAGE strongly support the results showing ectodomain shedding of RAGE by MMP9.

Although the results described here suggest a beneficial role for MMP9 in AD by cleavage of RAGE, MMP9 has been shown to play a detrimental role in other diseases such as stroke and metastasis. Thus, whether or not MMP9 is beneficial or harmful may depend on several factors, including the cellular sources, the extracellular environment, and the stage of lesion development in the diseases.

### **5.5 The cleavage of RAGE is not sequence specific**

The sequence P-T-A-G-S present in the membrane proximal portion of the extracellular domain of RAGE is consistent with a previously defined MMP9 specific recognition motif Pro-X-X-Hy-(Ser/Thr) (Kridel *et al.* 2001). Therefore it was speculated that this sequence comprises the MMP9 cleavage site of RAGE. Unexpectedly, neither a point mutation within this sequence nor the substitution of all five amino acids significantly affected RAGE shedding, indicating a lack of sequence specificity for the RAGE sheddase.

Several structural characteristics of a substrate are important for its recognition by an enzyme, including sequence, stalk length, membrane distance and features of the distal ectodomain, as well as the tertiary structure of the enzyme itself. Several lines of evidence suggest that the structure of the juxtamembrane stalk region, rather than the presence or absence of a specific amino acid sequence determines the susceptibility of a transmembrane protein to shedding. Mutational analysis of the cleavage sites for TNF- $\alpha$  (Tang *et al.* 1996), TNFRI (Brakebusch *et al.* 1994), L-selectin (Migaki *et al.* 1995), IL-6R (Mullberg *et al.* 1994) and APP (Sisodia 1992) have revealed relaxed sequence specificities surrounding the cleavage sites. For example, TNF- $\alpha$  shedding can only be abolished by deletion of at least 10 amino acid residues surrounding the cleavage site (Tang *et al.* 1996). Therefore, some sequence changes may maintain structural integrity and cleavability of the juxtamembrane domain, whereas others disrupt this structure. The identification of amino acids comprising a potential cleavage site for MMP9 in the extracellular region of RAGE will provide helpful insights to our understanding of this process.

## **5.6 The cytoplasmic domain of RAGE is not essential for shedding and membrane localization of RAGE**

The present results clearly demonstrate that the cytoplasmic domain of RAGE is not required for shedding of the ectodomain. In this regard, RAGE is similar to the ACE (Sadhukhan *et al.* 1998; Chubb *et al.* 2004), APP (da Cruz e Silva *et al.* 1993), kit ligand (Cheng and Flanagan 1994), L1 (Heiz *et al.* 2004) and IL-6 receptor (Mullberg *et al.* 1994). In contrast, the cytoplasmic domains of proTGF- $\alpha$  and the TNF- $\alpha$  receptor are necessary for their cleavage (Crowe *et al.* 1993; Bosenberg *et al.* 1992). Furthermore, the fact that the deletion of RAGE cytoplasmic domain has no significant influence on PMA stimulated shedding strongly support the conclusion that PMA stimulated RAGE shedding is not due to direct activation of RAGE by PKC. Whether a subtle difference in shedding efficiency can be detected between full-length RAGE and C-terminal truncated RAGE awaits the development of more sensitive assays.

Deficient transport has been proposed as an explanation for the previously reported lack of PMA activated ectodomain shedding of C-terminal truncated proTGF- $\alpha$  (Urena *et al.* 1999), since the ectodomain shedding machinery is known to be located at the cell surface. In fact, targeting of transmembrane proteins to several subcellular compartments is mainly dependent on sorting signals located in cytoplasmic domain. In contrast, the same study reported that the maturation and transport of betaglycan are unaffected by the absence of the cytoplasmic tail (Urena *et al.* 1999).

By a biotinylation assay it was demonstrated in this thesis that full-length RAGE is cleaved at cell surface constitutively or upon stimulation. Furthermore, cytoplasmic domain deleted RAGE is biotinlyted indicating that it is also cell surface anchored. This finding is consistent with a recent report which showed a clear membrane localization of full-length RAGE as well as C-terminal truncated RAGE (Bartling *et al.* 2005). In conclusion, cell surface localization of RAGE is independent of its cytoplasmic tail.

Cytoplasmic domain deleted RAGE is also called DN-RAGE because the lack of the cytoplasmic domain is thought to prevent its signaling by a dominant negative way. Recombinant DN-RAGE has been shown to abrogate RAGE-mediated neurite outgrowth, implying that the cytoplasmic domain of RAGE interacts with a signaling complex necessary to initiate neurite extension (Huttunen *et al.* 1999). However, the signaling mechanism of RAGE is poorly understood and up to date none of the cytoplasmic binding partners of RAGE have been identified. Because

shedding of RAGE was found to be independent from the presence of its cytoplasmic domain, modulators for RAGE shedding must attack other target sides.

### **5.7 Significance of RAGE shedding**

Ectodomain shedding represents a distinguished mechanism to regulate the signaling capacity of cell surface receptors. On one hand, ligands are synthesized as transmembrane proforms and inactively sequestered and converted to active forms able to bind receptors only by shedding. On the other hand, cleaving the ligand binding domain of receptors by shedding can terminate receptor signaling.

sRAGE has been cloned and expressed as a recombinant protein. The existence of natural sRAGE in biological fluids suggests that sRAGE has important roles in normal physiology as well as the development of pathological processes. The importance of sRAGE has been demonstrated by administering recombinant sRAGE to prevent diabetic atherosclerosis (Park *et al.* 1998), reduce diabetic late complications (Goova *et al.* 2001), inhibit tumor metastases and invasion (Taguchi *et al.* 2000), and block transport of A $\beta$  across the blood brain barrier (Deane *et al.* 2003).

However, the *in vivo* significance of RAGE shedding to generate sRAGE has not yet been studied. The relatively lower level of plasma sRAGE has been described to be associated with various diseases including Alzheimer's disease (Emanuele *et al.* 2005), hypertension (Geroldi *et al.* 2005), rheumatoid arthritis (Pullerits *et al.* 2005) and coronary artery disease (Falcone *et al.* 2005). Therefore, the formation of sRAGE by metalloproteinase cleavage might be important to regulate RAGE-mediated cellular functions. The presence of sRAGE in biological fluids could affect function of RAGE ligands by competing for ligand binding with membrane bound RAGE. Thus by preventing interaction of ligands with cell surface RAGE, sRAGE can disrupt ligand induced RAGE mediated signaling. For example, use of recombinant sRAGE reduced vascular levels of phosphorylated p38 MAP kinase and activated NF- $\kappa$ B. Given that RAGE is a multi-ligand receptor and a number of disorders have been reported to be associated with activation or defect of the ligand-RAGE axis, modulation of sRAGE generation by regulating proteolysis of RAGE provides a novel and favorable therapeutic way in addition to administration of recombinant sRAGE. Additionally, it has been suggested that RAGE should be considered a pattern recognition receptor (PRR), since it binds to a diversity of ligands (Bierhaus *et al.* 2005). By this opinion, it is proposed that the beneficial effects of sRAGE are not solely the result of preventing ligand engagement of cell surface RAGE but possibly also of other receptors.



Regulation of shedding of RAGE can be conducted via increase of MMP9 activity or its expression to generate more sRAGE. On the other hand, specific MMP9 inhibitors can be used to inhibit RAGE shedding. Given the complex roles of RAGE, and other receptors interacting with RAGE ligands, the decision to activate or inhibit RAGE shedding will depend on different physiopathological contexts. It has been speculated that sRAGE-ligand complexes are eliminated from the blood via the spleen and/or liver (Renard *et al.* 1997). If this is true, enhancement of RAGE shedding will give rise to clearance of circulating A $\beta$  from blood by soluble RAGE. Also, by shifting cell surface RAGE into sRAGE, it would be possible to reduce the uptake of A $\beta$  into the brain and diminish membrane-bound RAGE-mediated neurotoxicity. On the other side, soluble RAGE might also affect the bioavailability of RAGE ligands by forming a complex with ligands.

Lastly, either high or even low levels of soluble RAGE in human plasma might correlate with distinct pathological conditions and possibly serve as a prognostic marker for certain type of diseases. Indeed, a growing number of evidence suggests the possibility of soluble RAGE as a biomarker for many RAGE-related diseases including coronary artery disease (Falcone *et al.* 2005), rheumatoid arthritis (Pullerits *et al.* 2005), Alzheimer disease (Emanuele *et al.* 2005), type 1 diabetes (Forbes *et al.* 2005) and hypertension (Geroldi *et al.* 2005). Long-term, large-scale prospective clinical trials will be required to evaluate the rationality of soluble RAGE as biomarker for RAGE-mediated diseases. Furthermore, antibodies specifically recognizing only the secreted form of RAGE which is generated by proteolysis should be included in such studies. In this aspect, it is also important to detect the changes in activity or expression of MMP9 or other sheddases that account for the shedding of RAGE and to reveal the corresponding relationship between levels of sheddases and sRAGE in various diseased conditions.

## 6. Summary

RAGE mediates diverse physiological and pathological effects by binding a variety of ligands. Despite incomplete understanding of RAGE-mediated disorders soluble RAGE (sRAGE) has been identified as a potential biomarker for RAGE-related diseases and possibly represents a hopeful pharmaceutical against RAGE-mediated disorders. Nevertheless, the source of sRAGE remains poorly investigated. Currently sRAGE is thought to be derived exclusively from alternative splicing of mRNA.

In this thesis it was investigated whether sRAGE can also be released as a result of ectodomain shedding of full-length RAGE. Using cells overexpressing RAGE as a model system, it was demonstrated clearly that RAGE undergoes ectodomain shedding in both constitutive and regulated manner. Several stimuli including PMA, AMPA, calcium and chelerythrine stimulated the release of sRAGE into cell culture medium. Moreover, possible mechanisms that regulate ectodomain shedding of RAGE were investigated and it was found that shedding of RAGE is likely independent from PKC and MAPK pathways. By using gain of function and loss of function approaches MMP9 but not ADAM10, ADAM17 or MT1-MMP was characterized as the metalloproteinase that mediates shedding of RAGE. Furthermore, it was shown that cytoplasmic domain of RAGE is not essential for shedding of RAGE. In addition, the potential cleavage site of RAGE by MMP9 was investigated and a lack of sequence specificity for the RAGE processing proteinase was demonstrated by mutation analysis. Finally the physiopathological significance of shedding of RAGE is discussed.

In conclusion, for the first time ectodomain shedding of human RAGE and the underlying regulatory mechanisms were investigated. The data open a new field for modulation of RAGE shedding as a novel intervention approach against RAGE-mediated diseases.

## Reference

### Reference List

- Allinson TM, Parkin ET, Condon TP, Schwager SL, Sturrock ED, Turner AJ, Hooper NM (2004) The role of ADAM10 and ADAM17 in the ectodomain shedding of angiotensin converting enzyme and the amyloid precursor protein. *Eur.J Biochem.* **271**, 2539-2547.
- Arancio O, Zhang HP, Chen X, Lin C, Trinchese F, Puzzo D, Liu S, Hegde A, Yan SF, Stern A, Luddy JS, Lue LF, Walker DG, Roher A, Buttini M, Mucke L, Li W, Schmidt AM, Kindy M, Hyslop PA, Stern DM, Du Yan SS (2004) RAGE potentiates Abeta-induced perturbation of neuronal function in transgenic mice. *EMBO J* **23**, 4096-4105.
- Arribas J, Borroto A (2002) Protein ectodomain shedding. *Chemical Reviews* **102**, 4627-4637.
- Arribas J, Coodly L, Vollmer P, Kishimoto TK, Rose-John S, Massague J (1996) Diverse cell surface protein ectodomains are shed by a system sensitive to metalloprotease inhibitors. *J Biol.Chem.* **271**, 11376-11382.
- Arribas J, Massague J (1995) Transforming growth factor-alpha and beta-amyloid precursor protein share a secretory mechanism. *J Cell Biol.* **128**, 433-441.
- Backstrom JR, Lim GP, Cullen MJ, Tokes ZA (1996) Matrix metalloproteinase-9 (MMP-9) is synthesized in neurons of the human hippocampus and is capable of degrading the amyloid-beta peptide (1-40). *J Neurosci.* **16**, 7910-7919.
- Bartling B, Hofmann HS, Weigle B, Silber RE, Simm A (2005) Down-regulation of the receptor for advanced glycation end-products (RAGE) supports non-small cell lung carcinoma. *Carcinogenesis* **26**, 293-301.
- Baumbach WR, Horner DL, Logan JS (1989) The growth hormone-binding protein in rat serum is an alternatively spliced form of the rat growth hormone receptor. *Genes and Development* **3**, 1199-1205.
- Begg MJ, Sturrock ED, van der Westhuyzen DR (2004) Soluble LDL-R are formed by cell surface cleavage in response to phorbol esters. *Eur.J Biochem.* **271**, 524-533.
- Behl C, Davis JB, Lesley R, Schubert D (1994) Hydrogen peroxide mediates amyloid beta protein toxicity. *Cell* **77**, 817-827.
- Bierhaus A, Haslbeck KM, Humpert PM, Liliensiek B, Dehmer T, Morcos M, Sayed AA, Andrassy M, Schiekofer S, Schneider JG, Schulz JB, Heuss D, Neundorfer B, Dierl S, Huber J, Tritschler H, Schmidt AM, Schwaninger M, Haering HU, Schleicher E, Kasper M, Stern DM, Arnold B, Nawroth PP (2004) Loss of pain perception in diabetes is dependent on a receptor of the immunoglobulin superfamily. *J Clin.Invest* **114**, 1741-1751.
- Bierhaus A, Humpert PM, Morcos M, Wendt T, Chavakis T, Arnold B, Stern DM, Nawroth PP (2005) Understanding RAGE, the receptor for advanced glycation end products. *J Mol.Med.* **83**, 876-886.
- Birkedal-Hansen H (1995) Proteolytic remodeling of extracellular matrix. *Curr.Opin.Cell Biol.* **7**, 728-735.
- Black RA, Rauch CT, Kozlosky CJ, Peschon JJ, Slack JL, Wolfson MF, Castner BJ, Stocking KL, Reddy P, Srinivasan S, Nelson N, Boiani N, Schooley KA, Gerhart M, Davis R, Fitzner JN, Johnson RS, Paxton RJ, March CJ, Cerretti DP (1997) A metalloproteinase disintegrin that releases tumour-necrosis factor-alpha from cells. *Nature* **385**, 729-733.

- Black RA, White JM (1998) ADAMs: focus on the protease domain. *Curr.Opin.Cell Biol.* **10**, 654-659.
- Bode W, Fernandez-Catalan C, Tschesche H, Grams F, Nagase H, Maskos K (1999) Structural properties of matrix metalloproteinases. *Cell Mol.Life Sci.* **55**, 639-652.
- Borroto A, Ruiz-Paz S, de la Torre TV, Borrell-Pages M, Merlos-Suarez A, Pandiella A, Blobel CP, Baselga J, Arribas J (2003) Impaired trafficking and activation of tumor necrosis factor-alpha-converting enzyme in cell mutants defective in protein ectodomain shedding. *J Biol.Chem.* **278**, 25933-25939.
- Bosenberg MW, Pandiella A, Massague J (1992) The cytoplasmic carboxy-terminal amino acid specifies cleavage of membrane TGF alpha into soluble growth factor. *Cell* **71**, 1157-1165.
- Brakebusch C, Varfolomeev EE, Batkin M, Wallach D (1994) Structural requirements for inducible shedding of the p55 tumor necrosis factor receptor. *J Biol.Chem.* **269**, 32488-32496.
- Brett J, Schmidt AM, Yan SD, Zou YS, Weidman E, Pinsky D, Nowygrod R, Neeper M, Przysiecki C, Shaw A, . (1993) Survey of the distribution of a newly characterized receptor for advanced glycation end products in tissues. *Am.J.Pathol.* **143**, 1699-1712.
- Brown CL, Coffey RJ, Dempsey PJ (2001) The proamphiregulin cytoplasmic domain is required for basolateral sorting, but is not essential for constitutive or stimulus-induced processing in polarized Madin-Darby canine kidney cells. *J.Biol.Chem.* **276**, 29538-29549.
- Bucciarelli LG, Wendt T, Rong L, Lalla E, Hofmann MA, Goova MT, Taguchi A, Yan SF, Yan SD, Stern DM, Schmidt AM (2002) RAGE is a multiligand receptor of the immunoglobulin superfamily: implications for homeostasis and chronic disease. *Cell Mol.Life Sci.* **59**, 1117-1128.
- Budagian V, Bulanova E, Orinska Z, Ludwig A, Rose-John S, Saftig P, Borden EC, Bulfone-Paus S (2004) Natural soluble interleukin-15Ralpha is generated by cleavage that involves the tumor necrosis factor-alpha-converting enzyme (TACE/ADAM17). *J Biol.Chem.* **279**, 40368-40375.
- Cao J, Rehemtulla A, Pavlaki M, Kozarekar P, Chiarelli C (2005) Furin directly cleaves proMMP-2 in the trans-Golgi network resulting in a nonfunctioning proteinase. *J Biol.Chem.* **280**, 10974-10980.
- Cao X, Sudhof TC (2001) A transcriptionally [correction of transcriptively] active complex of APP with Fe65 and histone acetyltransferase Tip60. *Science* **293**, 115-120.
- Chakraborti S, Mandal M, Das S, Mandal A, Chakraborti T (2003) Regulation of matrix metalloproteinases: an overview. *Mol.Cell Biochem.* **253**, 269-285.
- Cheng HJ, Flanagan JG (1994) Transmembrane kit ligand cleavage does not require a signal in the cytoplasmic domain and occurs at a site dependent on spacing from the membrane. *Mol.Biol.Cell* **5**, 943-953.
- Choi ME (1999) Cloning and characterization of a naturally occurring soluble form of TGF-beta type I receptor. *Am.J Physiol* **276**, F88-F95.
- Chubb AJ, Schwager SL, van der ME, Ehlers MR, Sturrock ED (2004) Deletion of the cytoplasmic domain increases basal shedding of angiotensin-converting enzyme. *Biochem.Biophys.Res.Commun.* **314**, 971-975.
- Cisse MA, Sunyach C, Lefranc-Jullien S, Postina R, Vincent B, Checler F (2005) The disintegrin ADAM9 indirectly contributes to the physiological processing of cellular prion by modulating ADAM10 activity. *J Biol.Chem.* **280**, 40624-40631.
- Crowe PD, VanArsdale TL, Goodwin RG, Ware CF (1993) Specific induction of 80-kDa tumor necrosis

- factor receptor shedding in T lymphocytes involves the cytoplasmic domain and phosphorylation. *J Immunol* **151**, 6882-6890.
- da Cruz e Silva OA, Iverfeldt K, Oltersdorf T, Sinha S, Lieberburg I, Ramabhadran TV, Suzuki T, Sisodia SS, Gandy S, Greengard P (1993) Regulated cleavage of Alzheimer beta-amyloid precursor protein in the absence of the cytoplasmic tail. *Neuroscience* **57**, 873-877.
- Dagert M, Ehrlich SD (1979) Prolonged incubation in calcium chloride improves the competence of *Escherichia coli* cells. *Gene* **6**, 23-28.
- Daniels GM, Amara SG (1998) Selective labeling of neurotransmitter transporters at the cell surface. *Methods Enzymol.* **296**, 307-318.
- Deane R, Du YS, Subramanian RK, LaRue B, Jovanovic S, Hogg E, Welch D, Manness L, Lin C, Yu J, Zhu H, Ghiso J, Frangione B, Stern A, Schmidt AM, Armstrong DL, Arnold B, Liliensiek B, Nawroth P, Hofman F, Kindy M, Stern D, Zlokovic B (2003) RAGE mediates amyloid-beta peptide transport across the blood-brain barrier and accumulation in brain. *Nat.Med.* **9**, 907-913.
- Dethlefsen SM, Raab G, Moses MA, Adam RM, Klagsbrun M, Freeman MR (1998) Extracellular calcium influx stimulates metalloproteinase cleavage and secretion of heparin-binding EGF-like growth factor independently of protein kinase C. *J Cell Biochem.* **69**, 143-153.
- Devaux Y, Senior R, Ray P (2004) a new target for MMP-9 in the regulation of inflammatory response in the lung during oxidative stress. *Am.J.Respir.Crit.Care Med.* **169**, A456. (Abstract)
- Ding Q, Keller JN (2005a) Evaluation of rage isoforms, ligands, and signaling in the brain. *Biochim.Biophys.Acta* **1746**, 18-27.
- Ding Q, Keller JN (2005b) Splice variants of the receptor for advanced glycosylation end products (RAGE) in human brain. *Neurosci.Lett.* **373**, 67-72.
- Du YS, Zhu H, Fu J, Yan SF, Roher A, Tourtellotte WW, Rajavashisth T, Chen X, Godman GC, Stern D, Schmidt AM (1997) Amyloid-beta peptide-receptor for advanced glycation endproduct interaction elicits neuronal expression of macrophage-colony stimulating factor: a proinflammatory pathway in Alzheimer disease. *Proc.Natl.Acad.Sci.U.S.A* **94**, 5296-5301.
- Dzwonek J, Rylski M, Kaczmarek L (2004) Matrix metalloproteinases and their endogenous inhibitors in neuronal physiology of the adult brain. *FEBS Lett.* **567**, 129-135.
- Eguchi S, Numaguchi K, Iwasaki H, Matsumoto T, Yamakawa T, Utsunomiya H, Motley ED, Kawakatsu H, Owada KM, Hirata Y, Marumo F, Inagami T (1998) Calcium-dependent epidermal growth factor receptor transactivation mediates the angiotensin II-induced mitogen-activated protein kinase activation in vascular smooth muscle cells. *J.Biol.Chem.* **273**, 8890-8896.
- Elbashir SM, Harborth J, Lendeckel W, Yalcin A, Weber K, Tuschl T (2001) Duplexes of 21-nucleotide RNAs mediate RNA interference in cultured mammalian cells. *Nature* **411**, 494-498.
- Emanuele E, D'Angelo A, Tomaino C, Binetti G, Ghidoni R, Politi P, Bernardi L, Maletta R, Bruni AC, Geroldi D (2005) Circulating levels of soluble receptor for advanced glycation end products in Alzheimer disease and vascular dementia. *Arch.Neurol.* **62**, 1734-1736.
- Endo K, Takino T, Miyamori H, Kinsen H, Yoshizaki T, Furukawa M, Sato H (2003) Cleavage of syndecan-1 by membrane type matrix metalloproteinase-1 stimulates cell migration. *J Biol.Chem.* **278**, 40764-40770.

- Endres K, Postina R, Schroeder A, Mueller U, Fahrenholz F (2005) Shedding of the amyloid precursor protein-like protein APLP2 by disintegrin-metalloproteinases. *FEBS J* **272**, 5808-5820.
- Ethell DW, Kinloch R, Green DR (2002) Metalloproteinase shedding of Fas ligand regulates beta-amyloid neurotoxicity. *Curr.Biol.* **12**, 1595-1600.
- Falcone C, Emanuele E, D'Angelo A, Buzzi MP, Belvito C, Cuccia M, Geroldi D (2005) Plasma levels of soluble receptor for advanced glycation end products and coronary artery disease in nondiabetic men. *Arterioscler.Thromb.Vasc.Biol.* **25**, 1032-1037.
- Fiore E, Fusco C, Romero P, Stamenkovic I (2002) Matrix metalloproteinase 9 (MMP-9/gelatinase B) proteolytically cleaves ICAM-1 and participates in tumor cell resistance to natural killer cell-mediated cytotoxicity. *Oncogene* **21**, 5213-5223.
- Forbes JM, Thorpe SR, Thallas-Bonke V, Pete J, Thomas MC, Deemer ER, Bassal S, El Osta A, Long DM, Panagiotopoulos S, Jerums G, Osicka TM, Cooper ME (2005) Modulation of soluble receptor for advanced glycation end products by angiotensin-converting enzyme-1 inhibition in diabetic nephropathy. *J Am.Soc.Nephrol.* **16**, 2363-2372.
- Franklin RA, Atherfold PA, McCubrey JA (2000) Calcium-induced ERK activation in human T lymphocytes occurs via p56(Lck) and CaM-kinase. *Mol.Immunol.* **37**, 675-683.
- Gandy S (2005) The role of cerebral amyloid beta accumulation in common forms of Alzheimer disease. *J Clin.Invest* **115**, 1121-1129.
- Garton KJ, Gough PJ, Blobel CP, Murphy G, Greaves DR, Dempsey PJ, Raines EW (2001) Tumor necrosis factor-alpha-converting enzyme (ADAM17) mediates the cleavage and shedding of fractalkine (CX3CL1). *J Biol.Chem.* **276**, 37993-38001.
- Gechtman Z, Alonso JL, Raab G, Ingber DE, Klagsbrun M (1999) The shedding of membrane-anchored heparin-binding epidermal-like growth factor is regulated by the Raf/mitogen-activated protein kinase cascade and by cell adhesion and spreading. *J Biol.Chem.* **274**, 28828-28835.
- Genersch E, Hayess K, Neuenfeld Y, Haller H (2000) Sustained ERK phosphorylation is necessary but not sufficient for MMP-9 regulation in endothelial cells: involvement of Ras-dependent and -independent pathways. *J Cell Sci.* **113 Pt 23**, 4319-4330.
- Geroldi D, Falcone C, Emanuele E, D'Angelo A, Calcagnino M, Buzzi MP, Scioli GA, Fogari R (2005) Decreased plasma levels of soluble receptor for advanced glycation end-products in patients with essential hypertension. *J.Hypertens.* **23**, 1725-1729.
- Giri R, Selvaraj S, Miller CA, Hofman F, Yan SD, Stern D, Zlokovic BV, Kalra VK (2002) Effect of endothelial cell polarity on beta-amyloid-induced migration of monocytes across normal and AD endothelium. *Am.J Physiol Cell Physiol* **283**, C895-C904.
- Gitter BD, Cox LM, Rydel RE, May PC (1995) Amyloid beta peptide potentiates cytokine secretion by interleukin-1 beta-activated human astrocytoma cells. *Proc.Natl.Acad.Sci.U.S.A* **92**, 10738-10741.
- Goova MT, Li J, Kislinger T, Qu W, Lu Y, Bucciarelli LG, Nowygrod S, Wolf BM, Caliste X, Yan SF, Stern DM, Schmidt AM (2001) Blockade of receptor for advanced glycation end-products restores effective wound healing in diabetic mice. *Am.J.Pathol.* **159**, 513-525.
- Gough PJ, Garton KJ, Wille PT, Rychlewski M, Dempsey PJ, Raines EW (2004) A disintegrin and metalloproteinase 10-mediated cleavage and shedding regulates the cell surface expression of CXC chemokine ligand 16. *J Immunol* **172**, 3678-3685.

- Gutwein P, Oleszewski M, Mechttersheimer S, Agmon-Levin N, Krauss K, Altevogt P (2000) Role of Src kinases in the ADAM-mediated release of L1 adhesion molecule from human tumor cells. *J Biol.Chem.* **275**, 15490-15497.
- Hahn D, Pischitzis A, Roesmann S, Hansen MK, Leuenberger B, Luginbuehl U, Sterchi EE (2003) Phorbol 12-myristate 13-acetate-induced ectodomain shedding and phosphorylation of the human meprinbeta metalloprotease. *J Biol.Chem.* **278**, 42829-42839.
- Hammond SM, Caudy AA, Hannon GJ (2001) Post-transcriptional gene silencing by double-stranded RNA. *Nat.Rev.Genet.* **2**, 110-119.
- Hanford LE, Enghild JJ, Valnickova Z, Petersen SV, Schaefer LM, Schaefer TM, Reinhart TA, Oury TD (2004) Purification and characterization of mouse soluble receptor for advanced glycation end products (sRAGE). *Journal of Biological Chemistry* **279**, 50019-50024.
- Hannon GJ (2002) RNA interference. *Nature* **418**, 244-251.
- Hardy JA, Higgins GA (1992) Alzheimer's disease: the amyloid cascade hypothesis. *Science* **256**, 184-185.
- Haro H, Crawford HC, Fingleton B, Shinomiya K, Spengler DM, Matrisian LM (2000) Matrix metalloproteinase-7-dependent release of tumor necrosis factor-alpha in a model of herniated disc resorption. *J Clin.Invest* **105**, 143-150.
- Hartung HP, Kieseier BC (2000) The role of matrix metalloproteinases in autoimmune damage to the central and peripheral nervous system. *J Neuroimmunol.* **107**, 140-147.
- Haudenschild D, Moseley T, Rose L, Reddi AH (2002) Soluble and transmembrane isoforms of novel interleukin-17 receptor-like protein by RNA splicing and expression in prostate cancer. *J Biol.Chem.* **277**, 4309-4316.
- Hawari FI, Rouhani FN, Cui X, Yu ZX, Buckley C, Kaler M, Levine SJ (2004) Release of full-length 55-kDa TNF receptor 1 in exosome-like vesicles: a mechanism for generation of soluble cytokine receptors. *Proc.Natl.Acad.Sci.U.S.A* **101**, 1297-1302.
- Heiz M, Grunberg J, Schubiger PA, Novak-Hofer I (2004) Hepatocyte Growth Factor-induced Ectodomain Shedding of Cell Adhesion Molecule L1: ROLE OF THE L1 CYTOPLASMIC DOMAIN. *Journal of Biological Chemistry* **279**, 31149-31156.
- Hirata M, Umata T, Takahashi T, Ohnuma M, Miura Y, Iwamoto R, Mekada E (2001) Identification of serum factor inducing ectodomain shedding of proHB-EGF and sStudies of noncleavable mutants of proHB-EGF. *Biochem.Biophys.Res. Commun.* **283**, 915-922.
- Hofmann MA, Drury S, Fu C, Qu W, Taguchi A, Lu Y, Avila C, Kambham N, Bierhaus A, Nawroth P, Neurath MF, Slattery T, Beach D, McClary J, Nagashima M, Morser J, Stern D, Schmidt AM (1999) RAGE mediates a novel proinflammatory axis: a central cell surface receptor for S100/calgranulin polypeptides. *Cell* **97**, 889-901.
- Hooper NM, Karran EH, Turner AJ (1997) Membrane protein secretases. *Biochem.J* **321** ( Pt 2), 265-279.
- Hori O, Brett J, Slattery T, Cao R, Zhang JH, Chen JX, Nagashima M, Lundh ER, Vijay S, Nitecki D, Morser J, Stern D, Schmidt AM (1995) The Receptor for Advanced Glycation End-Products (Rage) Is A Cellular-Binding Site for Amphoterin - Mediation of Neurite Outgrowth and Coexpression of Rage and Amphoterin in the Developing Nervous-System. *Journal of Biological Chemistry* **270**, 25752-25761.
- Hudson BI, Schmidt AM (2004) RAGE: a novel target for drug intervention in diabetic vascular disease.

*Pharm.Res.* **21**, 1079-1086.

Hug H, Sarre TF (1993) Protein kinase C isoenzymes: divergence in signal transduction? *Biochem.J* **291** ( Pt 2), 329-343.

Huttunen HJ, Fages C, Rauvala H (1999) Receptor for advanced glycation end products (RAGE)-mediated neurite outgrowth and activation of NF-kappaB require the cytoplasmic domain of the receptor but different downstream signaling pathways. *J Biol.Chem.* **274**, 19919-19924.

Huttunen HJ, Kuja-Panula J, Rauvala H (2002) Receptor for advanced glycation end products (RAGE) signaling induces CREB-dependent chromogranin expression during neuronal differentiation. *J Biol.Chem.* **277**, 38635-38646.

Iwata N, Tsubuki S, Takaki Y, Shirotani K, Lu B, Gerard NP, Gerard C, Hama E, Lee HJ, Saido TC (2001) Metabolic regulation of brain Abeta by neprilysin. *Science* **292**, 1550-1552.

Kajita M, Itoh Y, Chiba T, Mori H, Okada A, Kinoh H, Seiki M (2001) Membrane-type 1 matrix metalloproteinase cleaves CD44 and promotes cell migration. *J Cell Biol.* **153**, 893-904.

Kaltschmidt B, Uherek M, Volk B, Baeuerle PA, Kaltschmidt C (1997) Transcription factor NF-kappaB is activated in primary neurons by amyloid beta peptides and in neurons surrounding early plaques from patients with Alzheimer disease. *Proc.Natl.Acad.Sci.U.S.A* **94**, 2642-2647.

Karsdal MA, Larsen L, Engsig MT, Lou H, Ferreras M, Lochter A, Delaisse JM, Foged NT (2002) Matrix metalloproteinase-dependent activation of latent transforming growth factor-beta controls the conversion of osteoblasts into osteocytes by blocking osteoblast apoptosis. *J Biol.Chem.* **277**, 44061-44067.

Kheradmand F, Werb Z (2002) Shedding light on sheddases: role in growth and development. *Bioessays* **24**, 8-12.

Kim J, Lin J, Adam RM, Lamb C, Shively SB, Freeman MR (2005) An oxidative stress mechanism mediates chelerythrine-induced heparin-binding EGF-like growth factor ectodomain shedding. *J Cell Biochem.* **94**, 39-49.

Kislinger T, Fu C, Huber B, Qu W, Taguchi A, Du YS, Hofmann M, Yan SF, Pischetsrieder M, Stern D, Schmidt AM (1999) N(epsilon)-(carboxymethyl)lysine adducts of proteins are ligands for receptor for advanced glycation end products that activate cell signaling pathways and modulate gene expression. *J.Biol.Chem.* **274**, 31740-31749.

Klegeris A, Walker DG, McGeer PL (1994) Activation of macrophages by Alzheimer beta amyloid peptide. *Biochem.Biophys.Res.Comm.* **199**, 984-991.

Kridel SJ, Chen E, Kotra LP, Howard EW, Mobashery S, Smith JW (2001) Substrate hydrolysis by matrix metalloproteinase-9. *J Biol.Chem.* **276**, 20572-20578.

Lakka SS, Gondi CS, Rao JS (2005) Proteases and glioma angiogenesis. *Brain Pathol.* **15**, 327-341.

Lambert DW, Yarski M, Warner FJ, Thornhill P, Parkin ET, Smith AI, Hooper NM, Turner AJ (2005) Tumor necrosis factor-alpha convertase (ADAM17) mediates regulated ectodomain shedding of the severe-acute respiratory syndrome-coronavirus (SARS-CoV) receptor, angiotensin-converting enzyme-2 (ACE2). *J Biol.Chem.* **280**, 30113-30119.

Lammich S, Kojro E, Postina R, Gilbert S, Pfeiffer R, Jasionowski M, Haass C, Fahrenholz F (1999) Constitutive and regulated alpha-secretase cleavage of Alzheimer's amyloid precursor protein by a disintegrin metalloprotease. *Proc.Natl.Acad.Sci.U.S.A* **96**, 3922-3927.



- Le Gall SM, Auger R, Dreux C, Mauduit P (2003) Regulated cell surface pro-EGF ectodomain shedding is a zinc metalloprotease-dependent process. *J Biol.Chem.* **278**, 45255-45268.
- Li J, Schmidt AM (1997) Characterization and functional analysis of the promoter of RAGE, the receptor for advanced glycation end products. *J Biol.Chem.* **272**, 16498-16506.
- Li JJ, Dickson D, Hof PR, Vlassara H (1998) Receptors for advanced glycosylation endproducts in human brain: role in brain homeostasis. *Mol.Med.* **4**, 46-60.
- Liaw PCY, Mather T, Oganessian N, Ferrell GL, Esmon CT (2001) Identification of the Protein C/Activated Protein C Binding Sites on the Endothelial Cell Protein C Receptor. IMPLICATIONS FOR A NOVEL MODE OF LIGAND RECOGNITION BY A MAJOR HISTOCOMPATIBILITY COMPLEX CLASS 1-TYPE RECEPTOR. *Journal of Biological Chemistry* **276**, 8364-8370.
- Lorenzl S, Albers DS, Relkin N, Ngyuen T, Hilgenberg SL, Chirichigno J, Cudkowicz ME, Beal MF (2003) Increased plasma levels of matrix metalloproteinase-9 in patients with Alzheimer's disease. *Neurochem.Int.* **43**, 191-196.
- Ludwig A, Hundhausen C, Lambert MH, Broadway N, Andrews RC, Bickett DM, Leesnitzer MA, Becherer JD (2005) Metalloproteinase inhibitors for the disintegrin-like metalloproteinases ADAM10 and ADAM17 that differentially block constitutive and phorbol ester-inducible shedding of cell surface molecules. *Comb.Chem.High Throughput Screen.* **8**, 161-171.
- Mackic JB, Stins M, McComb JG, Calero M, Ghiso J, Kim KS, Yan SD, Stern D, Schmidt AM, Frangione B, Zlokovic BV (1998) Human blood-brain barrier receptors for Alzheimer's amyloid-beta 1- 40. Asymmetrical binding, endocytosis, and transcytosis at the apical side of brain microvascular endothelial cell monolayer. *J Clin.Invest* **102**, 734-743.
- Malherbe P, Richards JG, Gaillard H, Thompson A, Diener C, Schuler A, Huber G (1999) cDNA cloning of a novel secreted isoform of the human receptor for advanced glycation end products and characterization of cells co-expressing cell-surface scavenger receptors and Swedish mutant amyloid precursor protein. *Brain Res.Mol.Brain Res.* **71**, 159-170.
- Matthews V, Schuster B, Schutze S, Bussmeyer I, Ludwig A, Hundhausen C, Sadowski T, Saftig P, Hartmann D, Kallen KJ, Rose-John S (2003) Cellular cholesterol depletion triggers shedding of the human interleukin-6 receptor by ADAM10 and ADAM17 (TACE). *J Biol.Chem.* **278**, 38829-38839.
- McQuibban GA, Gong JH, Tam EM, McCulloch CA, Clark-Lewis I, Overall CM (2000) Inflammation dampened by gelatinase A cleavage of monocyte chemoattractant protein-3. *Science* **289**, 1202-1206.
- Mechtersheimer S, Gutwein P, Agmon-Levin N, Stoeck A, Oleszewski M, Riedle S, Postina R, Fahrenholz F, Fogel M, Lemmon V, Altevogt P (2001) Ectodomain shedding of L1 adhesion molecule promotes cell migration by autocrine binding to integrins. *J Cell Biol.* **155**, 661-673.
- Merlos-Suarez A, Ruiz-Paz S, Baselga J, Arribas J (2001) Metalloprotease-dependent protransforming growth factor-alpha ectodomain shedding in the absence of tumor necrosis factor-alpha-converting enzyme. *J Biol.Chem.* **276**, 48510-48517.
- Michel J, Langstein J, Hofstadter F, Schwarz H (1998) A soluble form of CD137 (ILA/4-1BB), a member of the TNF receptor family, is released by activated lymphocytes and is detectable in sera of patients with rheumatoid arthritis. *Eur.J Immunol* **28**, 290-295.
- Migaki GI, Kahn J, Kishimoto TK (1995) Mutational analysis of the membrane-proximal cleavage site of L-selectin: relaxed sequence specificity surrounding the cleavage site. *J Exp.Med.* **182**, 549-557.

- Monea S, Jordan BA, Srivastava S, DeSouza S, Ziff EB (2006) Membrane localization of membrane type 5 matrix metalloproteinase by AMPA receptor binding protein and cleavage of cadherins. *J Neurosci.* **26**, 2300-2312.
- Montero JC, Yuste L, Diaz-Rodriguez E, Esparis-Ogando A, Pandiella A (2000) Differential shedding of transmembrane neuregulin isoforms by the tumor necrosis factor-alpha-converting enzyme. *Mol.Cell Neurosci.* **16**, 631-648.
- Mortier E, Bernard J, Plet A, Jacques Y (2004) Natural, proteolytic release of a soluble form of human IL-15 receptor alpha-chain that behaves as a specific, high affinity IL-15 antagonist. *J Immunol* **173**, 1681-1688.
- Moss ML, Lambert MH (2002) Shedding of membrane proteins by ADAM family proteases. *Essays Biochem.* **38**, 141-153.
- Mu D, Cambier S, Fjellbirkeland L, Baron JL, Munger JS, Kawakatsu H, Sheppard D, Broaddus VC, Nishimura SL (2002) The integrin alpha(v)beta8 mediates epithelial homeostasis through MT1-MMP-dependent activation of TGF-beta1. *J Cell Biol.* **157**, 493-507.
- Mullberg J, Oberthur W, Lottspeich F, Mehl E, Dittrich E, Graeve L, Heinrich PC, Rose-John S (1994) The soluble human IL-6 receptor. Mutational characterization of the proteolytic cleavage site. *The Journal of Immunology* **152**, 4958-4968.
- Nagase H, Visse R, Murphy G (2006) Structure and function of matrix metalloproteinases and TIMPs. *Cardiovasc.Res.* **69**, 562-573.
- Nakamura H, Suenaga N, Taniwaki K, Matsuki H, Yonezawa K, Fujii M, Okada Y, Seiki M (2004) Constitutive and induced CD44 shedding by ADAM-like proteases and membrane-type 1 matrix metalloproteinase. *Cancer Res.* **64**, 876-882.
- Neeper M, Schmidt AM, Brett J, Yan SD, Wang F, Pan YC, Elliston K, Stern D, Shaw A (1992) Cloning and expression of a cell surface receptor for advanced glycosylation end products of proteins. *J Biol.Chem.* **267**, 14998-15004.
- Nishizuka Y (1984) The role of protein kinase C in cell surface signal transduction and tumour promotion. *Nature* **308**, 693-698.
- Nishizuka Y (1986) Studies and perspectives of protein kinase C. *Science* **233**, 305-312.
- Ochieng J, Fridman R, Nangia-Makker P, Kleiner DE, Liotta LA, Stetler-Stevenson WG, Raz A (1994) Galectin-3 is a novel substrate for human matrix metalloproteinases-2 and -9. *Biochemistry* **33**, 14109-14114.
- Pandiella A, Massague J (1991) Multiple signals activate cleavage of the membrane transforming growth factor-alpha precursor. *Journal of Biological Chemistry* **266**, 5769-5773.
- Park IH, Yeon SI, Youn JH, Choi JE, Sasaki N, Choi IH, Shin JS (2004) Expression of a novel secreted splice variant of the receptor for advanced glycation end products (RAGE) in human brain astrocytes and peripheral blood mononuclear cells. *Mol.Immunol* **40**, 1203-1211.
- Park L, Raman KG, Lee KJ, Lu Y, Ferran LJ, Jr., Chow WS, Stern D, Schmidt AM (1998) Suppression of accelerated diabetic atherosclerosis by the soluble receptor for advanced glycation endproducts. *Nat.Med.* **4**, 1025-1031.
- Parkin ET, Tan F, Skidgel RA, Turner AJ, Hooper NM (2003) The ectodomain shedding of

- angiotensin-converting enzyme is independent of its localisation in lipid rafts. *J Cell Sci.* **116**, 3079-3087.
- Parkin ET, Trew A, Christie G, Faller A, Mayer R, Turner AJ, Hooper NM (2002) Structure-activity relationship of hydroxamate-based inhibitors on the secretases that cleave the amyloid precursor protein, angiotensin converting enzyme, CD23, and pro-tumor necrosis factor-alpha. *Biochemistry* **41**, 4972-4981.
- Perl AK, Wilgenbus P, Dahl U, Semb H, Christofori G (1998) A causal role for E-cadherin in the transition from adenoma to carcinoma. *Nature* **392**, 190-193.
- Peschon JJ, Slack JL, Reddy P, Stocking KL, Sunnarborg SW, Lee DC, Russell WE, Castner BJ, Johnson RS, Fitzner JN, Boyce RW, Nelson N, Kozlosky CJ, Wolfson MF, Rauch CT, Cerretti DP, Paxton RJ, March CJ, Black RA (1998) An essential role for ectodomain shedding in mammalian development. *Science* **282**, 1281-1284.
- Phong MC, Gutwein P, Kadel S, Hexel K, Altevogt P, Linderkamp O, Brenner B (2003) Molecular mechanisms of L-selectin-induced co-localization in rafts and shedding [corrected]. *Biochem.Biophys.Res.Commun.* **300**, 563-569.
- Prevost JM, Pelley JL, Zhu W, D'Egidio GE, Beaudry PP, Pihl C, Neely GG, Claret E, Wijdenes J, Brown CB (2002) Granulocyte-Macrophage Colony-Stimulating Factor (GM-CSF) and Inflammatory Stimuli Up-Regulate Secretion of the Soluble GM-CSF Receptor in Human Monocytes: Evidence for Ectodomain Shedding of the Cell Surface GM-CSF Receptor {alpha} Subunit. *The Journal of Immunology* **169**, 5679-5688.
- Primakoff P, Myles DG (2000) The ADAM gene family: surface proteins with adhesion and protease activity. *Trends Genet.* **16**, 83-87.
- Pullerits R, Bokarewa M, Dahlberg L, Tarkowski A (2005) Decreased levels of soluble receptor for advanced glycation end products in patients with rheumatoid arthritis indicating deficient inflammatory control. *Arthritis Res.Ther.* **7**, R817-R824.
- Racchi M, Solano DC, Sironi M, Govoni S (1999) Activity of alpha-secretase as the common final effector of protein kinase C-dependent and -independent modulation of amyloid precursor protein metabolism. *J Neurochem.* **72**, 2464-2470.
- Renard C, Chappey O, Wautier MP, Nagashima M, Lundh E, Morser J, Zhao L, Schmidt AM, Scherrmann JM, Wautier JL (1997) Recombinant advanced glycation end product receptor pharmacokinetics in normal and diabetic rats. *Mol.Pharmacol.* **52**, 54-62.
- Rong LL, Trojaborg W, Qu W, Kostov K, Yan SD, Gooch C, Szabolcs M, Hays AP, Schmidt AM (2004) Antagonism of RAGE suppresses peripheral nerve regeneration. *FASEB J* **18**, 1812-1817.
- Sadhukhan R, Sen GC, Ramchandran R, Sen I (1998) The distal ectodomain of angiotensin-converting enzyme regulates its cleavage-secretion from the cell surface. *Proc.Natl.Acad.Sci.U.S.A* **95**, 138-143.
- Sakaguchi T, Yan SF, Du Yan S, Belov D, Rong LL, Sousa M, Andrassy M, Marso SP, Duda S, Arnold B, Liliensiek B, Nawroth PP, Stern DM, Schmidt AM, Naka Y (2003) Central role of RAGE-dependent neointimal expansion in arterial restenosis. *Journal of Clinical Investigation* **111**, 959-972.
- Sanderson MP, Erickson SN, Gough PJ, Garton KJ, Wille PT, Raines EW, Dunbar AJ, Dempsey PJ (2005) ADAM10 mediates ectodomain shedding of the betacellulin precursor activated by p-aminophenylmercuric acetate and extracellular calcium influx. *J Biol.Chem.* **280**, 1826-1837.
- Schafer B, Gschwind A, Ullrich A (2004) Multiple G-protein-coupled receptor signals converge on the epidermal growth factor receptor to promote migration and invasion. *Oncogene* **23**, 991-999.

- Schlondorff J, Blobel CP (1999) Metalloprotease-disintegrins: modular proteins capable of promoting cell-cell interactions and triggering signals by protein-ectodomain shedding. *J Cell Sci.* **112** ( Pt 21), 3603-3617.
- Schlondorff J, Lum L, Blobel CP (2001) Biochemical and pharmacological criteria define two shedding activities for TRANCE/OPGL that are distinct from the tumor necrosis factor alpha convertase. *J Biol.Chem.* **276**, 14665-14674.
- Schlueter C, Hauke S, Flohr AM, Rogalla P, Bullerdiek J (2003) Tissue-specific expression patterns of the RAGE receptor and its soluble forms--a result of regulated alternative splicing? *Biochim.Biophys.Acta* **1630**, 1-6.
- Schmidt AM, Mora R, Cao R, Yan SD, Brett J, Ramakrishnan R, Tsang TC, Simionescu M, Stern D (1994) The endothelial cell binding site for advanced glycation end products consists of a complex: an integral membrane protein and a lactoferrin-like polypeptide. *J Biol.Chem.* **269**, 9882-9888.
- Schmidt AM, Vianna M, Gerlach M, Brett J, Ryan J, Kao J, Esposito C, Hegarty H, Hurley W, Claus M, . (1992) Isolation and characterization of two binding proteins for advanced glycosylation end products from bovine lung which are present on the endothelial cell surface. *J Biol.Chem.* **267**, 14987-14997.
- Schmidt AM, Yan SD, Yan SF, Stern DM (2001) The multiligand receptor RAGE as a progression factor amplifying immune and inflammatory responses. *J Clin.Invest* **108**, 949-955.
- Schmidt R, Bultmann A, Ungerer M, Joghetaei N, Bulbul O, Thieme S, Chavakis T, Toole BP, Gawaz M, Schomig A, May AE (2006) Extracellular matrix metalloproteinase inducer regulates matrix metalloproteinase activity in cardiovascular cells: implications in acute myocardial infarction. *Circulation* **113**, 834-841.
- Schurig U, Stopfel N, Huckel M, Pfirschke C, Wiederanders B, Brauer R (2005) Local expression of matrix metalloproteinases, cathepsins, and their inhibitors during the development of murine antigen-induced arthritis. *Arthritis Res.Ther.* **7**, R174-R188.
- Seals DF, Courtneidge SA (2003) The ADAMs family of metalloproteases: multidomain proteins with multiple functions. *Genes Dev.* **17**, 7-30.
- Selkoe DJ (2001a) Alzheimer's disease: genes, proteins, and therapy. *Physiol Rev.* **81**, 741-766.
- Selkoe DJ (2001b) Clearing the brain's amyloid cobwebs. *Neuron* **32**, 177-180.
- Sheu BC, Hsu SM, Ho HN, Lien HC, Huang SC, Lin RH (2001) A novel role of metalloproteinase in cancer-mediated immunosuppression. *Cancer Res.* **61**, 237-242.
- Shibata M, Yamada S, Kumar SR, Calero M, Bading J, Frangione B, Holtzman DM, Miller CA, Strickland DK, Ghiso J, Zlokovic BV (2000) Clearance of Alzheimer's amyloid-ss(1-40) peptide from brain by LDL receptor-related protein-1 at the blood-brain barrier. *J Clin.Invest* **106**, 1489-1499.
- Simm A, Munch G, Seif F, Schenk O, Heidland A, Richter H, Vamvakas S, Schinzel R (1997) Advanced glycation endproducts stimulate the MAP-kinase pathway in tubulus cell line LLC-PK1. *FEBS Lett.* **410**, 481-484.
- Sisodia SS (1992) {beta}-Amyloid Precursor Protein Cleavage by a Membrane-Bound Protease. *Proceedings of the National Academy of Sciences* **89**, 6075-6079.
- Slater SJ, Kelly MB, Taddeo FJ, Rubin E, Stubbs CD (1994) Evidence for discrete diacylglycerol and phorbol ester activator sites on protein kinase C. Differences in effects of 1-alkanol inhibition, activation by

- phosphatidylethanolamine and calcium chelation. *J Biol.Chem.* **269**, 17160-17165.
- Springman EB, Angleton EL, Birkedal-Hansen H, Wart HEV (1990) Multiple Modes of Activation of Latent Human Fibroblast Collagenase: Evidence for the Role of a Cys73 Active-Site Zinc Complex in Latency and a "Cysteine Switch" Mechanism for Activation. *Proceedings of the National Academy of Sciences* **87**, 364-368.
- Srikrishna G, Huttunen HJ, Johansson L, Weigle B, Yamaguchi Y, Rauvala H, Freeze HH (2002) N-Glycans on the receptor for advanced glycation end products influence amphoterin binding and neurite outgrowth. *J.Neurochem.* **80**, 998-1008.
- Stocker W, Grams F, Baumann U, Reinemer P, Gomis-Ruth FX, McKay DB, Bode W (1995) The metzincins--topological and sequential relations between the astacins, adamalysins, serralysins, and matrixins (collagenases) define a superfamily of zinc-peptidases. *Protein Sci.* **4**, 823-840.
- Sugaya K, Fukagawa T, Matsumoto K, Mita K, Takahashi E, Ando A, Inoko H, Ikemura T (1994) Three genes in the human MHC class III region near the junction with the class II: gene for receptor of advanced glycosylation end products, PBX2 homeobox gene and a notch homolog, human counterpart of mouse mammary tumor gene int-3. *Genomics* **23**, 408-419.
- Sunnarborg SW, Hinkle CL, Stevenson M, Russell WE, Raska CS, Peschon JJ, Castner BJ, Gerhart MJ, Paxton RJ, Black RA, Lee DC (2002) Tumor necrosis factor-alpha converting enzyme (TACE) regulates epidermal growth factor receptor ligand availability. *J.Biol.Chem.* **277**, 12838-12845.
- Taguchi A, Blood DC, del Toro G, Canet A, Lee DC, Qu W, Tanji N, Lu Y, Lalla E, Fu C, Hofmann MA, Kislinger T, Ingram M, Lu A, Tanaka H, Hori O, Ogawa S, Stern DM, Schmidt AM (2000) Blockade of RAGE-amphoterin signalling suppresses tumour growth and metastases. *Nature* **405**, 354-360.
- Tang P, Hung MC, Klostergaard J (1996) Length of the Linking Domain of Human pro-Tumor Necrosis Factor Determines the Cleavage Processing. *Biochemistry* **35**, 8226-8233.
- Tanzi RE (1999) A genetic dichotomy model for the inheritance of Alzheimer's disease and common age-related disorders. *J Clin.Invest* **104**, 1175-1179.
- Thabard W, Collette M, Bataille R, Amiot M (2001) Protein kinase C delta and eta isoenzymes control the shedding of the interleukin 6 receptor alpha in myeloma cells. *Biochem.J* **358**, 193-200.
- Thathiah A, Carson DD (2004) MT1-MMP mediates MUC1 shedding independent of TACE/ADAM17. *Biochem.J* **382**, 363-373.
- Tomita S, Kirino Y, Suzuki T (1998) A basic amino acid in the cytoplasmic domain of Alzheimer's beta-amyloid precursor protein (APP) is essential for cleavage of APP at the alpha-site. *J Biol.Chem.* **273**, 19304-19310.
- Toth M, Gervasi DC, Fridman R (1997) Phorbol ester-induced cell surface association of matrix metalloproteinase-9 in human MCF10A breast epithelial cells. *Cancer Res.* **57**, 3159-3167.
- Tsakadze NL, Sithu SD, Sen U, English WR, Murphy G, D'Souza SE (2006) Tumor necrosis factor-alpha-converting enzyme (TACE/ADAM-17) mediates the ectodomain cleavage of intercellular adhesion molecule-1 (ICAM-1). *Journal of Biological Chemistry* **281**, 3157-3164.
- Urena JM, Merlos-Suarez A, Baselga J, Arribas J (1999) The cytoplasmic carboxy-terminal amino acid determines the subcellular localization of proTGF-(alpha) and membrane type matrix metalloprotease (MT1-MMP). *J Cell Sci.* **112** ( Pt 6), 773-784.

- Vinogradova O, Velyvis A, Velyviene A, Hu B, Haas T, Plow E, Qin J (2002) A structural mechanism of integrin alpha(IIb)beta(3) "inside-out" activation as regulated by its cytoplasmic face. *Cell* **110**, 587-597.
- Vollmer P, Peters M, Ehlers M, Yagame H, Matsuba T, Kondo M, Yasukawa K, Buschenfelde KH, Rose-John S (1996) Yeast expression of the cytokine receptor domain of the soluble interleukin-6 receptor. *J.Immunol.Methods* **199**, 47-54.
- Wang WS, Chen PM, Su Y (2006) Colorectal carcinoma: from tumorigenesis to treatment. *Cell Mol.Life Sci.* **63**, 663-671.
- Wang X, He K, Gerhart M, Huang Y, Jiang J, Paxton RJ, Yang S, Lu C, Menon RK, Black RA, Baumann G, Frank SJ (2002) Metalloprotease-mediated GH Receptor Proteolysis and GHBP Shedding. DETERMINATION OF EXTRACELLULAR DOMAIN STEM REGION CLEAVAGE SITE. *Journal of Biological Chemistry* **277**, 50510-50519.
- Woessner JF, Jr. (1995) Quantification of matrix metalloproteinases in tissue samples. *Methods Enzymol.* **248**, 510-528.
- Woo MS, Jung SH, Kim SY, Hyun JW, Ko KH, Kim WK, Kim HS (2005) Curcumin suppresses phorbol ester-induced matrix metalloproteinase-9 expression by inhibiting the PKC to MAPK signaling pathways in human astrogloma cells. *Biochem.Biophys.Res.Commun.* **335**, 1017-1025.
- Xing Y, Xu Q, Lee C (2003) Widespread production of novel soluble protein isoforms by alternative splicing removal of transmembrane anchoring domains. *FEBS Lett.* **555**, 572-578.
- Yan SD, Chen X, Fu J, Chen M, Zhu H, Roher A, Slattery T, Zhao L, Nagashima M, Morser J, Migheli A, Nawroth P, Stern D, Schmidt AM (1996) RAGE and amyloid-beta peptide neurotoxicity in Alzheimer's disease. *Nature* **382**, 685-691.
- Yan SD, Stern D, Kane MD, Kuo YM, Lampert HC, Roher AE (1998) RAGE-Abeta interactions in the pathophysiology of Alzheimer's disease. *Restor.Neurol.Neurosci.* **12**, 167-173.
- Yan SD, Stern D, Schmidt AM (1997) What's the RAGE? The receptor for advanced glycation end products (RAGE) and the dark side of glucose. *Eur.J Clin.Invest* **27**, 179-181.
- Yan Y, Shirakabe K, Werb Z (2002) The metalloprotease Kuzbanian (ADAM10) mediates the transactivation of EGF receptor by G protein-coupled receptors. *J Cell Biol.* **158**, 221-226.
- Yonekura H, Yamamoto Y, Sakurai S, Petrova RG, Abedin MJ, Li H, Yasui K, Takeuchi M, Makita Z, Takasawa S, Okamoto H, Watanabe T, Yamamoto H (2003) Novel splice variants of the receptor for advanced glycation end-products expressed in human vascular endothelial cells and pericytes, and their putative roles in diabetes-induced vascular injury. *Biochem.J.* **370**, 1097-1109.
- Yu Q, Stamenkovic I (1999) Localization of matrix metalloproteinase 9 to the cell surface provides a mechanism for CD44-mediated tumor invasion. *Genes Dev.* **13**, 35-48.
- Yu Q, Stamenkovic I (2000) Cell surface-localized matrix metalloproteinase-9 proteolytically activates TGF-beta and promotes tumor invasion and angiogenesis. *Genes Dev.* **14**, 163-176.
- Yu R, Mandlekar S, Tan TH, Kong AN (2000) Activation of p38 and c-Jun N-terminal kinase pathways and induction of apoptosis by chelerythrine do not require inhibition of protein kinase C. *J Biol.Chem.* **275**, 9612-9619.
- Yu XF, Han ZC (2006) Matrix metalloproteinases in bone marrow: roles of gelatinases in physiological hematopoiesis and hematopoietic malignancies. *Histol.Histopathol.* **21**, 519-531.

Zhang G, Kazanietz MG, Blumberg PM, Hurley JH (1995) Crystal structure of the cys2 activator-binding domain of protein kinase C delta in complex with phorbol ester. *Cell* **81**, 917-924.

Zheng Y, Saftig P, Hartmann D, Blobel C (2004) Evaluation of the contribution of different ADAMs to tumor necrosis factor alpha (TNFalpha) shedding and of the function of the TNFalpha ectodomain in ensuring selective stimulated shedding by the TNFalpha convertase (TACE/ADAM17). *J Biol.Chem.* **279**, 42898-42906.

Zlokovic B (1997) Can blood-brain barrier play a role in the development of cerebral amyloidosis and Alzheimer's disease pathology. *Neurobiol.Dis.* **4**, 23-26.

Zlokovic BV (2004) Clearing amyloid through the blood-brain barrier. *J Neurochem.* **89**, 807-811.

Zlokovic BV, Martel CL, Matsubara E, McComb JG, Zheng G, McCluskey RT, Frangione B, Ghiso J (1996) Glycoprotein 330/megalin: probable role in receptor-mediated transport of apolipoprotein J alone and in a complex with Alzheimer disease amyloid beta at the blood-brain and blood-cerebrospinal fluid barriers. *Proc.Natl.Acad.Sci.U.S.A* **93**, 4229-4234.

## Abbreviations

<b>A<math>\beta</math></b>	Amyloid $\beta$ Peptide
<b>AD</b>	Alzheimer's disease
<b>ADAM</b>	a Disintegrin and Metalloprotease
<b>AGE</b>	advanced glycation end products
<b>AICD</b>	APP Intracellular Domain
<b>APP</b>	Amyloid precursor protein
<b>sAPP<math>\alpha</math></b>	$\alpha$ -Secretase cleaved soluble APP
<b>sAPP<math>\beta</math></b>	$\beta$ -secretase cleaved soluble APP
<b>ATP</b>	adenosin triphosphate
<b>BBB</b>	Blood Brain Barrier
<b>bp</b>	Base pair
<b>BSA</b>	Bovine serum albumine
<b>DMSO</b>	dimethylsulfoxide
<b>DNA</b>	desoxyribonucleic acid
<b>dNTP</b>	desoxynucleotidetriphosphate
<b>DTT</b>	dithiothreitol
<b>ECL</b>	enhanced chemoluminescence
<b>EDTA</b>	ethylenediaminetetraacetate
<b>FCS</b>	fetal calf serum
<b>HA</b>	Hemagglutinin
<b>His</b>	Histidine
<b>kDa</b>	Kilo Dalton
<b>MMP</b>	Matrix-Metalloproteinase
<b>PAGE</b>	Polyacrylamide gel electrophoresis
<b>PBS</b>	phosphate buffered saline
<b>PCR</b>	polymerase chain reaction
<b>PMA</b>	Phorbol-12-Myristat-13-Acetate
<b>RNA</b>	ribonucleic acid
<b>RAGE</b>	Receptor for advanced glycaion end products
<b>ROS</b>	reactive oxygen species
<b>rpm</b>	rounds per minute
<b>SDS</b>	sodium dodecyl sulfate
<b>TCA</b>	Trichloroacetic acid
<b>Tris</b>	tris(-hydroxymethyl)-aminomethane



## Index of Tables and Figures

<b>Figure 1 Processing of APP and consequential accumulation of A<math>\beta</math>.</b> .....	2
<b>Figure 2 Transport-clearance model for A<math>\beta</math> regulations in the brain.</b> .....	3
<b>Figure 3 Structure of Receptor for advanced glycation end products.</b> .....	5
<b>Figure 4 RAGE signaling pathways.</b> .....	7
<b>Figure 5 Multiple isoforms of RAGE.</b> .....	9
<b>Figure 6 Modular domain structures of MMPs.</b> .....	17
<b>Figure 7 Expression of either myc-tagged RAGE or wild-type RAGE in Flp-In 293 cells and COS-7 cells.</b> .....	49
<b>Figure 8 Cleavage of epitope-tagged RAGE and glycosylation of sRAGE.</b> .....	50
<b>Figure 9 RAGE is cell surface associated and the cleavage of RAGE occurs at the plasma membrane.</b> .....	52
<b>Figure 10 Constitutive and PMA-stimulated shedding of RAGE.</b> .....	53
<b>Figure 11 Shedding of RAGE stimulated by APMA.</b> .....	54
<b>Figure 12 Shedding of RAGE stimulated by a calcium ionophore.</b> .....	55
<b>Figure 13 Effects of chelerythrine and PD98059 on RAGE shedding.</b> .....	56
<b>Figure 14 Proteolysis of RAGE is unaffected by several protease inhibitors.</b> .....	59
<b>Figure 15 Shedding of RAGE inhibited by the metalloproteinase inhibitor GI254023X.</b> .....	60
<b>Figure 16 Shedding of RAGE inhibited by the metalloproteinase inhibitor GW280264X.</b> .....	61
<b>Figure 17 Shedding of RAGE inhibited by the metalloproteinase inhibitor GM6001.</b> .....	62
<b>Figure 18 Shedding of RAGE is unaffected by ADAM10.</b> .....	65
<b>Figure 19 Shedding of RAGE is unaffected by ADAM17.</b> .....	66
<b>Figure 20 Overexpression of MT1-MMP does not influence shedding of RAGE.</b> .....	68
<b>Figure 21 Expression and activity of human MMP9 in secretion medium from COS-7 cells.</b> .....	70
<b>Figure 22 MMP9 increases constitutive and PMA-stimulated shedding of RAGE.</b> .....	72
<b>Figure 23 Scheme of the RNAi Pathway.</b> .....	73
<b>Figure 24 Activity of human MMP9 inhibited by MMP9 Stealth RNAi.</b> .....	75
<b>Figure 25 Shedding of RAGE decreased by MMP9 knockdown.</b> .....	76
<b>Figure 26 Shedding of RAGE is decreased by MMP9 but not ADAM10 knockdown.</b> .....	77
<b>Figure 27 Deletion of its cytoplasmic domain does not abrogate ectodomain shedding of RAGE.</b> .....	79
<b>Figure 28 Deletion of its cytoplasmic domain does not abrogate APMA-stimulated shedding of RAGE.</b> .....	79
<b>Figure 29 RAGE-<math>\Delta</math>C is present and cleaved at the cell surface.</b> .....	80
<b>Figure 30 Schematic representation of the putative cleavage sequence of RAGE and the P328E mutation.</b> .....	81
<b>Figure 31 Mutation or deletion of the P-T-A-G-S motif does not abrogate ectodomain shedding of RAGE.</b> .....	82
<b>Table 1 Ligands for RAGE and their associated pathophysiologic roles</b> .....	6
<b>Table 2 Splicing forms of RAGE</b> .....	11
<b>Table 3 Examples of proteins undergoing ectodomain shedding and the corresponding sheddases</b> .....	13
<b>Table 4 Category of MMPs and their Substrates (adapted from Chakraborti <i>et al.</i> 2003)</b> .....	15
<b>Table 5 Reaction Components of PCR</b> .....	39
<b>Table 6 Preparation of BSA standard series</b> .....	40
<b>Table 7 Summary of inhibitors and activators used for analysis of shedding of RAGE</b> .....	47
<b>Table 8 Protease inhibitors, inhibition profile and experiment concentration</b> .....	57
<b>Table 9 IC50 values of two metalloproteinase inhibitors for recombinant metalloproteinases</b> ....	63

